Underlying principles of bistability in the expression of the pivotal virulence regulator RovA of *Yersinia pseudotuberculosis* and its role for virulence

Von der Fakultät für Lebenswissenschaften

der Technischen Universität Carolo-Wilhelmina zu Braunschweig

zur Erlangung des Grades einer

Doktorin der Naturwissenschaften

(Dr. rer. nat.)

genehmigte

D i s s e r t a t i o n

von Franziska Schuster
aus Salzwedel

1. Referentin oder Referent: Prof. Dr. Petra Dersch
2. Referentin oder Referent: Prof. Dr. Susanne Engelmann
eingereicht am: 14.09.2015
mündliche Prüfung (Disputation) am: 27.11.2015

Druckjahr 2015

Vorveröffentlichungen der Dissertation

Teilergebnisse aus dieser Arbeit wurden mit Genehmigung der Fakultät für Lebenswissenschaften, vertreten durch die Mentorin der Arbeit, in folgenden Beiträgen vorab veröffentlicht:

Publikationen

Nuss A.M.[*], Schuster F.[*], Roselius L., Klein J., Bücker R., Heroven AK., Herbst K., Wittmann C., Müller J., Münch R., Jahn D., Dersch P.: A precise temperature-responsive bistable switch controlling virulence. In preparation. ([*]shared first authorship)

Nuss A.M.[*], Schuster F.[*], Heroven AK., Heine, W., Pisano F., Dersch P. (2014): A direct link between the global regulator PhoP and the Csr regulon in *Y. pseudotuberculosis* through the small regulatory RNA CsrC. *RNA Biology*, *11*(5), 580–593. doi:10.4161/rna.28676 ([*]shared first authorship)

Tagungsbeiträge

Schuster F., Nuss A.M., Dersch P. (2013): Bistable expression of the pivotal virulence regulator RovA of *Yersinia pseudotuberculosis*. SPP1617, Kloster Banz, Bad Staffelstein

Schuster F., Nuss A.M., Heroven AK., Heine, W., Pisano F., Dersch P. (2014): A direct link between the global regulator PhoP and the Csr regulon in *Y. pseudotuberculosis* through the small regulatory RNA CsrC. 4. nationales *Yersinia* Meeting, Hamburg

Table of contents

List of figures

List of tables

Abbreviations

A	adenine
Amp	ampicillin
APS	ammonium persulfate
bp	base pair
BHI	brain heart infusion
BSA	bovine serum albumin
C	cytosine
°C	degree Celsius
CFU	colony forming units
Cm	chloramphenicol
Crp	cAMP receptor protein
Csr	carbon storage regulator
Da	Dalton
DAPI	49,6- diamidino-2-phenylindole
DIG	digoxygenin
DNA	desoxyribonucleic acid
e.g.	for example
et al.	et alii
EDTA	ethylenediaminetetraacetic acid
FACS	fluorescence activated cell sorting
FELASA	European Health Recommendations of the Federation of Laboratory Animal Science Associations
G	guanine
g	gram
GFP	green fluorescent protein
GV-SOLAS	German Recommendations of the Society for Laboratory Animal Science
h	hour(s)
HRP	horseradish peroxidase
IPTG	isopropyl-β-d-thiogalactopyranosid
Kan	kanamycin
kDa	kilo-Dalton
KEGG	Kyoto Encyclopedia of Genes and Genomes
kb	kilo-base
l	liter
lacZ	gene encoding for β-galactosidase
LD_{50}	lethal dose, 50%
LPS	lipopolysaccharide
M	molar
mA	milli-Ampère
M-cells	microfold cells

min	minute
µ	micro
ml	milliliter
MLNs	mesenteric lymph nodes
NCBI	National Center for Biotechnology Information
NEB	New England Biolabs
NF-κB	nuclear factor κB
nm	nanometer
nM	nanomolar
OD	optical density
ori	origin of replication
PAGE	polyacrylamide gelelectrophoresis
PBS	phosphate buffer saline
PCR	polymerase chain reaction
PFA	paraformaldehyde
PP	Peyer's patch
PVDF	polyvinylidene fluoride
pYV	*Yersinia* virulence plasmid
RBS	ribosomal binding site
RNA	ribonucleic acid
Rov	regulator of virulence
rpm	revolutions per minute
s	seconds
SDS	sodiumdodecylsulfate
SOC	super optimal broth
T	thymine
TAE	tris-acetate EDTA
Taq	DNA polymerase of *Thermus aquaticus*
TBE	tris-borate EDTA
TEMED	tetramethylethylenediamine
Tris	trishydroxymethylaminomethane
TSS	transcriptional start site
T3SS	type three secretion system
UTR	untranslated region
UV	ultra violet
wt	wild type
V	Volt

1 Introduction

Infectious diseases still belong to one of the leading causes of deaths worldwide with about 15% deaths per year, coming immediately after cardiovascular diseases. Besides respiratory infections, gastrointestinal diseases are one of the predominant infectious diseases. In 2004 2.2 million people died due to diarrheal diseases, which are a major problem in developing countries (WHO, GBD report 2004 update). Even in Germany 50% of all reported infectious diseases are infections of the gastrointestinal tract. The agents of gastrointestinal diseases are mainly *Salmonella*, enterohaemorrhagic *Escherichia coli* (EHEC), *Campylobacter* and *Yersinia* (Epidemiologisches Bulletin 46/2003, RKI). In 2014 2485 cases of Yersiniosis were reported in Germany (Epidemiologisches Bulletin 20/2015, RKI).

However, in general infection processes are still not fully understood. For instance, questions regarding regulatory mechanisms controlling the expression of virulence factors during the infection remain to be analyzed. Recently, it was shown that gene expression is not always unimodal within one bacterial population (Casadesús and Low, 2013). The role and mechanisms of heterogeneous expression of a virulence gene regulator in *Y. pseudotuberculosis* are investigated in this study.

1.1 The genus *Yersinia*

The genus *Yersinia* belongs to the family of *Enterobacteriaceae* and was named after Alexandre Émile Jean Yersin, who first isolated *Y. pestis* from buboes in Hongkong in 1894 (Treille and Yersin, 1894). *Yersinia* are Gram-negative, rod-shaped bacteria, which can grow under facultative anaerobic conditions. *Yersinia* are psychotolerant and are able to grow between temperatures of 4°C to 43°C with an optimum between 20°C and 30°C. Until now 18 species have been reported of which three are pathogenic to humans - *Y. pestis, Y. pseudotuberculosis* and *Y. enterocolitica* (Bottone, 1997; Chen *et al*., 2010; Savin *et al*., 2014). While *Y. enterocolitica* and *Y. pseudotuberculosis* only share a nucleotide identity of 60% and emerged from each other 42 to 187 million years ago, *Y. pestis* evolved from *Y. pseudotuberculosis* just 1.500 - 20.000 years ago and has a 90% nucleotide identity with *Y. pseudotuberculosis* (Achtman *et al*., 1999).

Y. pestis is the agent of bubonic and pneumonic plague and causes severe fever, swollen buboes and haemorrhages. The main reservoirs of *Y. pestis* are rodents, but the bacteria were also found in prairie dogs. They are normally transmitted from animals to humans by fleabites and rarely from human to human by inhalation of aerosols (Perry and Fetherston, 1997).

Y. pseudotuberculosis and *Y. enterocolitica* are food-borne pathogens that cause Yersiniosis, gut-associated diseases like gastroenteritis, enterocolitis and mesenterial lymphadenitis with symptoms such as vomiting, fever, abdominal pain and diarrhea (Galindo *et al*., 2011; Koornhof *et al*., 1999). Yersiniosis is typically a self-limiting disease, however in immune-compromised persons it can lead to septicemica with mortality rates of up to 75% (Deacon *et al*., 2003). In rare cases *Y. pseudotuberculosis* and *Y. enterocolitica* can also cause autoimmune diseases like reactive arthritis and erythema nodosum (Naktin and Beavis, 1999). The main reservoir of *Y. pseudotuberculosis* and *Y. enterocolitica* are animals, soil and water. The transmission route is fecal-oral via contaminated food or water (Galindo *et al*., 2011). Even though Yersiniosis is rarely lethal, it is one of the most abundant bacterial zoonotic infectious diseases in the European Union (Rosner *et al*., 2010).

Although transmission of the bacteria as well as the disease symptoms differ significantly between the human pathogenic *Yersiniae*, these species share a tropism for lymphatic tissues and resistance to phagocytosis and killing by macrophages (Perry and Fetherston, 1997). Furthermore they all harbor the 70 kb *Yersinia* virulence plasmid pYV (pCD1 in *Y. pestis*), which is important for full virulence of these species. The plasmid encodes several virulence factors like the *Yersinia* adhesin A (YadA), the *Yersinia* outer proteins (Yops) and the type three secretion system (T3SS). However, *yadA* is not expressed in *Y. pestis* due to an inactivating mutation in the gene (Chain *et al.*, 2004). Besides plasmid pCD1, *Y. pestis* carries two additional virulence plasmids, the 100 kb plasmid pMT1 and the 9,5 kb plasmid pPCP1, which are important for transmission and tissue invasion of *Y. pestis* in fleas (Chain *et al*., 2004; Perry and Fetherston, 1997; Smego *et al*., 1999).

1.2 Pathogenesis of enteropathogenic *Yersinia*

The infectious process of enteropathogenic *Yersinia* species is biphasic and can be classified in an early- and a late-phase of infection. The early-phase represents the start of the infection and is characterized by the expression of virulence genes necessary for the colonization and invasion of the host. In the later phase, genes are expressed which are crucial for the evasion of the immune system and for dissemination to deeper organs (Fig. 1.1).

Ingestion of the bacteria takes place via uptake of contaminated food or water, e. g. vegetables, milk and meat products, mainly raw pork (Fredriksson-Ahomaa *et al*., 2006). When entering the host *Yersinia* enocunter a temperature change from environmental to host body temperature, which is besides nutrient and iron availability an important signal for the bacteria to adapt their gene expression pattern to host conditions. After passing the stomach the bacteria reach the small intestine and interact in the ileum with microfold cells (M-cells), which are specialized epithelial cells. M-cells are part of the follicle-associated epithelial layer and characterized by a low amount of flat microvilli and a reduced glycocalyx. They are additionally characterized by a pocket at the basolateral membrane in which phagocytes are located (Grützkau *et al.*, 1990). The main function of M-cells is the sampling and transport of antigens and microorganisms to the underlying lymphatic tissues (Kraehenbuhl and Neutra, 2000). Many enteropathogens like *Yersinia*, *Salmonella* and *Shigella* use the M-cells as an entry gate into the host (Grützkau *et al*., 1990; Sansonetti, 2002). The bacteria adhere to and invade the M-cells and subsequently reach the underlying Peyer's patches (PP) by transcytosis. The PPs are part of the mucosa associated lymphoid tissue and most frequently located in the ileum. Inside the PP the bacteria can replicate and disseminate via the lymphatic system to mesenteric lymph nodes as well as systemic organs like liver, kidney and spleen (Marra and Isberg, 1997; Pepe and Miller, 1993).

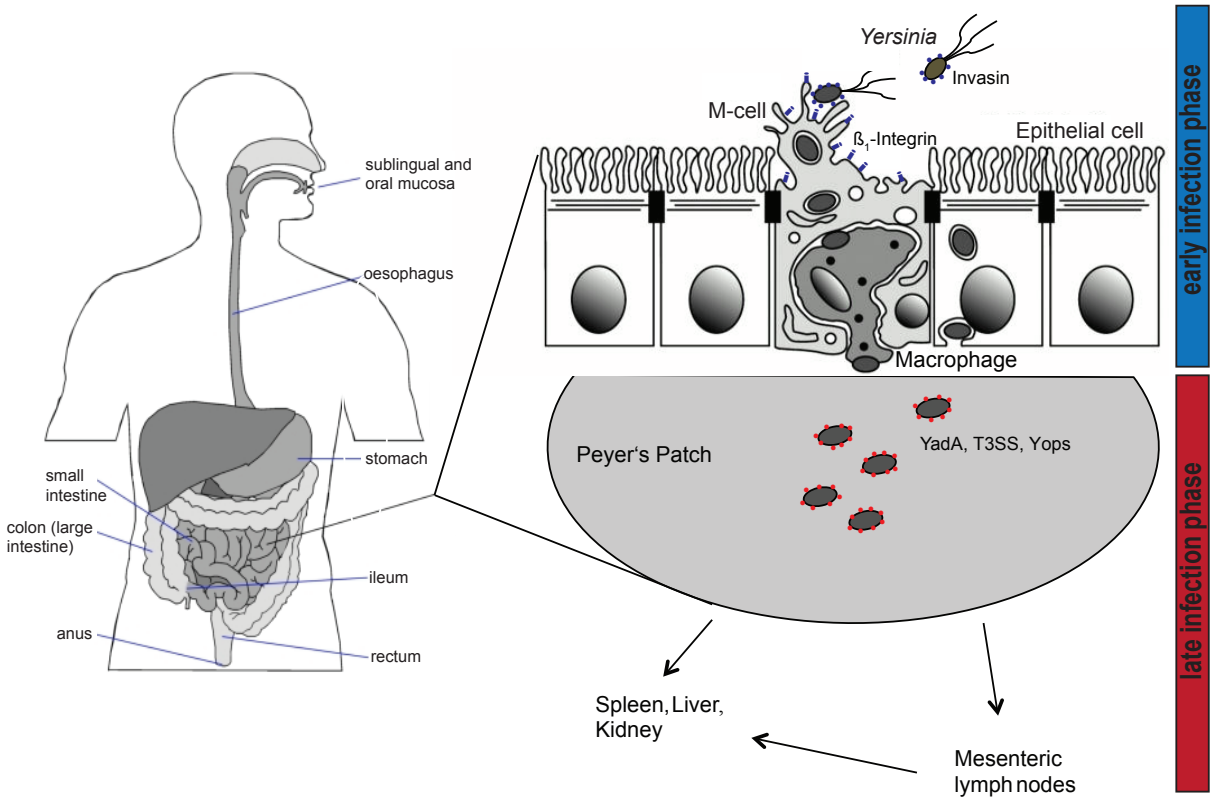

Fig. 1.1 Infection route of *Y. pseudotuberculosis*.
The bacteria are ingested together with contaminated food or water. After passing the stomach, they reach the small intestine. *Yersinia* are motile and express invasin, which mediates the interaction with M-cells in the epithelial layer via binding to β_1-intergrins. The bacteria transmigrate through the M-cells and reach the underlying PP. Once inside the tissue they express virulence factors such as YadA, the T3SS and the Yop effectors to resist immune responses. From the PP bacteria disseminate to the mesenteric lymph nodes as well as to deeper organs like spleen, liver and kidneys (modified from Azizi *et al*., 2010; Sansonetti, 2002).

1.3 Virulence factors of *Y. pseudotuberculosis*

Pathogenic bacteria differ from their non-pathogenic relatives by the expression of virulence factors and the ability to cause disease. Usually a set of different virulence factors are required for colonization and invasion of a host as well as for evasion of the immune system. The virulence factors of *Y. pseudotuberculosis* are either encoded on the 70 kb virulence plasmid or on the chromosome.

1.3.1 Adhesins and invasins

The enteropathogenic *Yersinia* strains express three main adhesins - invasin (InvA), the attachment and invasion locus (Ail), and the *Yersinia* adhesion A (YadA). InvA and Ail are encoded on the chromosome, while the *yadA* gene is located on the

virulence plasmid pYV (Balligand *et al*., 1985; Bölin *et al*., 1982; Isberg *et al*., 1987; Miller and Falkow, 1988). Invasin is the predominant and most efficient invasion factor and binds to β_1-integrins on the surface of M-cells and leads to the uptake into host cells (Dersch and Isberg, 1999; Isberg and Leong, 1990). The expression of *invA* is induced at temperatures below 30°C and crucial for the initial phase of infection (Nagel *et al*., 2001). YadA expression is induced at 37°C by the temperature-dependent regulator LcrF (Skurnik and Toivanen, 1992). By binding extracellular matrix proteins such as fibronectin, laminin and collagen, YadA also causes cell invasion, serum resistance, autoagglutination and resistance to phagocytosis (China *et al*., 1993; Heise and Dersch, 2006; Ruckdeschel *et al*., 1996; Skurnik *et al*., 1984). Ail, which is expressed at 37°C, also increases adhesion to epithelial cells and mediates serum resistance (Bliska and Falkow, 1992; Miller and Falkow, 1988).

The first step in the infectious process is the adhesion to and invasion of intestinal epithelial layer. Two mechanisms of host cell entry can be distinguished: the “trigger” and the “zipper” mechanism (Cossart and Sansonetti, 2004; O Cróinín and Backert, 2012). The “trigger” mechanism is used by e.g. *Salmonella* and *Shigella.* Effectors of the T3SS are translocated directly into host cells and activate rearrangements of the cytoskeleton, which results in membrane ruffling and uptake of the bacteria. The internalization of *Yersinia* into host cell occurs via the “zipper” mechanism, which is mediated through adherence of the bacteria to cell-surface receptors (Fig. 1.2). The interaction of the surface molecule invasin with β_1-integrins leads to a signal transduction to the cytoskeleton of the host cell. Induction of actin cytoskeleton rearrangements mediate the formation of filopodia and lamellipodia and thereby the engulfment of bacteria into a membrane-bound phagosome (Oelschlaeger, 2001; Sansonetti, 2002).

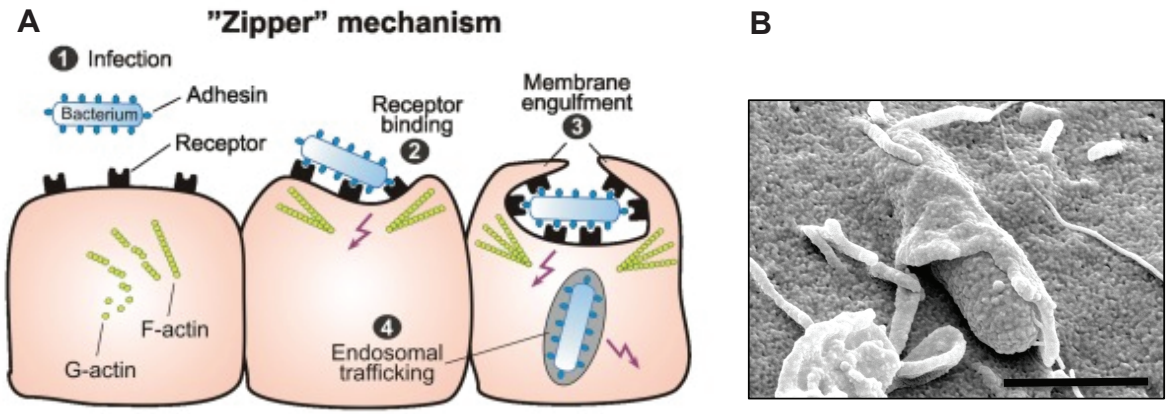

Fig. 1.2 Internalization of *Yersinia* by the "zipper" mechanism.
(A) Upon infection, the bacteria interact with receptors at the surface of the eukaryotic cell (1). Thereby, a signal is transmitted into the host cell that leads to the formation of filopodia and lamellipodia (2), the bacteria are engulfed (3) and internalized in vacuoles (4) (modified from O Cróinín and Backert, 2012). **(B)** Scanning electron microscopy picture of *Y. pseudotuberculosis* engulfed from the eukaryotic cell. Black bar indicates 1 µm (picture from M. Rohde, Helmholtz-Centre for Infection Research).

1.3.2 The Yop-virulon

Besides YadA, the virulence plasmid encodes the *Yersinia* outer proteins (Yops), as well as the Yop secretion machinery (Ysc), which assembles the T3SS (Cornelis *et al.*, 1998). The T3SS is built up by a needle-like structure with a basal body, which spans from the inner and outer membrane of the bacterium directly into the eukaryotic host cell (Fig. 1.3) (Cornelis, 2002). The Yops can be divided into two groups, first the effector proteins (YopE, YopH, YopJ, YopM, YopT and YpkA), which are translocated into the cytoplasm of target cells and second YopD and YopB, which form together with LcrV a pore in the host cell membrane. Translocation of Yops requires a close contact to the eukaryotic cell (Cornelis *et al*., 1998; Dewoody *et al*., 2013). The effector proteins inhibit the immune response, e. g. YopE, YopT and YpkA are described to act on Rho-GTPases and thereby disrupt cytoskeletal dynamics and prevent phagocytosis (Black and Bliska, 2000; Cornelis, 2002; Iriarte and Cornelis, 1998; Von Pawel-Rammingen *et al*., 2000). It was shown that YopJ is involved in preventing the inflammatory response e. g. by the inhibition of NF-kB, which results in a decreased cytokine expression (Schesser *et al*., 1998).

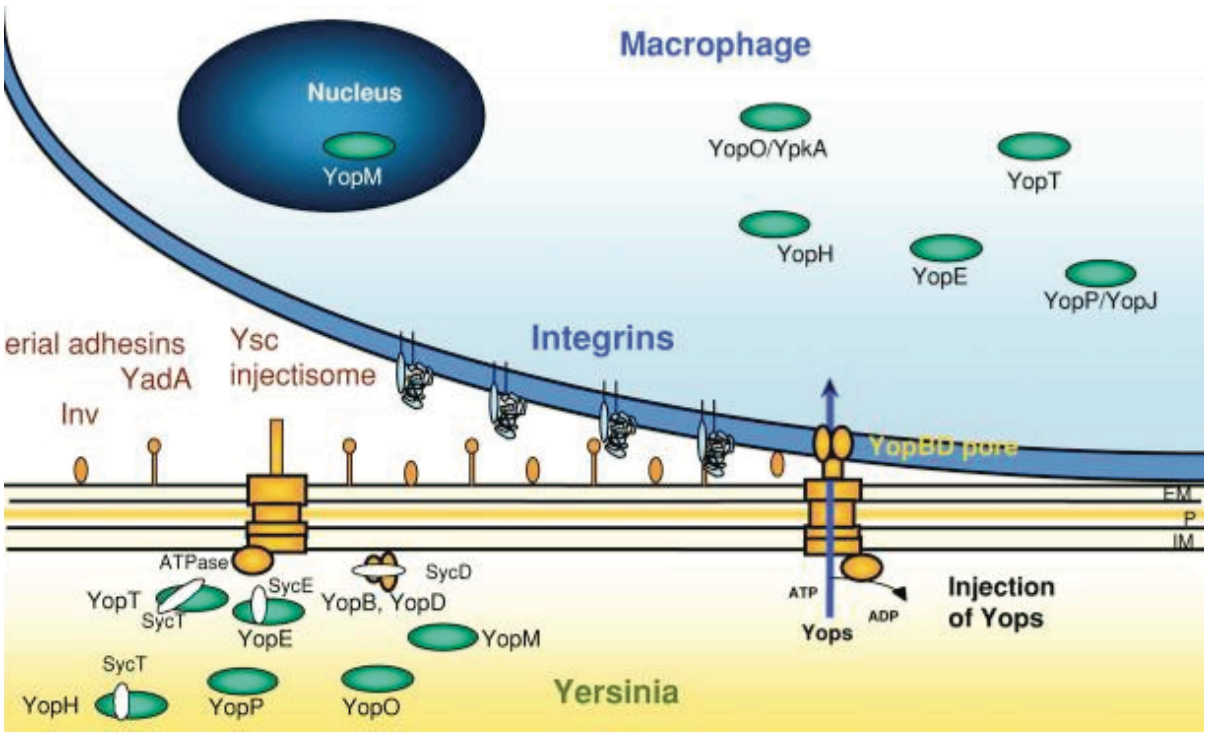

Fig. 1.3 The T3SS and secretion of Yops into the host cell.
At 37°C expression of the T3SS and Yops is activated. Upon host cell contact YopD and YopB form a pore in the eukaryotic cell membrane and the effector proteins YopE, YopH, YopJ, YopM, YpkA and YopT are secreted through the T3SS directly into to host cell, where they prevent phagocytosis and cytokine release (Cornelis, 2002).

1.3.3 Other virulence factors

One of the first challenges for *Y. pseudotuberculosis* during the infection is the survival in the acidic milieu of the stomach. Therefore, the bacteria express urease and aspartase, which produce ammonia, leading to an increase of the pH (Hu *et al*., 2009, 2010).

Inside the host, bacteria are also facing limited iron availabilities. One main strategy to overcome iron depletion is the expression of siderophores, which are low molecular mass compounds, which efficiently chelate Fe^{2+}/Fe^{3+}-ions. They have a very high affinity to Fe^{2+}/Fe^{3+}-ions and are secreted to the surrounding media. The ferric-ions, bound to the siderophore, are subsequently taken up by special iron-uptake systems. In *Y. pseudotuberculosis* the siderophore yersiniabactin, encoded on the high-pathogenicity island (HPI), functions as iron chelator and is important for virulence (Carniel *et al*., 1992; Heesemann, 1987).

The cytotoxic necrotizing factor CNF_Y, which is only present in some *Y. pseudotuberculosis* strains such as YPIII, targets Rho-GTPases in particular RhoA

(Hoffmann *et al*., 2004; Lockman *et al*., 2002). The toxin enhances the delivery of Yop effector proteins, targets the host-immune response and is crucial for virulence of *Y. pseudotuberculosis* YPIII (Schweer *et al*., 2013).

1.4 Regulation of gene expression in *Y. pseudotuberculosis*

Tight regulation of gene expression is important for rapid adaptation to changing environments. Most pathogenic bacteria frequently change between an internal and an external lifestyle, where temperature, ion and nutrient availabilities differ dramatically. For instance, genes involved in the evasion of host immune responses are not needed under environmental conditions. To adjust the gene expression pattern to these different conditions, bacteria have to recognize whether they are outside or inside a host. Temperature belongs to the most important parameters, which are used by pathogenic bacteria to sense their environment.

The expression of genes on the virulence plasmid pYV for example is controlled by the low calcium response F protein (LcrF), an AraC-type DNA-binding protein that is regulated by temperature on transcriptional and translational level (Fig. 1.4) (Hoe *et al.*, 1992; Rouvroit *et al*., 1992; Skurnik and Toivanen, 1992). *lcrF* is located in an operon with *yscW* on the virulence plasmid (Böhme *et al.*, 2012). YscW is one of the Ysc proteins, which are involved in the assembly of the T3SS and functions as pilot protein of YscS (Burghout *et al.*, 2004). At moderate temperatures the polycistronic *yscW-lcrF* mRNA forms two stem-loops in the intergenic region of *yscW* and *lcrF.* This structure masks the ribosomal binding site (RBS) and prevents translation of *lcrF*. The stem-loop structure melts at 37°C which facilitates translation of *lcrF* and subsequent binding of LcrF to its target genes (Böhme *et al*., 2012). Additionally, *lcrF* expression is regulated by the *Yersinia* modulator A (YmoA). At moderate temperatures YmoA binds to the 5'UTR of the *yscW-lcrF* operon and represses the transcription of *lcrF*. At 37°C YmoA is degraded by Clp and Lon proteases, whereby transcription of *lcrF* can occur (Böhme *et al*., 2012).

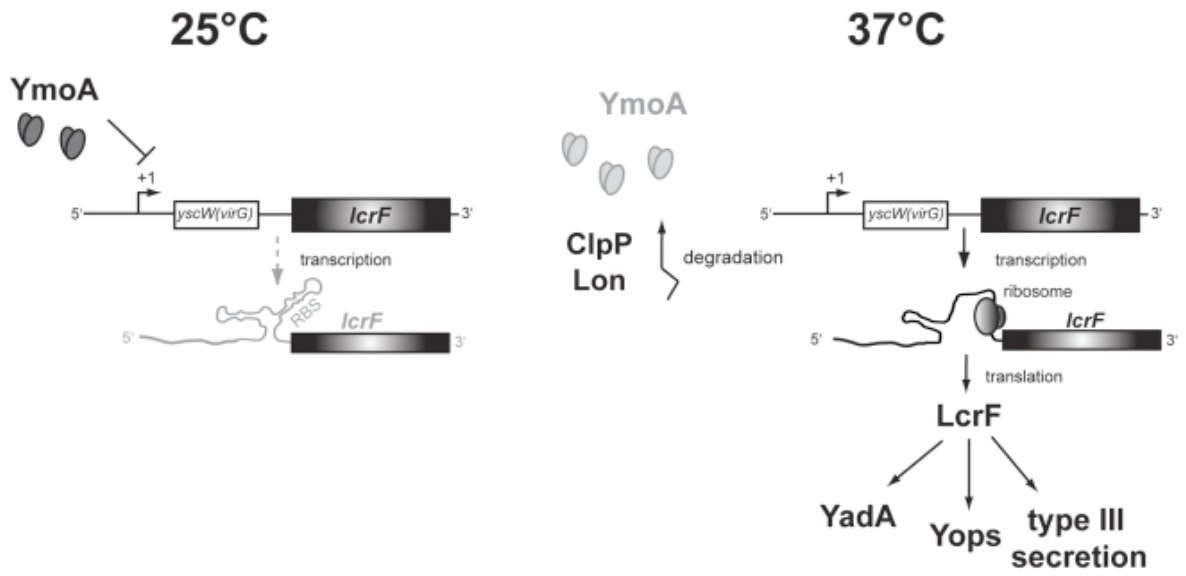

Fig. 1.4 Model of temperature-dependent regulation of *lcrF*.
At 25°C transcription of *yscW-lcrF* is repressed by YmoA. Additionally, stem-loop structures in the intergenic region of the polycistronic *yscW-lcrF* mRNA mask the RBS and prevents translation of *lcrF*. At 37°C YmoA is degraded by proteases. Furthermore, the stem-loop structure melts, translation of *lcrF* can occur and LcrF-dependent genes are expressed (according to Böhme *et al.*, 2012).

Another strategy for bacteria to sense whether they are inside or outside a host are two-component systems. They mostly consist of a membrane-spanning sensor kinase and a response regulator. The sensor kinase recognizes certain extracellular signals such as nutrients or ions and transduces the signal to the response regulator, which is phosphorylated by the sensor kinase. This leads to DNA-binding of the response regulator and thereby to activation or repression of target genes. *Y. pseudotuberculosis* expresses several two-component systems, which are relevant for pathogenesis like PhoP/PhoQ and BarA/UvrY (Grabenstein *et al*., 2004; Heroven *et al*., 2008).

1.4.1 The two-component system PhoP/PhoQ

The PhoP/PhoQ two-component system can be found in many pathogenic bacteria such as *S. enterica* serovar Typhimurium, *Mycobacterium tuberculosis*, *Shigella flexneri*, *Pseudomonas aeruginosa* and *Yersinia* spp. It plays an important role in virulence, for instance in the survival and proliferation inside macrophages (Grabenstein *et al.*, 2004; Macfarlane *et al.*, 2000; Miller *et al*., 1989; Moss *et al.*, 2000; Oyston *et al*., 2000; Pérez *et al.*, 2001). In *S. enterica* serovar Typhimurium it

was shown that a *phoP* deletion leads to an attenuation of virulence in mice (Galán and Curtiss, 1989; Miller *et al*., 1989).

The sensor kinase PhoQ is a membrane spanning protein and recognizes low Mg^{2+}- and Ca^{2+}-concentrations, acidic pH and the presence of antimicrobial peptides and activates the response regulator PhoP by phosphorylation (Fig. 1.5) (García Véscovi *et al*., 1996; Grabenstein *et al*., 2004; Groisman, 2001; Véscovi *et al*., 1997).

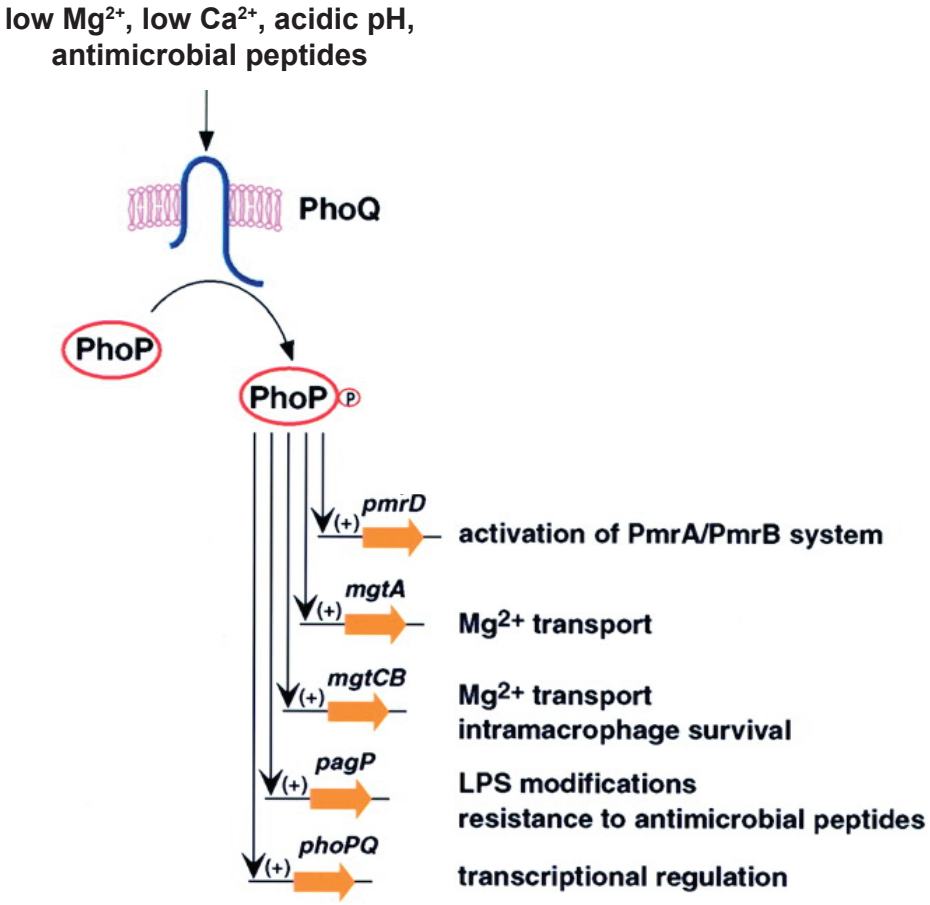

Fig. 1.5 Schematic overview of the PhoP/PhoQ two component system.
The sensor kinase PhoQ senses low Mg^{2+}- and low Ca^{2+}-concentrations as well as low pH and antimicrobial peptides. Thereby it activates the response regulator PhoP by phosphorylation. PhoP acts as transcriptional regulator and controls expression of target genes (modified from Groisman, 2001).

PhoP binds to PhoP box-like DNA sequences which are direct repeats of the sequence motif T/GGTTTAA/T leading to activation or repression of target gene expression (Lejona *et al*., 2003; Minagawa *et al*., 2003). For instance *mgtA* and *mgtCB,* encoding Mg^{2+}-uptake systems, are activated by PhoP in *S. enterica* serovar

Typhimurium (García Véscovi *et al*., 1996; Tao *et al*., 1995). Resistance to antimicrobial peptides is mediated by modifications of lipopolysaccharides (LPS), e.g. by activation of the synthesis of PagP, which incorporates palmitate into lipid A of the LPS (Guo *et al*., 1998). Furthermore, in *S. enterica* serovar Typhimurium PhoP activates the synthesis of PmrD, which leads to *pmrAB* expression. *pmrAB* encodes for another two-component system, PmrA/PmrB, that additionally promotes resistance against antimicrobial peptides (Gunn and Miller, 1996; Roland *et al*., 1993). PhoP also regulates the expression of global virulence regulators such as RovA in *Y. pestis* and SlyA in *S. enterica* serovar Typhimurium. While PhoP activates expression of *slyA* in *S. enterica* serovar Typhimurium, expression of *rovA* in *Y. pestis* is repressed by PhoP (Norte *et al*., 2003; Zhang *et al*., 2011). Expression of the *phoPQ* operon itself occurs from two different promoters, one that is constitutively expressed and another that is positively autoregulated by PhoP/PhoQ (Kato *et al*., 1999; Soncini *et al*., 1995).

1.4.2 The carbon storage regulator system

The carbon storage regulator (Csr) system is composed of the two small regulatory RNAs CsrB and CsrC and the dimeric RNA-binding protein CsrA (Heroven *et al*., 2008; Romeo *et al*., 2013; Vakulskas *et al*., 2015). The Csr-system acts on post-transcriptional level and is widely distributed among eubacteria including *S. enterica* serovar Typhimurium, *Y. pseudotuberculosis, V. cholerae* and *E. coli* (Altier *et al*., 2000; Heroven *et al*., 2008; Lenz *et al*., 2005; Romeo *et al*., 1993; White *et al*., 1996). CsrA is a homodimer, each monomer comprises five β-strands, a small α-helix and a flexible C-terminus (Gutiérrez *et al*., 2005). CsrA binds preferably to GGA-motifs, which are often located in the RBS of target mRNAs. This blocks binding of ribosomes and thereby translation of mRNAs and leads to faster mRNA degradation by RNases (Babitzke *et al*., 2009; Dubey, 2005; Dubey *et al*., 2003). The small regulatory RNAs CsrB and CsrC harbor 18 and 14 GGA-motifs in *Y. pseudotuberculosis,* respectively, and antagonize the function of CsrA by direct sequestration, which leads to de-repression of target mRNA translation (Heroven *et al*., 2008; Liu *et al*., 1997; Romeo, 1998). Vice versa, the small RNAs require CsrA for stabilisation (Böhme, K., PhD thesis; Reimmann *et al*., 2005). Furthermore, the

two small RNAs are counter-regulated. Up-regulation of one RNA leads to down-regulation of the other (Fig. 1.6) (Heroven *et al*., 2012a).

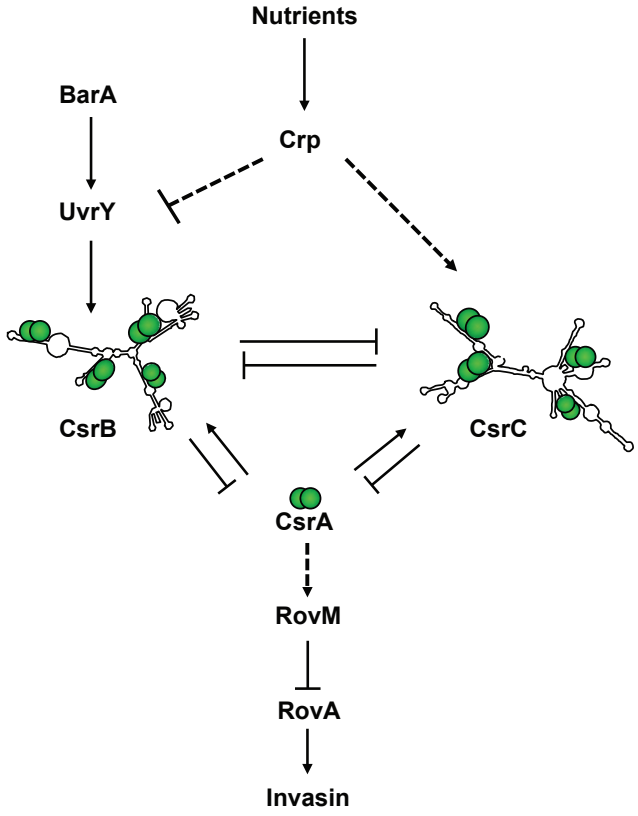

Fig. 1.6 Regulatory network of the carbon storage regulator system.
The Csr-system consists of the two non-coding RNAs CsrB and CsrC and the RNA-binding protein CsrA. CsrB and CsrC are stabilized by CsrA through binding to several GGA-motifs, while the small RNAs sequester CsrA from their target mRNAs and thereby inhibit CsrA activity. The two small RNAs counter-regulate each other, a high amount of one RNA leads to a decrease of the other. CsrB is activated by the two-component system BarA/UvrY in response to so far unknown environmental signals and is negatively influenced by Crp (cAMP receptor protein). Crp also activates the expression of *csrC*. A high amount of the small RNAs CsrB or CsrC leads to sequestration of CsrA, which results in an up-regulation of *rovA* and thereby in a higher amount of invasin (dashed lines – indirect control, solid lines – direct control).

The two-component system BarA/UvrY and its homologues are found in many Gram-negative bacteria. They belong to the control circuit of the Csr-system with BarA as sensor kinase and UvrY as cognate response regulator (Pernestig *et al*., 2003; Suzuki *et al*., 2002). The inducing signal for BarA is mostly unknown, however in *E. coli* it was shown that formate, acetate, intermediates of the tricarboxylic acid cycle and short-chain fatty acids activate BarA (Chavez *et al*., 2010). In contrast to *E. coli* and *Salmonella enterica* serovar Typhimurium leads the activation of the two-

component system BarA/UvrY to an induced expression of CsrB but not CsrC in *Y. pseudotuberculosis* (Heroven *et al.*, 2008).

The dimeric protein Crp is implicated in the overall control of the Csr-system in *Y. pseudotuberculosis* by regulating the small RNAs CsrB and CsrC (Heroven *et al*., 2012a). Crp is, together with cAMP, involved in the catabolite repression and regulates genes of the carbohydrate metabolism. Alternative sugars such as lactose are only catabolized in the absence of glucose, due to the repression of cAMP synthesis by glucose (Crasnier, 1996; Ishizuka *et al*., 1994; Zheng *et al*., 2004). It was shown that in *Y. pseudotuberculosis* Crp represses *csrB* expression indirectly through UvrY, while *csrC* expression is activated by Crp (Heroven *et al*., 2012a).

The Csr-system controls expression of genes involved in metabolism - stationary phase genes are often down-regulated by CsrA while genes of the exponential phase are up-regulated (Romeo, 1998). Furthermore, the Csr-system is important for virulence gene expression in *Y. pseudotuberculosis.* CsrA represses expression of the primary colonization factor invasin indirectly via the LysR-type regulator RovM and the MarR-type regulator RovA (Heroven *et al*., 2008, 2012a; Nagel *et al*., 2001).

1.4.3 MarR-type regulators

The family of multiple antibiotic resistance regulator (MarR) of transcriptional regulators was named after the first identified MarR protein in *E. coli,* due to a multiple antibiotic resistance phenotype (Cohen *et al*., 1993a; George and Levy, 1983). Members of this family are widespread and can be found in bacterial and archaeal genomes. MarR-type regulators are involved in the control of metabolism, virulence gene expression, stress responses and resistance against antibiotics (Ariza *et al*., 1994; Pérez-Rueda and Collado-Vides, 2001; Sulavik *et al*., 1995). In the plant pathogen *Erwinia chrysanthemi,* virulence gene expression is regulated by PecS, which controls the expression of pectate lyase, cellulase as well as indigoidine (Reverchon *et al.*, 1994, 2002). In *Vibrio cholera* AphA is important for the activation of the toxin-coregulated pilus, which is necessary for the intestinal colonization of the host (Kovacikova *et al*., 2004; Skorupski and Taylor, 1999; Taylor *et al*., 1987). MgrA of *Staphylococcus aureus* was found to regulate the expression of the type 8 capsular polysaccharide, protein A, nuclease, alpha-toxin and coagulase (Luong *et*

al., 2003). Further members of the MarR-family involved in regulation of virulence gene expression are SlyA of *S. enterica* serovar Typhimurium and RovA of *Y. pseudotuberculosis* (Libby *et al.*, 1994; Nagel *et al.*, 2001).

The first crystal structure of a MarR-type regulator revealed that this regulator family consist of six α-helices and three β-sheets and bind as homodimer to the DNA via a winged helix-turn-helix motif (Alekshun *et al.*, 2001). It was described for many MarR-homologues that DNA-binding is influenced by recognition of small anionic lipophilic molecules such as salicylate and related compounds (Wilkinson and Grove, 2006). In most cases, recognition of the small ligands attenuates binding to DNA through an overlap of DNA- and ligand-binding sites, e.g. for PecS of *Erwinia* and HucR of *Deinococcus radiodurans* which binds urate (Perera and Grove, 2010; Perera *et al.*, 2009; Wilkinson and Grove, 2004).

Many of the MarR-type regulators act as repressor and activator of target genes as described for PecS of *E. chrysanthemi* and RovA of *Y. pseudotuberculosis* (Heroven *et al.*, 2004; Nagel *et al*., 2001; Nasser *et al*., 1999; Praillet *et al*., 1996; Reverchon *et al*., 1994).

1.4.3.1 RovA of *Y. pseudotuberculosis*

All three pathogenic *Yersinia* species encode the transcriptional regulator RovA. The first discovery of RovA was in *Y. enterocolitica* in 2000 as a regulator of the early-stage virulence factor invasin, which is important for the primary colonization of the host (Revell and Miller, 2000). RovA was identified to also control *invA* expression in *Y. pseudotuberculosis* (Nagel *et al.*, 2001). It activates *invA* expression at moderate temperatures by interaction with two distinct binding sites 50 – 207 bp upstream of the transcriptional start site (Heroven *et al*., 2004; Nagel *et al*., 2001). In *Y. pestis,* RovA was found to regulate *psaA* expression, which encodes the pH 6 antigen, which is important for the development of bubonic plague (Cathelyn *et al.*, 2006; Lindler *et al.*, 1990). A *rovA* knock-out mutant of all of the pathogenic *Yersinia* species has a significantly higher LD_{50} value than the respective wild-type strain (Cathelyn *et al*., 2006; Heroven and Dersch, 2006; Revell and Miller, 2002). In contrast, the LD_{50} of an *inv* knock-out mutant is comparable to that of the wild-type strain indicating that RovA controls more virulence factors apart from invasin and has

a higher impact on the virulence of *Yersinia* (Pepe and Miller, 1993; Revell and Miller, 2002).

RovA consists of six α-helices and two β-sheets, and binds as homodimer via a winked helix-turn-helix motif to the DNA, similar to other MarR-type regulators (Alekshun *et al*., 2001; Quade *et al*., 2012). The activation of target genes occurs by direct interaction with the RNA-polymerase (RNAP) (Tran *et al*., 2005). The N-terminus of RovA was identified to be important for DNA-binding while the C-terminus is involved in dimerization (Fig. 1.7) (Quade *et al*., 2012; Tran *et al*., 2005).

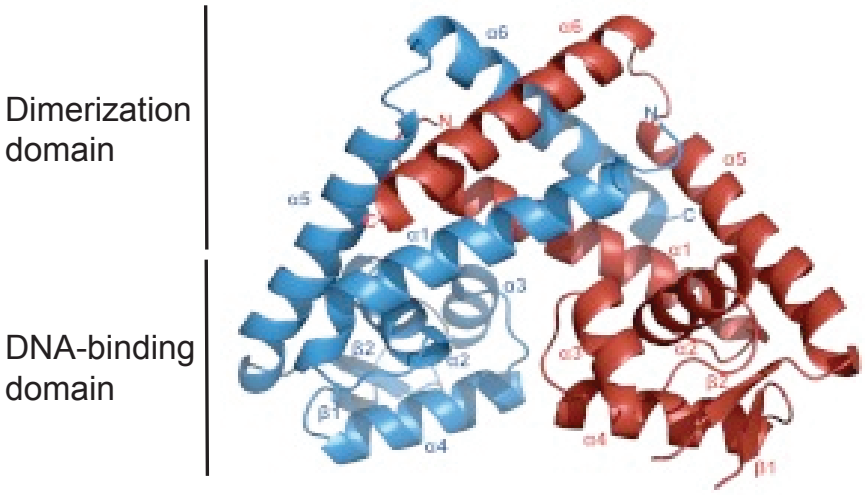

Fig. 1.7 Structure of RovA.
RovA forms a homodimer, each monomer consists of six α-helices and two β-sheets. The monomers are highlighted in blue and red (modified from Quade *et al*., 2012).

The expression of *rovA* itself is auto-regulated. This has been also described for several other MarR-type regulators such as SlyA of *S. typhimurium* (Heroven *et al*., 2004; Nagel *et al*., 2001; Stapleton *et al*., 2002). Expression occurs from two different promoters P1 and P2, which are located 76 and 343 nucleotides upstream of the transcriptional start site, respectively (Heroven *et al*., 2004). Binding of RovA upstream of promoter P2 results in activation of *rovA* expression, while binding downstream of promoter P1 leads to repression of *rovA* expression (Heroven *et al*., 2004; Nagel *et al*., 2001). Furthermore, competitive electrophoretic mobility shift assays revealed a higher affinity of RovA to the upstream region of promoter P2. This

suggests that RovA binds the low affinity site downstream of promoter P1 only when a certain threshold of RovA molecules is reached in the cell (Heroven *et al*., 2004).

In addition to the positive and negative autoregulation, *rovA* expression is repressed by the nucleoid-associated protein H-NS (Heroven *et al*., 2004). The binding site of H-NS overlaps with the RovA binding site upstream of promoter P2 with a higher affinity to RovA than to H-NS. This indicates that H-NS represses *rovA* expression only in the absence of RovA and that RovA acts as anti-repressor (Heroven *et al*., 2004; Tran *et al*., 2005).

Moreover, *rovA* expression is dependent on the nutrient availability, which is mediated via the transcriptional regulator RovM. RovM belongs to the family of LysR-type proteins and represses *rovA* expression by binding upstream of promoter P1. This effect is predominant when *Y. pseudotuberculosis* is grown in minimal media, due to a higher amount of RovM in the cell (Heroven and Dersch, 2006; Nagel *et al*., 2001). RovM is indirectly activated by CsrA, which links the RovM-RovA-InvA cascade with the Csr-system (Heroven *et al*., 2008).

Additionally, RovA synthesis is dependent on temperature. At moderate temperatures (20-28°C) *rovA* expression is activated, whereas expression is repressed at 37°C (Herbst *et al*., 2009; Nagel *et al*., 2001). RovA is a thermosensor; during a temperature shift, it undergoes a reversible conformational change, which alters the DNA-binding capacity. At 37°C the DNA binding affinity of RovA is reduced and amino acids, which are recognized by proteases are no longer protected through DNA-binding (Herbst *et al*., 2009). This renders RovA more susceptible to degradation by Lon and ClpP proteases at 37°C. Moreover, the expression of *lon* is increased at 37°C, which has an additional effect on the degradation of RovA (Herbst *et al*., 2009). Comparative studies of RovA and its homolog SlyA of *S. enterica* serovar Typhimurium revealed that a flexible loop between α-helix five and six is responsible for thermosensing activity of RovA (Quade *et al*., 2012). SlyA shares an amino acid sequence identity to RovA of 79%, but is stable at 37°C and does not act as a thermometer (Dolan *et al*., 2011; Quade *et al*., 2012). In this specific loop, RovA harbors a glycine at position 116, while SlyA harbors an alanine. An exchange of G116A in RovA results in the loss of the thermo-sensing activity and a higher DNA-binding affinity at 37°C (Fig. 1.8) (Quade *et al*., 2012).

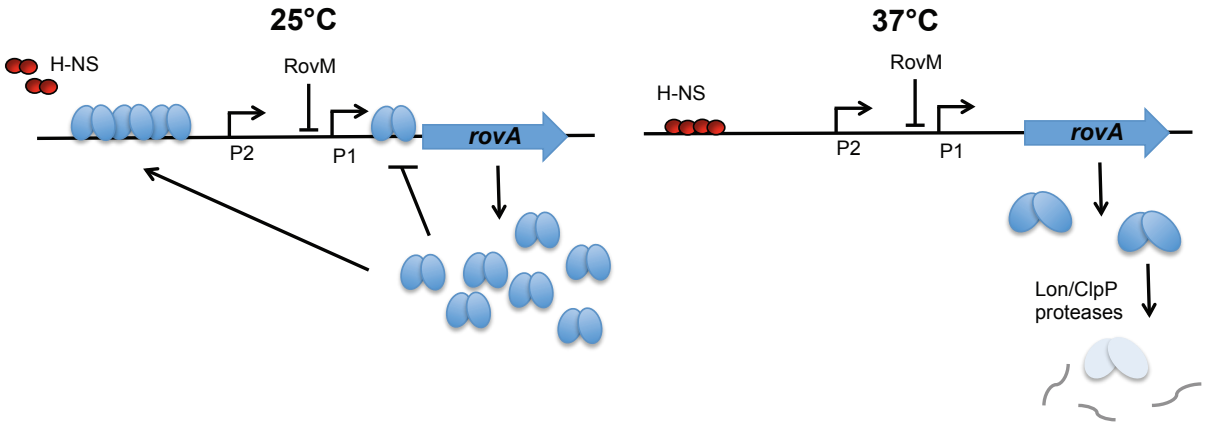

Fig. 1.8 Regulation of RovA.
At 25°C RovA binds to a high-affinity site upstream of promoter P2 and activates its own expression. After the RovA amounts reach a certain threshold in the cell, RovA also binds to a low affinity site downstream of promoter P1 and inhibits its own expression. Additionally, RovM represses *rovA* expression when nutrient availability is low by binding upstream of promoter P1. At 37°C RovA undergoes a conformational change, which results in a loss of the DNA-binding capacity and increased degradation by proteases. Moreover, *rovA* is repressed by H-NS (modified from Herbst *et al.*, 2009).

Expression analysis and stability assays of RovA at different temperatures and growth phases revealed that RovA is stabilized during stationary phase and activates its own expression even at 37°C (Herbst *et al.*, 2009; Nagel *et al.*, 2001). The supernatant of stationary phase cells harbors a factor that stabilizes RovA (Herbst, K., PhD thesis; Mendonca, C., PhD thesis). Binding of small ligands to MarR-type regulators is well known (Perera and Grove, 2010; Wilkinson and Grove, 2004). Indeed, it could be shown that RovA binds several diverse ligands (Mendonca, C., PhD thesis). However, it remains unclear whether these ligands are the natural substrates of RovA.

Taken together, *rovA* is maximally expressed at moderate temperatures, when grown in complex media. It is strongly auto-regulated and harbors an intrinsic thermosensor, which allows fast recognition of temperature changes and rapid adaption of target gene expression.

1.5 Phenotypic heterogeneity

For a long time it was assumed that the expression of a certain gene is unimodal under defined conditions. The steadily improving technologies for the analysis of single cells, like flow cytometry and fluorescence microscopy, now allow an

investigation of individual cells in a comparative approach. It became evident that genetically identical cells - grown under the same conditions - can develop and behave differently, which give rise to phenotypic heterogeneity of a population. The main source of phenotypic heterogeneity are stochastic fluctuations in gene expression, but also epigenetic modifications such as DNA methylation can lead to phenotypic heterogeneity (Casadesús and Low, 2006, 2013; Elowitz *et al*., 2002). Another origin of phenotypic heterogeneity might be cell ageing, e.g. in *Methylobacterium extorquens* cell size and timing of cell division depend on the pole age of a cell. Thereby, the cellular age contributes to phenotypic variability (Bergmiller and Ackermann, 2011).

Phenotypic heterogeneity is a form of bet-hedging and beneficial in fast changing environments, in which the regulation of gene expression is too slow to ensure rapid adaptation to new conditions. One part of the population is pre-adapted to new conditions, which increases the fitness of the whole population (Ackermann, 2015; Veening *et al*., 2008a). The formation of persister cells is a well-described example of bet-hedging and phenotypic heterogeneity. Persister cells are very slow growing or non-growing cells, which are tolerant to antibiotics. After removing the antibiotic, persisters are able to regrow and form a new population consisting of antibiotic-sensitive cells and persister cells (Lewis, 2007). In *E. coli* the toxin HipA is involved in the formation of persister cells (Moyed and Bertrand, 1983). If HipA exceeds a certain threshold, the cell become dormant and thereby resistant to antibiotics (Rotem *et al*., 2010).

The division of labor between individual cells is another advantage of phenotypic heterogeneity (Ackermann, 2015). For instance, under nutrient-limiting conditions some *B. subtilis* cells synthesize and secrete the exoproteases bacillopeptidase and subtilisin E and thereby supply the enzyme to the whole population (Veening *et al*., 2008b). This is also an example for social behavior of bacteria as one subpopulation takes over the costs for the production of exoenzymes, whereas the entire population benefits from these exoenzymes (Veening *et al*., 2008a). Social interactions between cells of one population are common for phenotypic heterogeneity. For example, in cyanobacteria nitrogen fixation and photosynthetic carbon fixation are separated into different cells types, but each cell type provides carbon or nitrogen to the other cell type, respectively (Reuven and Eldar, 2011). An extreme form of division of labor is

self-destructive cooperation as it is described for the heterogeneous expression of genes encoding for the T3SS-1 of *S. enterica* serovar Typhimurium (Ackermann *et al*., 2008). Cells, that express the *t3ss-1* are impaired in growth and mainly killed by the host-immune system during invasion of the epithelium, while the other part of the population is fast growing and benefits from the inflammation by outcompeting the commensals in the gut (Ackermann *et al*., 2008; Diard *et al.*, 2013; Sturm *et al*., 2011). Moreover, the bistable expression of the *t3ss-1* is also an example for bet-hedging as the slow-growing T3SS-1-positive subpopulation is more tolerant to antibiotics and thereby promotes survival during exposure to antibiotics (Arnoldini *et al.*, 2014)

The heterogeneous expression of the T3SS-1 in *S. enterica* serovar Typhimurium gives evidence that phenotypic heterogeneity also contributes to virulence of bacteria. Several other examples of heterogeneous expression of virulence factors are described, e.g. expression of flagella genes in *S. enterica* serovar Typhimurium (Casadesús and Low, 2013; Zieg *et al.*, 1977). Two different flagella genes are located in the genome of *S. enterica* serovar Typhimurium and due to the reversible inversion of a DNA fragment one or the other type of flagella is expressed. The regulated expression of two different flagella genes is believed to avoid recognition by the host immune system (Rossez *et al*., 2015; Zieg *et al*., 1977).

1.5.1 Bistability

A special kind of heterogeneity is bistability, which is characterized by the bifurcation of one bacterial population into two or more distinct subpopulations without any mutations or DNA-rarrangements (Dubnau and Losick, 2006; Graumann, 2006). Requirements for bistable expression of a gene are positive or double negative feedback loops together with a non-linear response in the regulatory network of a transcriptional regulator (Casadesús and Low, 2013; Ferrell, 2002; Smits *et al*., 2006). In biological systems gene expression is subjected to random fluctuations – noise. Noise, amplified by a positive or double negative feedback loop can lead to expression of a certain gene in some cells, whereas other cells do not reach the threshold and gene expression is “OFF” (Elowitz *et al*., 2002; Ozbudak *et al*., 2002).

In *Bacillus subtilis* for example bistable expression is well described for the development of competence under limiting nutrient conditions, which arises in 10% - 20% of all cells in stationary phase (Cahn and Fox, 1968; Graumann, 2006; Hadden and Nester, 1968). Responsible for the bistability is the positive feedback loop of the transcriptional activator ComK, which leads to expression of competence genes such as the DNA-uptake apparatus (Gamba *et al*., 2015; Maamar and Dubnau, 2005; van Sinderen *et al*., 1995).

Besides competence, genes related to swimming and chaining are also heterogeneously expressed in *B. subtilis*. In an exponentially growing culture some cells are motile, while others do not separate after cell division and develop long chains (Dubnau and Losick, 2006; Kearns and Losick, 2005). The alternative sigma factor σ^D regulates motility as it is active in motile cells and inactive in sessile cells. The alternative sigma factor is responsible for the bifurcation of the culture in the two subpopulations (Cozy *et al*., 2012; Kearns and Losick, 2005).

However, bistability is not a phenomenon restricted to bacteria, it is also described for eukaryotes and viruses. Bacteriophage λ reveals bistability during infection of *E. coli.* The virus can undergo the lytic pathway and thereby release phage particles or integrate DNA into the host genome by using the lysogenic pathway (Casjens and Hendrix, 2015). The decision which part of λ-infected cells will be lysed depends on the number of co-infecting phages and the two transcriptional regulators Cro and CI (Joh and Weitz, 2011; Smits *et al*., 2006). Bistability was also reported during maturation of *Xenopus laevis* oocytes. The inducing signal for maturation is the steroid hormone progesterone, which activates the Mos-MEK-MAP kinase cascade. A positive feedback loop within this cascade is responsible for the bistable maturation phenotype (Ferrell, 1999, 2002).

The transcriptional regulator RovA of *Y. pseudotuberculosis* is a perfect candidate for bistable expression as it is positively and negatively auto-regulated. Additionally, a non-linear response is formed through cooperative binding of RovA to its own promoter region and enhanced proteolytic degradation at higher temperatures. Indeed, first experimental investigations revealed a temperature-dependent bistable expression of *rovA* (Herbst, K., PhD thesis; Nuss A. M., unpublished data). At moderate temperature (25°C) the entire population expresses *rovA*, while at higher temperature (37°C) no *rovA* expression was observed. However, at intermediate

temperature (32°C) two subpopulations with either high or low *rovA* expression were described and revealed bistability (Herbst, K., PhD thesis; Nuss A. M., unpublished data).

1.6 Aim of this study

The overall goal of this study is to investigate the molecular mechanisms underlying bistable expression of *rovA* of *Y. pseudotuberculosis* and the identification of its function during infection.

RovA is a transcriptional regulator of early-stage virulence factors such as invasin, which is important for the primary colonization of the host (Nagel *et al.*, 2001). Preliminary data revealed a temperature-dependent bistable expression of the transcriptional regulator RovA of *Y. pseudotuberculosis* (Herbst, K., PhD thesis, Nuss, A. M., unpublished data). One aim of this thesis is to analyze the dynamics of bistable *rovA* expression. To address this aim, time-lapse microscopy, following the fate of one cell, will be established. In order to gain deeper information about the molecular mechanisms involved in the establishment of bistable *rovA* expression, the impact of elements implicated in thermosensing and proteolysis of RovA should be analyzed. For this purpose, mutants altering in RovA stability and thermosensing will be constructed and tested for bistable *rovA* expression. Moreover, possible strain-specific differences in the bistable expression of *rovA* will be considered. Therefore, *rovA* expression will be analyzed in the two different clinical isolates YPIII and IP32953.

As the role of heterogeneity of RovA on virulence of *Y. pseudotuberculosis* is unknown, the impact of bistable *rovA* expression during the infectious process should be investigated. First, the expression of *rovA* within organs as well as their spatial distribution will be explored. Next, the impact of bistable *rovA* expression on virulence of *Y. pseudotuberculosis* will be analyzed. Therefore, a Δ*rovA* mutant as well as mutants expressing stabilized RovA variants will be compared to the wild type with respect to organ colonization and survival of mice.

2 Materials and methods

2.1 Materials

2.1.1 Equipment and material

The material and equipment used in this study were obtained from BD Biosciences, Biochrom, Biometra, Bio-Rad, Brand, Consort, Eppendorf, GE Healthcare, Gilson, Greiner, Heraeus, Heidolph, Hirschmann EM, Ibidi, Integra Biosciences, Janke & Kunkel IKA-Labortechnik, Laboport, Marienfeld, Millipore, Microflex Corporation, PeqLab, Roth, Sarstedt, Sartorius, Schott, Sigma Aldrich, Sorvall, TPP, Thermo Scientific, Oregon Scientific, VWR International, Whatman Schleicher & Schüll GmbH and Zeiss if not stated otherwise.

2.1.2 Chemicals and buffers

Chemicals were purchased from Applichem, BD Biosciences, Biochrom, Biolegend, BioMoll, BioXCell, Difco, eBioscience, Fermentas, Fischer Scientific, Fluka, GIBCO, Invitrogen, Jackson ImmunoResearch, J.T. Baker, Life Technologies, Merck, Metabion, New England Biolabs Inc. (NEB), PAA, Pierce, Perkin Elmer, PeqLab, Promega, PromoCell, Qiagen, Roche, Roth, Sigma Aldrich, Serva, T.H. Geyer and Zeiss if not stated otherwise. The composition of buffers and solutions is listed in Table 2.1.

Table 2.1 Composition of buffers and solutions.

Buffer/solution	Composition
Binding buffer	20 mM NaH_2PO_4, 100 mM KCl, 5% glycerol, 2 mM 1,4-dithiothreitol, pH 8.0
Coomassie staining solution	20% isopropanol, 10% acetic acid, 0.05% Coomassie™ Brilliant Blue G250
Lysis buffer for proteins	50 mM NaH_2PO_4, 300 mM NaCl, 10 mM imidazol, pH 8.0
Lysis buffer for RNA	0.01 M NaOAc pH 4.5, 2% SDS
20x MOPS buffer	200 mM MOPS, 50 mM sodium acetate, 10 mM EDTA

Buffer/solution	Composition
PBS	8 g/l NaCl, 0.2 g/l KCl, 1.44 g/l Na_2HPO_4, 0.24 g/l $KH_2PO_3^-$, pH 7.4
Elution buffer	50 mM NaH_2PO_4, 300 mM NaCl, 250 mM imidazol, pH 8.0
RNA-resuspension buffer	0.3 M sucrose, 0.01 M NaOAc pH 4.5
SDS running buffer	33 mM Tris-HCl pH 8.3, 192 mM glycine, 0,1% SDS
SDS sample buffer	0.1 M Tris pH 6.8, 40% glycerol, 10% β-mercaptoethanol, 3.2% SDS, 0.2% bromophenol blue
Seperating gel buffer	500 mM Tris-HCl, 4% SDS, pH 6.8
20x SSC buffer	3 M NaCl, 0.3 M sodium citrate, pH 7.0
Stacking gel buffer	1.5 M Tris-HCl, 4% SDS, pH 8.8
50x TAE (Tris-acetate-EDTA) buffer	2 M Tris-HCl pH 8.3, 1 M acetic acid, 0.1 M EDTA
10x TBE (Tris-borate-EDTA) buffer	900 mM Tris-HCl, 900 mM boric acid, 25 mM EDTA pH 8.0
TBST buffer	20 mM Tris-HCl pH 7.5, 150 mM NaCl, 0.05% Tween-20
TFBI-buffer	30 mM KAc, 10 mM $CaCl_2$, 50 mM $MnCl_2$, 100 mM RbCl, 15% glycerol, pH 5.8
TFBII-buffer	10 mM PIPES, 75 mM $CaCl_2$, 10 mM RbCl, 15% glycerol, pH 6.5
Transblot buffer	25 mM Tris, 192 mM glycine, 20% methanol
Transformation buffer	272 mM sucrose, 15% glycerol
Washing buffer	50 mM NaH_2PO_4, 300 mM NaCl, 20 mM imidazol, pH 8.0
Z-buffer	100 mM sodium phosphate buffer pH 7.0, 1 mM $MgSO_4$

2.1.3 Media

The media used in this study were prepared with distilled water and are listed in Table 2.2.

Table 2.2 Media.

Media	Composition
BHI broth (brain-heart infusion)	37 g/l BHI
LB broth (Sambrock *et al*., 1989)	5 g/l yeast extract, 5 g/l NaCl, 10 g/l tryptone
LB solid medium	LB-medium, 18 g/l agar
SOC medium (super optimal broth)	5 g/l yeast extract, 0.5 g/l NaCl, 20 g/l tryptone, 2.5 ml/l 1 M KCl, 10 ml/l 1 M $MgCl_2$, 10 m/l 1 M $MgSO_4$
Yersinia solid medium	*Yersinia* selective agar base and *Yersinia* selective supplement (Oxoid)

2.1.4 Enzymes, antibodies and kits

Enzymes applied with provided buffers and antibodies used in this study are listed in Table 2.3. The primary antibodies anti-RovA and anti-HNS are polyclonal antibodies produced in rabbits, the primary antibody anti-InvA is monoclonal and produced in mice.

Table 2.3 Enzymes and antibodies.

Enzymes/ Antibody (dilution)	Manufacturer
Enzyme	
Antarctic phosphatase	NEB
DNase I	Roche
Mango*Taq*™ DNA polymerase	Bioline
PfuUltra II Fusion HS DNA polymerase	Agilent
Phusion® High-Fidelity DNA polymerase	NEB
Restriction enzymes	NEB
T4 DNA ligase	NEB
Taq DNA polymerase	NEB
Antibody (dilution and buffer)	
Anti-HNS (1:1000 000 in TBST + 3% BSA)	Davids Biotechnology

Enzymes/ Antibody (dilution)	Manufacturer
Anti-InvA 3A2 (1:4000 in TBST + 5% skim milk powder)	Dersch and Isberg, 1999
Anti-RovA (1:4000 in TBST + 3% BSA)	Davids Biotechnology
Anti-RovM (1:4000 in TBST + 3% BSA)	Davids Biotechnology
Anti-rabbit-HRP (1:7000 in TBST + 3% BSA)	NEB
Anti-mouse-HRP (1:7000 in TBST + 5% skim milk powder)	NEB

Commercial kits used in this study are listed in Table 2.4.

Table 2.4 Kits.

Kit	Application	Manufacturer
Coomassie Reagent Protein Assay Kit	Determination of protein concentration	Pierce
DIG Luminescent Detection Kit	Detection of DIG-labeled probes	Roche
QIAprep® Spin Miniprep Kit	Preparation of plasmid DNA	Qiagen
QIAquick® Gel Extraction Kit	Extraction of DNA from agarose gels	Qiagen
QIAquick® PCR Purfication Kit	Purification of PCR products	Qiagen
SV total RNA Purification Kit	Purification of RNA	Promega
Western Lightning ECL II Kit	Detection of secondary antibodies (HRP) for Western blotting	Perkin Elmer

2.1.5 Oligonucleotides

Oligonucleotides used in this study were purchased from Metabion in a concentration of 100 µM. For PCR reactions the primer concentration was diluted to 10 µM (Table 2.5).

Table 2.5 Primer.

Name	Sequence 5' - 3'	Description
135	GCGGCGGTCGACCAACGTAGTCGGTGCCATCGG	sequencing primer for chromosomal integration of *rovA*
151	GCGGCGTCTAGATATATTATCTACATCCATCTGGC	sequencing primer for chromosomal integration of *rovA*
555	CGGCGCGGATCCCTCTCACACCAGCTGTG	sense primer of *csrB* for Northern blotting
556	GGGGGCGTCGACGGCAAACTCAATATCCTG	anti-sense primer of *csrB* for Northern blotting
582	GCGGCGGTCGACCCTTCATCCCGTGGTAGG	sense primer of *csrC* for Northern blotting
583	GGGCGCGGATCCGATTGGGCCGGAATCTAGC	anti-sense primer of *csrC* for Northern blotting
I79	GTCGTCTCCGTTAGAGATTAC	sense primer of *csrC* for footprint
I293	GCTCCGTTTATAGCGTCCTTG	DIG-labeled sense primer of *csrC* for footprint
II379	AACGGAACAGTCTTCA**TCG**ATAATCGAACAGGT	sense primer for RovA Quick-Change of P98S, creates codon CCG → TCG
II380	ACCTGTTCGATTAT**CGA**TGAAGACTGTTCCGTT	anti-sense primer for RovA Quick-Change of P98S, creates codon CCG → TCG
II480	GCGGGTCGACTCCCTATCAGTGATAGAGATTGACATCCCTATCAGTGATAGAGATACTGAGCACAAAGGAGGAGCAATTGGAATCG	sense primer for P_{tet}-*rovA*, creates *Sal*I site
II483	GCGCGCGGCCGCTTATTACTTAGTTTGTAATTG	anti- sense primer of *rovA* coding region, creates *Not*I site
II525	GCGCGCGCGGCCGCTTAAGCTACTAAAGCGTAGTTTTCGTCG	anti-sense primer for $egfp_{LVA}$, creates *Not*I site
II624	GCAAAGAAATACTT**GCG**GGGATTTCATCGG	sense primer for RovA Quick-Change of G116A creates codons GGG →GCG
II625	CCGATGAAATCCC**CGC**AAGTATTTCTTTGC	anti-sense primer for RovA Quick-Change of G116A creates codons GGG →GCG
II626	GATGAAATTGCAGTGTTA**ATAAAG**CTAATCGATAAGC	sense primer for RovA Quick-Change of SG127128IK creates codons TCAGGC →ATAAAG

Name	Sequence 5' - 3'	Description
II627	GCTTATCGATTAG**CTTTAT**TAA CACTGCAATTTCATC	anti-sense primer for RovA Quick-Change of SG127/128IK creates codons TCAGGC →ATAAAG
III186	TGTAGTCGGGGACGTTATCG	sense primer of *gyrA* for EMSA
III187	CCCATCCACCAGCATATAGC	anti-sense primer of *gyrA* for EMSA
III784	GCGGCGGCATGCGCAAGGCG TTCAGGGAGC	anti-sense primer for *rovA* amplification, creates *Sph*I site
III947	GCGGTCGACGGCGTGCTAAC GACAATGAC	sense primer for *rovA* amplification, creates *Sal*I site
IV483	GCGGGTCGACAAAGGAGGAG CAATTGGAATCG	sense primer for *rovA*-*egfp*$_{LVA}$ translational fusion, creates *Sal*I site
IV490	GCGGGACGTCGCTAACACAGC G GTGGCCTCAAG	sense primer for amplification of *rho* promoter, creates *Aat*II site
IV491	GCGGGTCGACGGGTATGTCTT GAACTATGGTCGTG	anti-sense primer for amplification of *rho* promoter, creates *Sal*I site
IV937	GATAGTTATAGTTTCTGATGGT C	sense primer of *csrC* for EMSAs
IV938	GGGCTATTATGCACAGCTCTC	sense primer of *csrC* for EMSAs
IV939	ATCCATTACGTTCCTTGTATAT C	anti-sense primer of *csrC* for EMSAs
IV940	GAGAGCTGTGCATAATAGCCC	anti-sense primer of *csrC* for EMSAs
V519	GGGCGCGAGCTCCAGGAGTC CAAGCGAGCTC	sense primer of chloramphenicol cassette, creates *Sac*I site
V520	GGGCGCGACGTCGATCACTAC CGGGCG	anti-sense primer of chloramphenicol cassette, creates *Aat*II site
V521	GGGCGCCCTAGGCGAATTGAG GGGTACTGG	sense primer of ori p15a, creates *Avr*II site
V522	GGGCGCGAGCTCCCTCGCTCA CTGACTCGC	anti-sense primer of ori p15a, creates *Sac*I site
V586	GTCGTCTCCGTTAGAGATTAC	DIG-labeled anti-sense primer of *csrC* for footprint
V587	GCTCCGTTTATAGCGTCCTTG	sense primer of *csrC* for footprint
V842	GCGGGTCGACAAAATAAGGAGG AAAAAAAATGGTT	sense primer of *mCherry*, creates *Sal*I site
V843	GCGGGCGGCCGCTTATTATTA TTTGTACAGCTCATCCAT	anti-sense primer of *mCherry*, creates *Not*I site

The corresponding restriction sites are underlined, introduction of base pair substitutions for mutagenesis are shown in bold letters.

2.1.6 Strains and Plasmids

Plasmids used in this study are listed in Table 2.6, *E. coli* and *Y. pseudotuberculosis* strains are listed in Table 2.7.

Table 2.6 Plasmids.

Plasmids	Description	Source and reference
pAKH3	*sacB*$^{+}$, Amp^{R}	Nagel *et al*., 2001
pAKH101	pHT124, *csrB-lacZ*(4)[a], Amp^{R}	Heroven *et al*., 2008
pAKH103	pHT124, *csrC-lacZ*(4)[a], Amp^{R}	Nuss and Schuster *et al*., 2014
pAKH120	*tet-crsB*, ori p15a, Cm^{R}	Heroven AK.
pAKH139	pFU67, *crp-lacZ*(1)[b], Amp^{R}	Nuss and Schuster *et al*., 2014
pAKH188	pFS31, *csrC*$_{\text{YPIII+20nt IP32953}}$, Amp^{R}	Nuss and Schuster *et al*., 2014
pCM33	*rovA-lacZ*(1)[b], ori pSC101*, Kan^{R}	Mendonca, C.
pDM4	R6K derivative, *sacB*$^{+}$, Cm^{R}	Böhme *et al*., 2012
pET28a	T7 promoter based expression vector, Kan^{R}	Novagen
pFS1	pDM4, *rovA*$^{+}_{\text{YPIII}}$, Cm^{R}	This study
pFS5	pKH70, P$_{rho}$-*egfp*$_{\text{LVA}}$, Amp^{R}	This study
pFS6	pJet1.2, *rovA*$^{+}_{\text{YPIII}}$, Amp^{R}	This study
pFS7	pFS6, *rovA*$_{\text{P98S}}$, Amp^{R}	This study
pFS8	pDM4, *rovA*$_{\text{P98S}}$, Cm^{R}	This study
pFS13	pET28a, *phoP*$^{+}$, Kan^{R}	Nuss and Schuster *et al*., 2014
pFS14	pFS6, *rovA*$_{\text{G116A}}$, Amp^{R}	This study
pFS15	pFS6, *rovA*$_{\text{SG127/128IK}}$, Amp^{R}	This study
pFS16	pDM4 *rovA*$_{\text{G116A}}$, Cm^{R}	This study
pFS17	pDM4, *rovA*$_{\text{SG127/128IK}}$, Cm^{R}	This study
pFS21	pFS7, *rovA*$_{\text{P98S, SG127/128IK}}$, Amp^{R}	This study
pFS22	pFS14, *rovA*$_{\text{G116A, SG127/128IK}}$, Amp^{R}	This study
pFS23	pFS7, *rovA*$_{\text{P98S, G116A}}$, Amp^{R}	This study
pFS24	pFS23, *rovA*$_{\text{P98S, G116A, SG127/128IK}}$, Amp^{R}	This study

Plasmids	Description	Source and reference
pFS25	pDM4, *rovA*$_{P98S, SG127/128IK}$, Cm^R	This study
pFS26	pDM4, *rovA*$_{G116A, SG127/128IK}$, Cm^R	This study
pFS27	pDM4, *rovA*$_{P98S, G116A}$, Cm^R	This study
pFS28	pDM4, *rovA*$_{P98S, G116A, SG127/128IK}$, Cm^R	This study
pFS29	pAKH3, *csrC*$_{IP32953}$, Amp^R	Nuss and Schuster *et al*., 2014
pFS30	pAKH3, *csrC*$_{IP32953–20\ nt}$, Amp^R	Nuss and Schuster *et al*., 2014
pFS31	pAKH3, *csrC*$_{YPIII}$, Amp^R	Nuss and Schuster *et al*., 2014
pFS42	pZE21, P$_{Ltet O-1}$-*dsRed2*, Kan^R	This study
pFS43	pFS42, P$_{Ltet O-1}$-*mCherry*, Kan^R	This study
pFS46	pFU69, *tet-rovA*$_{P98S, G116A, SG127/128IK}$, Kan^R	This study
pFS48	pFS43, ori p15a, Cm^R	This study
pFU69	promoterless *egfp*, colE1, Kan^R	Uliczka *et al*., 2011
pFU76	promoterless *dsRed2,* ori R6K, Amp^R	Uliczka F.
pFU228	*gapA-dsRed2,* ori colE1, Cm^R	Uliczka F.
pHT124	promoter-probe vector, *lacZ*$^+$, Amp^R	Heroven *et al*., 2008
pJet1.2	cloning vector, Amp^R	Thermo Scientific
pKB63	pTS02, *csrA-lacZ*(6)[b], Amp^R	Nuss and Schuster *et al*., 2014
pKH70	pFU76, P$_{rovA}$-*rovA*-*egfp*$_{LVA}$, Amp^R, ΔR6Kmob, ori29807, containing *rovA* promoter fragment from -622 to +170	Herbst, K., PhD thesis
pTB23	*mCherry*, attLambda, ori R6K, Cm^R	Erhardt M.
pTS02	promoterless l*acZ*, ori pSC101*, Amp^R	Nuss and Schuster *et al*., 2014
pZE21	P*Ltet*O-1, ori colE1, Kan^R	Lutz and Bujard, 1997

[a]The number indicates the nucleotide of the corresponding gene fused to *lacZ*. [b]The number indicates the codon of the corresponding gene fused to *lacZ*.

Table 2.7 Strains.

Strains	Description	Source and reference
E. coli		
DH10ß	F$^-$ *endA*1 *recA*1 *galE*15 *galK*16 *nupG rpsL* Δ*lacX*74 Φ80*lacZ*ΔM15 *araD*139Δ(*ara, leu*)7697 *mcrA* Δ(*mrr-hsdRMS-mcrBC*)λ$^-$	Casadaban and Cohen, 1980
BL21λDE3	F$^-$ *ompT gal dcm lon hsdSB* (*rB2 mB2*) *gal* λDE3	Studier and Moffatt, 1986
CC118 λpir	F$^-$ Δ(*ara-leu*)7697 Δ(*lacZ*)74 Δ(*phoA*)20 *araD139 galE galK thi rpsE rpoB arfE*^{am} *recA1*	Manoil and Beckwith, 1986
S17-1λpir	*recA1 thi pro hsdR*$^-$ RP4-2Tc::Mu Km::Tn7 λpir	Simon *et al*., 1983
Y. pseudotuberculosis		
IP32953	pIB1, wild type	Chain *et al*., 2004
YPIII	pYV, wild type	Bölin *et al*., 1982
YP69	YPIII, Δ*csrB*	Heroven *et al*., 2008
YP72	YPIII, Δ*rovM*	Heroven *et al*., 2012a
YP89	YPIII, Δ*crp*	Heroven *et al*., 2012a
YP107	YPIII, Δ*rovA*	Quade *et al*., 2012
YP126	YPIII, Δ*csrC*	Heroven *et al*., 2012a
YP149	YPIII, *phoPQ*$_{IP32953}$	Schweer *et al*., 2013
YP192	YP191, Δ*invA*	Geyer, R., PhD thesis
YP268	YP107, *rovA*$^+_{YPIII}$	This study
YP269	YP107, *rovA*$_{P98S}$	This study
YP270	YP107, *rovA*$_{G116A}$	This study
YP271	YP107, *rovA*$_{SG127/128IK}$	This study
YP279	YP107, *rovA*$_{P98S, SG127/128IK}$	This study
YP285	YP149, Δ*csrC*, Kan^R	Nuss and Schuster *et al*., 2014
YP286	YP107, *rovA*$_{G116A, SG127/128IK}$	This study
YP287	YP107, *rovA*$_{P98S, G116A, SG127/128IK}$	This study
YP288	YP107, *rovA*$_{P98S, SG127/128IK}$	This study

Strains	Description	Source and reference
YP306	YP285, *csrC*$_{YPIII+20nt\ IP32953}$	Nuss and Schuster *et al*., 2014
YP307	YP285, *csrC*$_{IP32953}$	Nuss and Schuster *et al*., 2014
YP308	YP285, *csrC*$_{YPIII}$	Nuss and Schuster *et al*., 2014
YPIP6	IP32953, *phoPQ*$_{YPIII}$	Nuss and Schuster *et al*., 2014

2.1.7 Software and databases

Software used in this study was ApE (A plasmid Editor), FlowJo (Tree Star Inc.), FACSDiva™ (BD Bioscience), Graph Pad PRISM 5.0 (Graphpad Software, Inc.), ImageJ (National Institutes of Health, Wayne Rasband) and ZEN 2012 (Zeiss). The following databases were used: Bioinformatical information from databases National Center for Biotechnology Information (NCBI; www.ncbi.nlm.gov) and Kyoto Encyclopedia of Genes and Genomes (KEGG; www.genome.jp/kegg/).

2.2 Methods

2.2.1 Microbiological methods

2.2.1.1 Cultivation and storage of bacteria

Y. pseudotuberculosis strains were routinely grown under aerobic conditions in liquid LB media overnight to stationary growth phase or as day cultures for 3-4 hours to exponential growth phase at indicated temperatures. For solid cultivation on agar plates bacteria were incubated for two days at 25°C. *E. coli* strains were routinely grown in LB media for liquid cultivation overnight at 37°C or as day cultures for 3-5 hours and on agar plates for solid cultivation at 37°C. If necessary, antibiotics were added at the following concentrations: ampicillin 100 µg ml^{-1} (Roth), chloramphenicol 30 µg ml^{-1} (Roth) and kanamycin 50 µg ml^{-1} (Merck).

Bacteria were frozen for long-term storage in 30% sterile glycerol at -80°C.

2.2.1.2 Sterilization

Solutions and media were heat sterilized in an autoclave for 20 min at 121°C with 1 bar overpressure. Solutions that could not be autoclaved like antibiotics or sucrose were sterile filtered (pore diameter 0.2 µm). Heat sterilization was done for glassware at 180°C for 6 hours.

2.2.1.3 Measurement of cell density

The cell density of liquid cultures was monitored with a spectrophotometer (Amersham Biosciences) at a wavelength of 600 nm ($OD_{600\ nm}$).

2.2.1.4 Flow cytometry analysis

For flow cytometry overnight cultures grown at different temperatures between 25°C and 37°C were used for inoculation of a fresh culture. For this purpose, bacteria were diluted 1:50 in prewarmed media and incubated at the same temperature as the overnight culture. Bacteria were harvested in exponential growth phase by centrifugation (1 min, 14.000 g, room temperature). The pellets were resuspended with 1 ml 4% PFA (paraformaldehyde) and incubated for 20 min at room temperature. Cells were washed twice with 1 ml 1x PBS and stored in PBS in the fridge until further analysis in an LSR-II-Sorp flow cytometer (BS Bioscience). At least 100.000 cells were measured. The data were acquired with FACS Diva software (BD Biosciences) and further analyzed with the software FlowJo v9.7.2 (Tree Star Inc.).

2.2.1.5 Fluorescence microscopy and live cell imaging

Fluorescence microscopy and live cell imaging was performed with an Axiovert II fluorescence microscope (Zeiss) using an Axiocam HR digital charge-coupled device (CCD) camera (Zeiss) and the software ZEN 2012 (Zeiss). For batch cultures bacteria were grown to exponential growth phase at indicated temperatures, harvested and fixed as described for flow cytometry (see 2.2.1.4), spotted onto a glass slide and examined under the microscope. To perform live cell imaging, bacteria were grown to exponential growth phase at 32°C, diluted 1:10 in LB medium

and grown on agar blocks of 1 mm diameter in a micro-Dish^{35mm} (ibidi) under the microscope for up to 10 hours at the same temperature. Pictures were taken every 15 min and the images further processed with the software ImageJ.

2.2.2 Genetic and molecular biological methods for DNA

2.2.2.1 Plasmid and genomic DNA preparation

Plasmid DNA was isolated with the QIAprep Spin Miniprep Kit (Qiagen) according to the manufacturer's instructions. Distilled water was used for elution of plasmid DNA.

To isolate genomic DNA, 750 µl overnight culture were mixed carefully with one volume of phenol-chloroform-isoamylalcohol (25:24:1) and centrifuged (2 min, 10.000 g, room temperature). The watery supernatant was transferred in a new tube and one volume of chloroform was added. The tube was inverted carefully and then centrifuged (2 min, 10.000 g, room temperature). Again, the watery supernatant was transferred in a new tube and DNA was precipitated by adding two volumes of pure ethanol. After centrifugation (20 min, 10.000 g, room temperature) the DNA pellet was washed twice with 70% ethanol and then air-dried. The DNA was resuspended in 100 µl TE-buffer (0.1 M Tric-HCl pH 7.5, 1 mM EDTA) and the concentration was measured photometrically with a NanoDrop spectrophotometer (PeqLab) at 260 nm.

2.2.2.2 Polymerase chain reaction (PCR)

Polymerase chain reaction was performed to amplify DNA fragments with heat stable DNA polymerases and specific primers. The annealing temperature is dependent on the primer length and sequence, whereas the elongation time and temperature depend on the polymerase and size of the amplified DNA fragment.

The Phusion High-Fidelity DNA polymerase has a low error rate because of its proof reading activity and was therefore used for the amplification of DNA fragments that were further used for cloning or sequencing. Fragments for test-PCRs and colony-PCRs were amplified with the Mango*Taq* polymerase. Site directed mutagenesis was performed with the PfuUltra II Fusion HS DNA polymerase. The *Taq* polymerase was used to amplify DNA fragments for EMSAs. The composition and reaction conditions

for PCR were performed in 50 µl or 100 µl volumes according to the manufacturer's instructions.

2.2.2.3 Agarose gel electrophoresis

For size estimation of DNA fragments agarose gel electrophoresis was performed. In an electric field the negatively charged DNA is separated by its size. Routinely, 0.8% [w/v] agarose TAE gels buffer were used. DNA samples were mixed with 6x loading dye (10 mM Tris-HCl, 0.03% bromophenol blue, 0.03% xylene cyanol, 60% glycerol, 60 mM EDTA, pH 7.6) and electrophoresis was performed at 100 to 120 V. Gene Ruler DNA Ladder Mix (Thermo Scientific) was used as size standard (Fig. 2.1). DNA fragments were visualized by ethidium bromide, a DNA intercalating molecule, which is fluorescent upon UV-light exposure. Gel images were taken via a documentation system (BioRad).

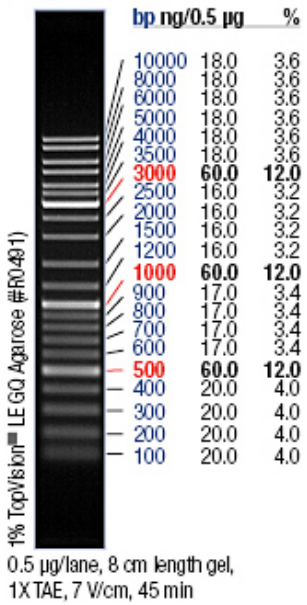

Fig. 2.1 Gene ruler DNA Ladder Mix (Thermo Scientific).

2.2.2.4 DNA extraction and purification from agarose gels

The QIAquick Gel Extraction Kit (Qiagen) was used for purification of DNA fragments from agarose gels according to the manufacturer's instructions. Purified DNA fragments were eluted with distilled water.

2.2.2.5 Cloning techniques

2.2.2.5.1 Restriction digestion

For cloning of DNA fragments into plasmids and to proof the size of an insert restriction digestion was applied. Restriction enzymes recognize specific palindromic sequences and cut them in such a way that overhanging (sticky) or blunt ends are generated. The restriction enzymes were purchased from NEB and reaction conditions were used as described by the manufacturer. The enzymes were heat-inactivated for 20 min at 65°C.

2.2.2.5.2 Dephosphorylation of plasmids

Dephosphorylation of plasmids was performed to remove phosphate groups at the 5' end of plasmids after restriction digestion to reduce the religation rate of the vector. The Antarctic Phosphatase (NEB) was used according to the manufacturer's description. The enzyme was heat-inactivated for 10 min at 65°C.

2.2.2.5.3 Ligation

The T4 DNA Ligase (NEB) was used to ligate plasmid and insert DNA. This enzyme catalyzes the formation of phosphodiester bonds between complementary sticky ends of the digested vector DNA and insert DNA. The ligation reaction was carried out in ligation buffer for 3-6 hours at room temperature or at 18°C overnight. The enzyme was heat-inactivated for 20 min at 65°C.

2.2.2.6 DNA sequencing

For quality control cloned and PCR amplified DNA was sequenced by the in house sequencing facility.

2.2.2.7 Transformation

2.2.2.7.1 Preparation of chemocompetent *E. coli* strains

E. coli cells were grown in LB medium containing 20 mM $MgSO_4$ at 37°C for 3-5 hours and centrifuged (10 min, 2.755 g, 4°C). The supernatant was discarded and the pellet was resuspended in 0.4 volumes of ice-cold TFBI-buffer. Cells were chilled on ice for about 10 min followed by centrifugation (10 min, 2.755 g, 4°C). The pellet was resuspended in 0.05 volume of ice-cold TFBII-buffer, chilled on ice for 15-60 min and aliquots of 50-100 µl were stored at -40°C till usage.

2.2.2.7.2 Heat shock transformation of *E. coli* strains

For transformation of plasmid DNA into chemocompetent *E. coli* strains, 50-100 µl of bacteria were incubated with an appropriate amount of plasmid DNA on ice for 15 min. Then bacteria were transferred to 42°C for 60 sec and immediately diluted in 1 ml SOC medium. Subsequently, the bacteria were incubated at 37°C for one hour, plated on solid medium with respective antibiotics and incubated overnight at 37°C.

2.2.2.7.3 Preparation of electrocompetent *Y. pseudotuberculosis* strains

Y. pseudotuberculosis cells were grown to exponential growth phase at 25°C in BHI medium. Bacteria were chilled on ice for 10-30 min and then centrifuged (15 min, 2.755 g, 4°C). After resuspension of the pellet in 0.2 volume ice-cold distilled water, the cells were centrifuged (15 min, 2.755 g, 4°C) and the pellet was resuspended in 0.2 volume ice-cold transformation buffer. After a further centrifugation step (15 min, 2.755 g, 4°C) the cells were resuspended in a 1/500 volume of transformation buffer and immediately used for transformation.

2.2.2.7.4 Electroporation

For transformation of electrocompetent *Y. pseudotuberculosis* cells 50-80 µl of the bacteria were mixed with plasmid DNA, transferred into a glass cuvette and electroporated at 2.5 kV, 25 µF and 200 Ω (GenePulser II, BioRad). Immediately after electroporation 1 ml SOC medium was added. The bacteria were incubated at

25°C and 750 rpm for 2 hours and then incubated overnight on solid medium with antibiotics at 25°C.

2.2.2.8 Construction of plasmids

Construction of plasmid pFS1 was done by amplification of *rovA* from *Y. pseudotuberculosis* YPIII chromosomal DNA with primers III784/III947, digestion of the PCR product with *Sal*I/*Sph*I and ligation into pDM4.

For the construction of pFS5 the promoter region of *rho* was amplified from *Y. pseudotuberculosis* YPIII chromosomal DNA with primers IV490/IV491 and cut with *Aat*II/*Sal*I. Furthermore, $egfp_{LVA}$ was amplified from plasmid pKH70 with primers II525/IV483 and cut with *Not*I/*Sal*I. The plasmid pKH70 was cut with *Aat*II/*Not*I and the two fragments *rho* and $egfp_{LVA,}$ were ligated into pKH70 resulting in plasmid pFS5.

Construction of plasmid pFS6 was performed by amplification of *rovA* from *Y. pseudotuberculosis* YPIII with primers III947/III784, restriction with *Sal*I/*Sph*I and ligation into the cloning vector pJet (Thermo Scientific). Plasmids pFS8, pFS16, pFS17, pFS25, pFS26, pFS27 and pFS28 were constructed by restriction of *rovA* with *Sal*I/*Sph*I from pFS7, pFS14, pFS15, pFS21, pFS22, pFS23 and pFS24 and ligation into pDM4.

In order produce $RovA_{P98S,\ G116A,\ SG127/128IK}$ under the control of the constitutive *tet*-promoter, plasmid pFS46 was constructed by amplification of *rovA* from plasmid pFS28 with primers II480/II483, cut with *Sal*I/*Not*I and ligated into pFU69.

To construct a plasmid with constitutive P_{tet}-*mCherry* expression plasmid pFU76 was cut with *Kpn*I/*Avr*II and ligated into pZE21 to obtain pFS42. *mCherry* was amplified from pTB23 with primers V842 and V843, cut with *Sal*I/*Not*I and ligated into pFS42 resulting in pFS43. For chloramphenicol resistance, the chloramphenicol cassette was amplified from pFU228 with primers V519/V520 and cut with *Aat*II/*Sac*I. The origin of replication p15a was amplified from pAKH120 with V521/V522, cut with *Avr*II/*Sac*I and ligated together with the chloramphenicol cassette into pFS43, which resulted in pFS48.

2.2.2.9 Site directed mutagenesis

For the integration of specific point mutations into a DNA sequence site directed mutagenesis was performed using the Quick-Change Site-directed Mutagenesis Kit (Stratagene). For this purpose, PCR was performed with the PfuUltra II Fusion HS DNA polymerase (Agilent) according to the manufacturer's instructions. The PCR-product was digested with *Dpn*I, transformed into *E. coli* K-12 cells and plated on LB agar with appropriate antibiotics. The plasmids pFS7, pFS14 and pFS15 were constructed by Quick-Change mutagenesis of plasmid pFS6 with the primers II379/II380, II624/II625 and II626/II627, respectively. Quick-Change mutagenesis of pFS7 and pFS14 with primers II626/II627 resulted in plasmid pFS21 and pFS22, respectively. Plasmid pFS23 was constructed from plasmid pFS7 with primers II624/II625 and plasmid pFS24 was generated from plasmid pFS23 with primers II626/II627 using Quick-Change mutagenesis.

2.2.2.10 Mutagenesis of *Y. pseudotuberculosis*

Mutagenesis of *Y. pseudotuberculosis* was achieved by homologous recombination. Suicide plasmids were transferred into *Yersinia* via conjugation-competent *E. coli* S17-1λpir strains. For this purpose, *Y. pseudotuberculosis* cells and *E. coli* S17-1λpir cells carrying the plasmid of interest were grown overnight at 25°C and 37°C, respectively. 300 µl of *E. coli* cells were centrifuged (3 min, 2.755 g, room temperature) and washed twice with LB medium to remove traces of antibiotics. Subsequently, 900 µl of *Y. pseudotuberculosis* cells were added and centrifuged (3 min, 2.755 g, room temperature). The cells were resuspended in LB medium and incubated on filter membranes for 6 h to 12 h at 25°C. Afterwards, the cells were removed from the filter by vortexing in 1x PBS, the cell suspension was washed once with 1x PBS and plated on *Yersinia* selective solid medium with the appropriate antibiotic. Only *Y. pseudotuberculosis* cells with the integrated plasmid were able to grow on the selective medium. After a 2 days incubation at 25°C the bacteria were transferred to LB agar supplemented with 10% sucrose. The *sacB* gene encoded on the integrated suicide plasmid inhibits growth on sucrose, therefore only bacteria without the plasmid could grow on these plates. Fast growing colonies were analyzed for correct insertion of cloned DNA fragment by PCR and sequencing with primers

135/151. The *Y. pseudotuberculosis* strains YP268, YP269, YP270, YP271, YP279, YP286, YP287 and YP288 were constructed with *Y. pseudotuberculosis* strain YP107 and the plasmids pFS1, pFS8, pFS16, pFS17, pFS25, pFS26, pFS28 and pFS27, respectively.

2.2.3 General molecular biological methods for RNA

2.2.3.1 RNA isolation with hot phenol

Isolation of total RNA was performed via the hot phenol method. For this purpose, 50 ml of exponentially grown cultures at 25°C or 37°C were harvested by centrifugation (5 min, 10.000 g, 25°C or 37°C). The pellets were snap-frozen in liquid nitrogen and then resuspended in 250 µl RNA-resuspension buffer on ice. The resuspended cells were transferred to a 2 ml tube, mixed with lysis buffer and incubated at 65°C for 90 s. 500 µl of 65°C phenol-water were added to the lysed cells, intensively shaked and incubated at 65°C for 3 min. The suspension was frozen in liquid nitrogen for at least 30 s, centrifuged (10 min, 10.000 g, room temperature) and the aqueous phase was transferred to a new tube. This process was performed two more times. Then 300 µl of chloroform:isoamylalcohol (24:1) were added to the aqueous phase, mixed vigorously by vortexing and centrifuged (3 min, 10.000 g, room temperature). This step was repeated one more time. To precipitate the RNA, 1/10 volume of 3 M NaOAc pH 4.5 and 2.5 volume of 95% ethanol were added, mixed and incubated for at least 1 h at -20°C. The RNA was recovered by centrifugation (30 min, 10.000 g, 4°C). The pellet was washed once with ice-cold 70% ethanol (10 min, 10.000 g, 4°C), dried and resuspended in distilled water. The concentration of the RNA was measured with a NanoDrop spectrophotometer (PeqLab) at 260 nm.

2.2.3.2 Northern blotting

For Northern blotting 5 µg of total RNA were mixed with loading dye (0.03% bromophenol blue, 4 mM EDTA, 0.1 mg/ml EtBr, 2.7% formaldehyde, 31% formamide, 20% glycerol in 4x MOPS buffer), heated for 10 min at 70°C and loaded onto a 1.2% MOPS agarose gel. Gelelectrophoresis was performed for 100 min at

120 V in 1x MOPS buffer and an image was taken via a gel documentation system (Biorad) under UV-light to visualize the 23S and 16S rRNAs as loading control. The RNA was transferred on a positively charged membrane (GE Healthcare) by vacuum blotting for 1.5 h at 5 bar in 10x SSC buffer.

Detection of the two CsrC transcripts was performed using a high-resolution urea-acrylamide gel (4.2 g urea, 0.6 ml 10x TBE pH 8.0, 3 ml 40% acrylamide, 3.25 ml distilled water, 6 µl TEMED, 60 µl 10% APS). 10 µg of total RNA were mixed with loading dye (0.03% bromophenol blue, 0.5 mM EDTA, 20% SDS, 9.5 ml formamide) and heated for 10 min. The RNA was transferred on positively charged membranes (GE Healthcare) by semi-dry blotting for 30 min at 20 V in 0.5% TBE.

The membrane was UV cross-linked twice in a UV cross-linker (Stratagene) at 120.000 microjoules. For detection of the specific RNAs CsrB and CsrC DIG-labeled PCR fragments were amplified with primers 555/556 and 582/583, respectively, using DIG-PCR nucleotide mix (Roche). Prehybridization (1-2 hours, 42°C), hybridization (overnight, 42°C), washing and immunological detection were done using the DIG Luminescent Detection Kit (Roche) according to the manufacturer's advices.

2.2.3.3 RNA stability assay

To determine the stability of the small regulatory RNA CsrC transcription was inhibited with 2 mg/ml rifampicin. At given time points samples were taken, 0.2 volumes of stop solution (5% water-saturated phenol, 95% ethanol) were added to the samples and snap-frozen in liquid nitrogen. After thawing on ice, the samples were centrifuged (10 min, 10.000 g, 4°C) and the RNA was isolated with the SV total RNA Purification Kit (Promega) according to the manufacturer's advices. The concentration of the RNA was determined in a NanoDrop spectrophotometer (PeqLab) at 260 nm. Separation of the RNA with agarose gels and detection with Northern blotting was performed as described in 2.2.3.2.

To measure the half-life of CsrC, the amount of CsrC was determined densitometrically using the software ImageJ, normalized to the 23S and 16S rRNAs and plotted in half-logarithmic scale against time. With the help of an exponential regression curve the half-life was calculated.

2.2.4 Biochemical methods

2.2.4.1 Expression and purification of recombinant PhoP protein

E. coli BL21λDE3 pFS13 cells were grown at 37°C for 2-3 h and expression of His_6-PhoP was induced by addition of 1 mM IPTG (isopropyl-β-D-thiogalactoside). The cells were shifted to 18°C and harvested after 3-5 h by centrifugation (20 min, 6.000-9.000 g, 4°C). After one washing step with lysis buffer the pellet was resuspended in 0.1 volumes of lysis buffer and cells were lysed in a French Press (Heinemann). The soluble His_6-PhoP protein was purified using a Ni-NTA agarose column (Machery Nagel). For this purpose, the column was loaded twice with the lysate, washed with four column volumes of washing buffer and eluted with 2 ml elution buffer. The purity of His_6-PhoP was verified by SDS-PAGE and staining of the gel with coomassie. The concentration of purified His_6-PhoP was determined by Bradford assay, using the Coomassie Reagent Protein Assay Kit (Pierce) according to the manufacturer's advices. 250 µl of the Coomassie reagent were mixed with undiluted, a 1:10 and a 1:100 protein dilution and incubated in a micro titer plate for 10 min at room temperature. The absorption was measured with an ELISA plate reader (BioRad) at 595 nm and the concentration was determined via a BSA standard curve .

2.2.4.2 SDS polyacrylamide gel electrophoresis (SDS-PAGE)

SDS-PAGE (Laemmli, 1970) is a technique for separation of proteins under denaturating conditions according to their molecular weight in an electric field. For sample preparation cells were centrifuged (60 sec, 14.000 g, room temperature), the pellet was resuspended in SDS sample buffer and heated for 10 min at 95°C. For an $OD_{600\ nm}$ of 1 a volume of 100 µl sample buffer was used to lyse a bacterial pellet obtained from 1 ml culture. The gel is composed of a separating and a stacking gel with a different pH and polyacrylamide concentrations (Table 2.8). For smaller proteins (up to 25 kDa) a separating gel of 15% was prepared, while separating gels of 10% to 12% were used for bigger proteins (above 25 kDa). Electrophoresis was performed in a BioRad electrophoresis chamber at 25 mA per gel for 30 to 45 min in SDS running buffer. As size standard the PageRuler Prestained Protein Ladder (Thermo Scientific) was used (Fig. 2.2).

Table 2.8 Composition of SDS gels

Buffer/Solution	stacking gel	separating gel 10%	separating gel 12%	separating gel 15%
Separating gel buffer pH 8.8	-	2.5 ml	2.5 ml	2.5 ml
Stacking gel buffer pH 6.8	1.25 ml	-	-	-
A. dest	3.25 ml	4.2 ml	3.5 ml	2.5 ml
Acrylamide	550 µl	3.3 ml	4 ml	5.0 ml
TEMED	12.5 µl	25 µl	25 µl	25 µl
APS (10%)	50 µl	100 µl	100 µl	100 µl

After electrophoresis the gel was used for Western blotting or directly stained with coomassie staining solution for one to two hours and subsequently destained with water by heating.

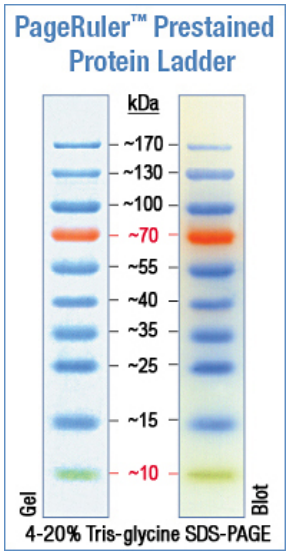

Fig. 2.2 PageRuler Prestained Protein Ladder (Thermo Scientific).

2.2.4.3 Western blotting

For Western blotting proteins were separated by SDS-PAGE and transferred electrophoretically on an Immobilon PVDF membrane (Millipore) for 60 min at 100 V in precooled transblot buffer in a blotting chamber (BioRad). To avoid unspecific binding of proteins the membrane was blocked afterwards for at least 1 hour in

blocking buffer (TBST buffer with either 3% BSA or 5% dried milk powder depending on the requirements of the primary antibody). Thereafter, the membrane was incubated with the primary antibody in blocking buffer under agitation for 1 hour at room temperature or overnight at 4°C. The membrane was washed 3 times for 5 min with TBST buffer and then incubated with the secondary antibody conjugated to horse radish peroxidase (HRP) for 1 hour at room temperature under agitation. After washing the membrane 3 times for 5 min with TBST buffer the blot was developed with the Western Lightning ECL II Kit (Perkin Elmer).

2.2.4.4 β-galactodsidase activity assay

Quantitative expression analyses were performed indirectly via the *lacZ* reporter system. The activity of the β-galactosidase enzyme encoded on a *lacZ*-fusion of choice was analyzed according to Miller (Miller, 1992). For this purpose, the promoter region of a gene of interest was fused to *lacZ* and expression quantified through β-galactosidase activity. This enzyme catalyzes the cleavage of colourless *ortho*-nitrophenyl-β-galactoside (ONPG), which results in the formation of yellow nitrophenol that can be measured photometrically. The amount of nitrophenol correlates directly with the β-galactosidase activity, which in turn depends on the strength of the expression.

The $OD_{600\ nm}$ of an exponential grown culture was measured and 200 µl of cells were lysed with one drop of 0.1% SDS and two drops of chloroform. After 5 min of incubation, 1.5 ml of Z-buffer were added. The reaction was started by the addition of 400 µl ONPG (4 mg/ml) and stopped with 1 ml Na_2CO_3 after a certain time period. The absorption of the sample was determined in a micro titer plate with an ELISA reader (BioRad) at 420 nm. The specific enzyme activity was calculated as follows: $OD_{420\ nm} * 6.648^{-1} * OD_{600\ nm} * t\ [min]^{-1} * V\ [ml]$.

$OD_{420\ nm}$: optical density of stopped reaction
6.648: extinction coefficient of cleaved ONPG
$OD_{600\ nm}$: optical density of bacterial culture
V: culture volume
t: time from start to stop of enzyme reaction

2.2.4.5 Electrophoretic mobility shift assay (EMSA)

For DNA-binding studies of PhoP with the *csrC* upstream region recombinant His_6-PhoP protein was dialysed against binding buffer. Three different fragments of the *csrC* upstream region were amplified by PCR from genomic DNA of *Y. pseudotuberculosis* YPIII. One fragment containing two putative binding sites of PhoP was amplified with primers IV937/IV939, while the other two fragments harboring either binding site one or two were amplified with primers IV938/IV939 and IV937/IV940, respectively. As negative control part of the *gyrA* gene was amplified with primer pair III186/III187. For the binding reaction, 200 fmol of each DNA fragment were used and incubated with increasing amounts of PhoP in binding buffer in a 20 µl reaction mixture for 20 min at 25°C. After incubation, the reaction mixture was loaded onto a 5% polyacrylamide gel, gel electrophoresis was performed at 70 V and subsequently the gel was stained with ethidium bromide. To measure the dissociation constant K_d of each fragment, the relative amount of unbound DNA was determined densitometrically using the software ImageJ and plotted against increasing amounts of PhoP. The K_d was calculated with the help of a regression curve of three independent experiments.

2.2.4.6 DNase I footprinting

To determine the precise binding region of PhoP within the promoter region of *csrC* a DNase I footprint assay was performed. For this purpose, the *csrC* upstream region was amplified from *Y. pseudotuberculosis* YPIII with either a sense (I293) or an anti-sense (V586) digoxigenin (DIG)-labeled primer and the unlabeled primer I79 or V587, respectively. The purified His_6-PhoP protein was either preincubated with 20 mM acetyl phosphate for 30 min at 25°C for phosphorylation or directly used for the footprinting reaction. The purified DIG-labeled DNA fragment was incubated with increasing concentrations of the His_6-PhoP protein for 20 min at 25°C in binding buffer as described for the EMSA. The reaction mixture was digested with a suitable dilution of DNase I for exactly 20 s and stopped by the addition of 50 µl stop solution (15 mM EDTA, 10 µg ml^{-1} yeast carrier tRNA). To extract the DNA, phenol-chloroform-isoamylalcohol (25:24:1) was added and the DNA was precipitated with ethanol. After washing with 70% ethanol, the pellet was dried and then resuspended

in 5 µl sequencing blue marker (Sequenase sequencing kit). The samples were loaded on a 6% polyacrylamide sequencing gel, run for 3 h at 60 W and afterwards transferred to a Nytran N membrane (GE Healthcare) by capillary blotting. After UV cross-linking, the DNase I footprint reaction was developed using CDP-star of the DIG Luminescent Detection kit (Roche) according to the manufacture's advices.

2.2.5 Mouse experiments

Mouse experiments were performed according to the standard recommendations of FELASA (Federation of Laboratory Animal Science Associations) and handled with appropriate care and welfare. Mice were housed in the animal facility at the Helmholtz Centre for Infection Research, Braunschweig, under specific pathogen-free conditions according to GV-SOLAS (German Recommendations of the Society for Laboratory Animal Science). For all mouse experiments, 6-8 weeks old female BALB/c mice were purchased from Janvier (Saint Berthevin Cedex, France).

2.2.5.1 Oral infection

Infection of mice with *Y. pseudotuberculosis* was performed orally with a buttoned cannula to mimic the natural infection route. Prior to infection, mice were starved overnight. The bacteria were grown at 25°C in 25 ml LB liquid media overnight and harvested by centrifugation (10 min, 2.775 g, 25°C). The pellet was washed twice with sterile PBS, resuspended in PBS and the $OD_{600\ nm}$ was measured and adjusted. 200 µl of the bacterial suspension were used for the infection of each mouse. Determination of the infection dose was achieved by plating different dilutions of the bacterial suspension on LB agar.

2.2.5.2 Survival experiments

The virulence of the bacteria was determined by survival experiments. Therefore mice were infected orally with $2*10^8$ CFU of different *Y. pseudotuberculosis* strains as described in 2.2.5.1 and health status as well as body weight were monitored for at least 14 days. The mice were sacrificed when the body weight was below 80% in comparison to the weight before infection.

2.2.5.3 Organ burden experiments

To determine the bacterial load in specific organs of mice, organ burden experiments were performed. Therefore, mice were orally infected as described in 2.2.5.1 with $2*10^8$ CFU of different *Y. pseudotuberculosis* strains. One, three and five days after infection, mice were euthanized by CO_2 asphyxiation and Peyer's patches (PP), mesenteric lymph nodes (MLN), spleen, liver and caecum were dissected. The organs were weighted and homogenized in sterile PBS with the Polytron PT 2100 homogenizer (Kinematica, Switzerland) at 30.000 rpm for 30 s. Different dilutions were plated on LB agar plates and the CFU was calculated per g organ/tissue.

2.2.5.4 Cryosections

Cryosections of different organs were performed to determine the localization of bacteria expressing *rovA*. Therefore BALB/c mice were orally infected as described in 2.2.5.1 with $2*10^8$ CFU of *Y. pseudotuberculosis* harboring plasmid pFS48 (P_{tet}-*mCherry*) and plasmid pKH70 (P_{rovA}-*egfp*$_{LVA}$). Three days post infection mice were euthanized by CO_2 asphyxiation and PP and caecum were isolated. The organs were frozen on dry ice in Tissue-Tek OCT freezing medium (Sakura Finetek). Cryosections of 6-8 µm were prepared with a Microm HM 560 cryostat (Thermo Scientific), mounted on SuperFrost Plus slides (Thermo Scientific) and fixed for 20 min with ice-cold 4% PFA. The fixed slides were washed twice with 1x PBS and air-dried. For cell-nuclei staining and mounting of samples Roti-Mount FluorCare (Roth) was used. Samples were imaged using the Axiovert II fluorescence microscope (Zeiss) with an Axiocam HR digital charge-coupled device (CCD) camera (Zeiss) and the software ZEN 2012 (Zeiss).

3 Results

The enteropathogenic bacterium *Y. pseudotuberculosis* enters the host via M-cells in the epithelial layer of the gut. For the invasion and colonization of the host several early-phase virulence factors like the invasin InvA are necessary (Marra and Isberg, 1997). The expression of *invA* is especially important for the start of infection, as InvA mediates the interaction with M-cells, while it is not required for the later-phase of infection (Clark *et al.*, 1998; Isberg and Leong, 1990). Moreover, InvA is highly immunogenic and therefore a disadvantage for the bacteria after entering the host (Gillenius and Urban, 2015; Grassl *et al.*, 2003a). Thus, constitutive expression of virulence factors is not profitable with respect to immune evasion and also energy consumptive. Hence, the expression of virulence factors has to be tightly controlled in order to ensure a successful infection. RovA, the regulator of virulence A, is one major regulator of early-phase virulence factors like InvA (Nagel *et al.*, 2001). RovA acts as thermosensor by altering its conformation during a temperature shift from 25°C to 37°C and is thereby able to distinguish between environment and host (Herbst *et al*., 2009). In a mathematical model the expression of *rovA* was predicted to be bistable in a temperature-dependent manner (Müller J.; Münch R., unpublished data). Requirements for the bistable expression of a protein are positive or double negative feedback loops within the regulatory network of a transcriptional regulator in combination with a non-linear response, such as cooperative DNA-binding or regulated proteolysis (Ferrell, 2002; Smits *et al*., 2006). In first experiments the temperature-dependent bistable expression of *rovA* could be confirmed (Herbst, K., PhD thesis; Nuss, A. M., unpublished data).

The present study investigates the underlying molecular mechanisms leading to bistable *rovA* expression as well as their role for virulence of *Y. pseudotuberculosis*.

3.1 Temperature-dependent bistable expression of *rovA*

Monitoring heterogeneous gene expression involves the analysis on single cell level, usually via a suitable reporter gene. For the analysis of bistable *rovA* expression the reporter gene *egfp*$_{LVA}$ was used. Since eGFP is a very stable protein with a half-life of approximately 24 hours, rapid changes in gene expression cannot be detected. To

overcome this problem, a LVA-tag for faster protein degradation was attached (Andersen *et al*., 1998; Herbst, K., PhD thesis). LVA is a variant of SsrA-tags and mainly degraded by Clp-proteases. eGFP carrying the LVA-tag has a decreased half-life of about 40 min, which is more useful for studying dynamics of gene expression (Andersen *et al.*, 1998).

3.1.1 Validation of bistable *rovA* expression

To confirm bistable *rovA* expression plasmid pKH70 carrying a P_{rovA}-*egfp*$_{LVA}$ fusion was transformed into competent *Y. pseudotuberculosis* YPIII cells, which were grown to exponential growth phase at different temperatures and analyzed for P_{rovA}-*egfp*$_{LVA}$ expression by fluorescence microscopy (Fig. 3.1). Microscopic pictures show a homogenous expression of the reporter fusion at 25°C and 37°C, in which all cells are eGFP-positive or eGFP-negative, respectively (Fig. 3.1 A). However, at 32°C P_{rovA}-*egfp*$_{LVA}$ is heterogeneously expressed. Two cell types were detectable, one with green fluorescence due to RovA-dependent *egfp*$_{LVA}$ expression (“ON”) and a second one, in which *rovA* is not expressed without any green fluorescence (“OFF”). To examine the temperature range in which bistable expression of P_{rovA}-*egfp*$_{LVA}$ can be observed, bacteria were grown at 25°C and between 30°C to 37°C and P_{rovA}-*egfp*$_{LVA}$ expression was analyzed by flow cytometry (Fig. 3.1 B, D). At intermediate temperatures (30°C to 34°C) two distinct subpopulations with either high (“ON”) or low/no P_{rovA}-*egfp*$_{LVA}$ expression (“OFF”) could be detected. With increasing temperatures, the amount of eGFP-positive cells gradually decreases. The gating strategy for eGFP-positive and eGFP-negative bacteria of an *in vitro* culture is shown in Fig. S1. Furthermore, the amount of RovA expressed from the chromosomal copy was determined (Fig. 3.1 C). The RovA-levels analyzed by Western blot reflect the eGFP-levels of the flow cytometry analysis: with increasing temperatures a lower amount of RovA was observed.

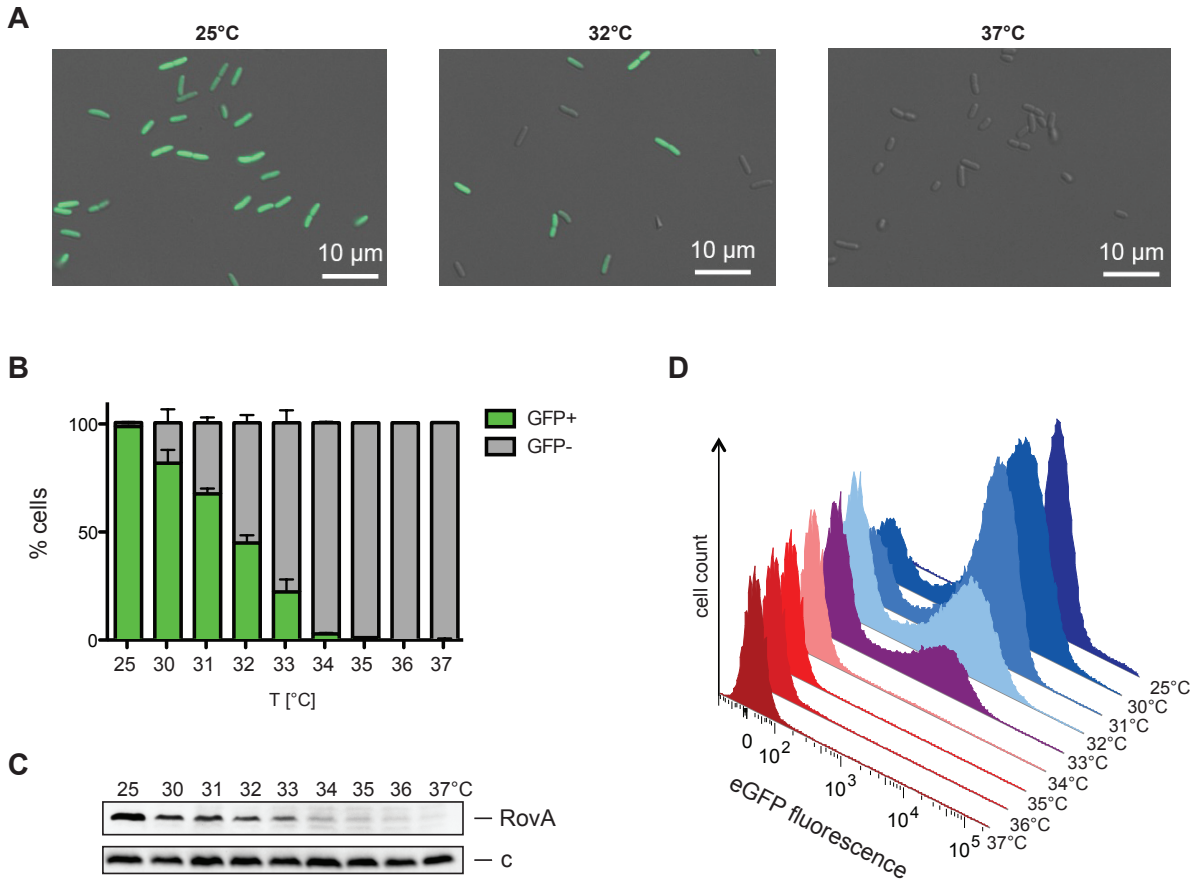

Fig. 3.1 Expression of a P_{rovA}-$egfp_{LVA}$ reporter fusion at various temperatures.
Y. pseudotuberculosis YPIII cells harboring plasmid pKH70 (P_{rovA}-$egfp_{LVA}$) were grown to exponential growth phase and samples were taken at different temperatures for microscope, flow cytometry and Western blot analysis. **(A)** Microscopic pictures at 25°C, 32°C and 37°C. **(B)** Quantification of eGFP-positive and eGFP-negative cells at indicated temperatures measured by flow cytometry. The data show the mean ± SEM of three independent experiments performed in triplicates. **(C)** Whole cell extracts were prepared, separated on 15% SDS-polyacrylamide gels and RovA expressed from the chromosomal *rovA* gene was analyzed by blotting using a specific RovA antibody, (c – loading control). **(D)** Intensity of eGFP fluorescence at different temperatures is shown in a histogram.

To proof that bistable *rovA* expression is not based on a temperature-dependent $eGFP_{LVA}$ synthesis or proteolysis, $egfp_{LVA}$ was expressed under the control of the constitutive *rho* promoter in plasmid pFS5 and its expression was tested at different temperatures by flow cytometry (Fig. 3.2). At the investigated temperatures all cells express $eGFP_{LVA}$ with a high intensity. This demonstrates that bistable *rovA* expression is specific and not a result of a temperature-dependent expression or degradation of $eGFP_{LVA}$.

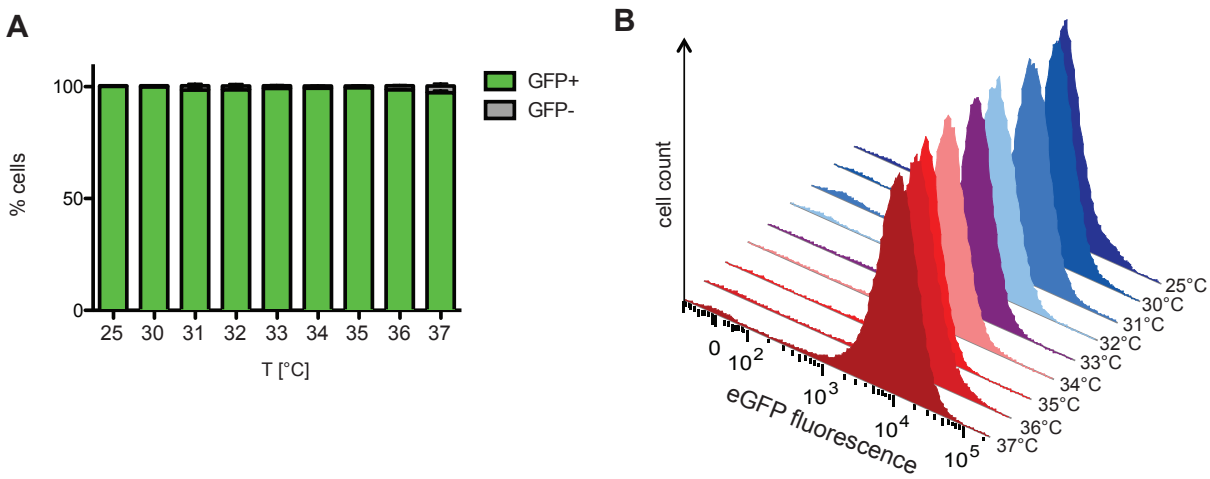

Fig. 3.2 Expression of a P_{rho}-*egfp*$_{LVA}$ reporter fusion at various temperatures.
Y. pseudotuberculosis YPIII cells harboring plasmid pFS5 (P_{rho}-*egfp*$_{LVA}$) were grown to exponential growth phase and samples were taken at different temperatures for flow cytometry. **(A)** Quantification of eGFP-positive and eGFP-negative cells at indicated temperatures measured by flow cytometry. The data show the mean ± SEM of two independent experiments performed in duplicates or triplicates. **(B)** Intensity of eGFP fluorescence within the bacterial population at different temperatures is shown in a histogram.

3.1.2 Time-lapse microscopy reveals reversibility and hysteresis

In order to follow RovA-dependent expression of *egfp*$_{LVA}$ on single cell level over several generations time-lapse microscopy was performed. For this purpose, bacteria were grown to exponential growth phase at 32°C and observed using time-lapse microscopy for several hours (Fig. 3.3). The data show heterogeneous expression of P_{rovA}-*egfp*$_{LVA}$ in a growing microcolony. Observing cells starting in the “ON” state (P_{rovA}-*egfp*$_{LVA}$ expression) shows that these cells tend to stay in the “ON” state (Fig. 3.3 A). Vice versa a microcolony that starts from an “OFF” cell (no P_{rovA}-*egfp*$_{LVA}$ expression) remains preferably in this state (Fig. 3.3 B). Nevertheless, spontaneous switching from one state to the other can be observed and shows reversibility and hysteresis, a characteristic of bistable systems. Hysteresis describes a memory-like behavior of cells in which they tend to stay in the state of their ancestors (Ninfa and Mayo, 2004; Veening *et al*., 2008a).

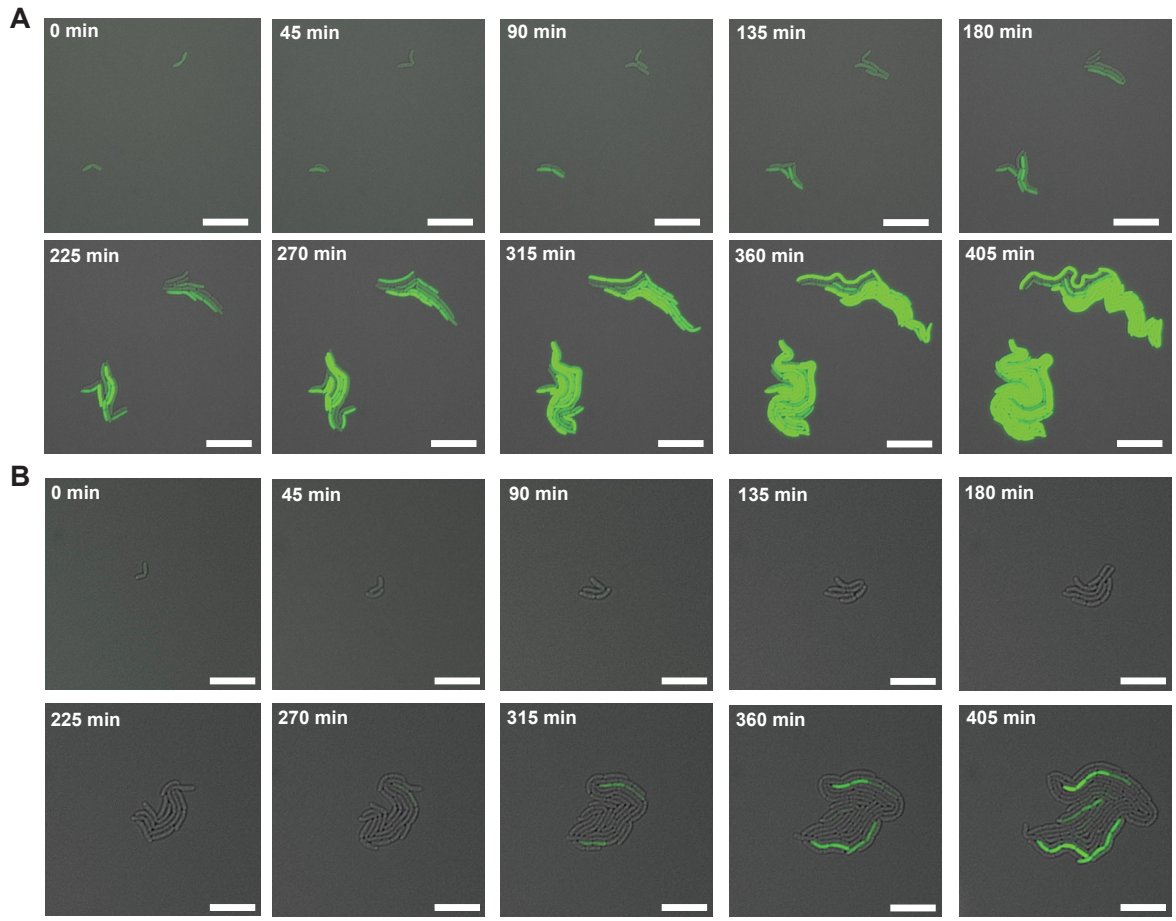

Fig. 3.3 Time-lapse microscopy of *Y. pseudotuberculosis* at 32°C.
Y. pseudotuberculosis YPIII cells harboring plasmid pKH70 (P_{rovA}-*egfp*$_{LVA}$) were grown for two hours at 32°C, diluted 1:10 in LB media and incubated in a micro-dish under the microscope at 32°C. Growth of cells was monitored using the Axiovert II fluorescence microscope (Zeiss) and images were taken every 15 min. Analysis started either from eGFP-positive cells **(A)** or eGFP-negative cells **(B)**. White bars indicate 10 µm.

3.1.3 Bistable *rovA* expression is affected by thermosensing and proteolysis

To gain information about the molecular mechanisms underlying bistable *rovA* expression, mutants altered in stability and thermosensing of RovA were constructed and analyzed. Previous investigations revealed that RovA stability is enhanced at 37°C in *Y. enterocolitica* O:3 (Uliczka *et al*., 2011). A substitution of proline to serine at position 98 is responsible for the increased stability, but does not affect thermosensing of RovA (Uliczka *et al*., 2011). An exchange of P98S in *Y. pseudotuberculosis* YPIII also affects stability of RovA and leads to increased stability at 37°C (Mendonca, C., PhD thesis). Moreover, a comparison of RovA of *Y. pseudotuberculosis* and SlyA of *Salmonella enterica* serovar Typhimurium revealed differences in stability and DNA-binding affinity at 37°C. Amino acid G116

was identified to be responsible for the thermosensing capacity of RovA, while amino acids SG127/128 renders the protein more susceptible to degradation (Quade *et al*., 2012). As a consequence, an exchange of G116A leads to an increased DNA-binding affinity at 37°C. Additionally, substitution of amino acids SG127/128IK increases stability of RovA (Quade *et al*., 2012).

Based on these findings, gene variants of *rovA* were constructed within the original *rovA* locus on the chromosome leading to RovA mutations with amino acid substitutions of P98S, G116A and SG127/128IK. *Y. pseudotuberculosis* wild type strain and the different *rovA* mutants carrying plasmid pKH70 (P_{rovA}-*egfp*$_{LVA}$) were grown to exponential growth phase at temperatures ranging from 25°C to 37°C and *rovA* expression was analyzed by flow cytometry and Western blot (Fig. 3.4). As previously described, bistable expression of P_{rovA}-*egfp*$_{LVA}$ was observed at growth temperatures between 30°C and 34°C in the wild type strain (Fig. 3.4 A). About 50% of cells were in the “ON” and 50% in the “OFF” state was observed at 32°C. Loss of the thermosensing activity of RovA due to the G116A substitution affects the pattern of bistable P_{rovA}-*egfp*$_{LVA}$ expression (Fig. 3.4 B). The temperature range, in which bistable expression occurs, appears to be broader in comparison to the wild type, two subpopulations can be observed between 31°C and 36°C. Exchange of the amino acids SG127/128IK had a similar effect on the distribution of bistable expression, but in contrast to YP270 (RovA$_{G116A}$) less eGFP-positive cells could be observed at 36°C (Fig. 3.4 C). The lowest impact on bistable P_{rovA}-*egfp*$_{LVA}$ expression was visible for YP269 (RovA$_{P98S}$) (Fig. 3.4 D). The results were verified by Western blotting. A gradual temperature up-shift leads to a decrease of the RovA-level within the entire population, which equals the percentage of eGFP-positive cells at the respective temperature.

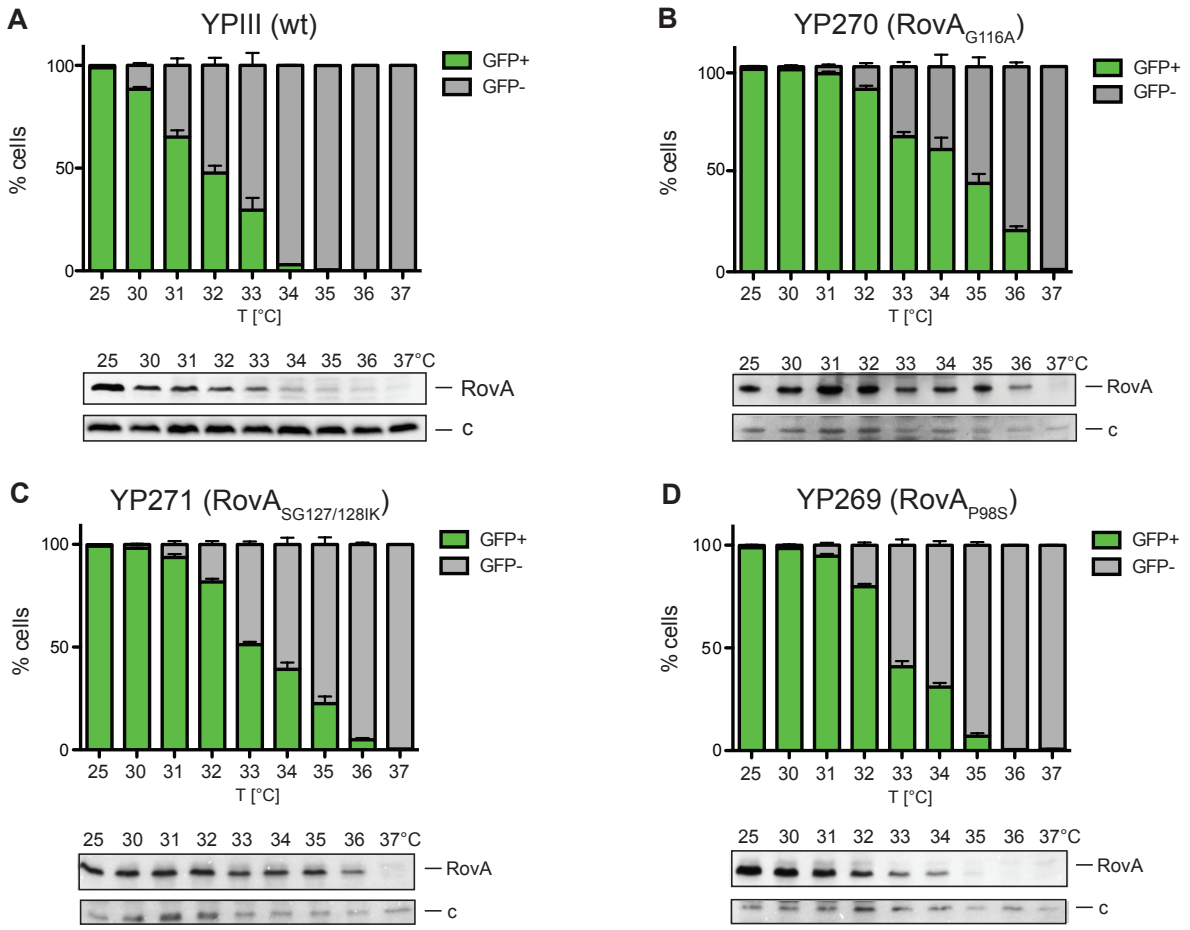

Fig. 3.4 Analysis of bistable *rovA* expression in YPIII expressing different RovA variants.
Y. pseudotuberculosis YPIII wild type strain as well as mutants expressing a stabilized version of RovA harboring the plasmid pKH70 (P_{rovA}-*egfp*$_{LVA}$) were grown to exponential growth phase and samples were taken at indicated temperatures for flow cytometry and Western blot analysis. Upper panels show quantification of eGFP-positive and eGFP-negative cells measured by flow cytometry. The data show the mean ± SEM of three independent experiments performed in triplicates. Lower panels show Western blots of chromosomally encoded RovA using a RovA specific antibody (c – loading control). **(A)** YPIII wild type RovA (wt), **(B)** YP270 (RovA$_{G116A}$), **(C)** YP271 (RovA$_{SG127/128IK}$), **(D)** YP269 (RovA$_{P98S}$).

The stabilized variants RovA$_{P98S}$, RovA$_{G116A}$ and RovA$_{SG217/128IK}$ led to a modulation of bistable P_{rovA}-*egfp*$_{LVA}$ expression pattern and to expression of *rovA* at higher temperatures, but not at host body temperature (37°C). In order to further shift *rovA* expression to higher temperatures and to abolish RovA bistability entirely, multiple substitutions were integrated into the RovA protein to further increase stability and DNA binding affinity. The generated mutants were analyzed by flow cytometry and Western blotting (Fig. 3.5). The bistable expression of P_{rovA}-*egfp*$_{LVA}$ is still present, but shifted to higher temperatures. Only a very low P_{rovA}-*egfp*$_{LVA}$ expression could be observed in strain YP279 (RovA$_{P98S, SG127/128IK}$) at 37°C, in which degradation but not thermosensing is affected (Fig. 3.5 A). Loss of the thermosensing capacity in

connection with decreased proteolysis, either through substitution of G116A and SG127/128IK or G116A and P98S leads to expression of P_{rovA}-*egfp*$_{LVA}$ in about 20% to 25% of the bacteria at 37°C (Fig. 3.5 B, C). In order to further increase the ratio of cells in the "ON" state at 37°C, a stabilized RovA variant with multiple substitutions was constructed and tested on bistable of P_{rovA}-*egfp*$_{LVA}$ expression (Fig. 3.5 D). However, only a slight increase of cells in the "ON" state could be observed at 37°C in strain YP287 expressing the stabilized $RovA_{G116A, P98S, SG127/128IK}$ variant.

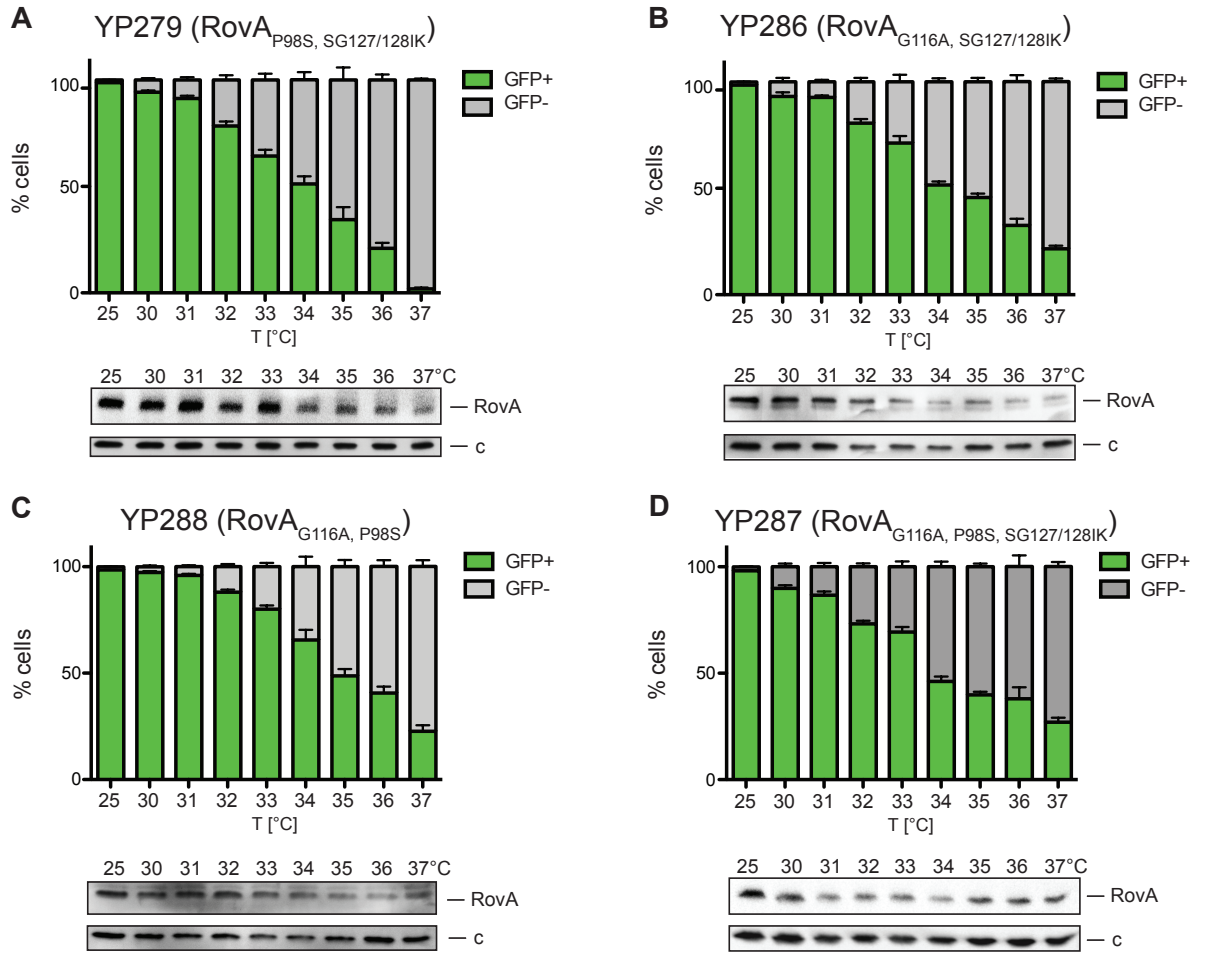

Fig. 3.5 Effect of multiple amino acid substitutions within the RovA protein on bistable *rovA* expression.
Mutants expressing different stabilized versions of RovA harboring the plasmid pKH70 (P_{rovA}-*egfp*$_{LVA}$) were grown to exponential growth phase and samples were taken at indicated temperatures for flow cytometry and Western blot analysis. Upper panels show quantification of eGFP-positive and eGFP-negative cells measured by flow cytometry. The data show the mean ± SEM of three independent experiments performed in triplicates. Lower panles show Western blots of chromosomally encoded RovA using a RovA specific antibody (c – loading control). **(A)** YP279 ($RovA_{P98S, SG127/128IK}$), **(B)** YP286 ($RovA_{G116A, SG127/128IK}$) **(C)** YP288 ($RovA_{G116A, P98S}$), **(D)** YP287 ($RovA_{G116A, P98S, SG127/128IK}$).

Taken together, the thermosensing capacity as well as the temperature-dependent proteolysis of RovA strongly affect bistable expression of *rovA*. Nevertheless, uncoupling of these factors does not lead to an abrogation of bistability.

3.1.4 *rovA* is bistably expressed under the control of a constitutive promoter and in a Δ*rovM* mutant

As mentioned before, a positive or double negative feedback loop combined with a non-linear response, such as regulated proteolysis, is required for the formation of bistability (Ferrell, 2002; Smits *et al*., 2006). Diminished degradation and enhanced DNA-binding affinity of RovA led to a shift of bistable *rovA* expression to higher temperatures, but did not abolish RovA bistability (see Fig. 3.4, 3.5).

To test the impact of the positive and negative feedback loop on bistable *rovA* expression when a stabilized variant of RovA is expressed, $rovA_{P98S,\ G116A,\ SG127/128IK}$ was expressed under the control of a constitutive promoter. Therefore, plasmids pFS46 (P_{tet}-$rovA_{P98S,\ G116A,\ SG127/128IK}$) and pKH70 ($P_{rovA}$-$egfp_{LVA}$) were transformed into *Y. pseudotuberculosis* YP107 (Δ*rovA).* The *rovA* deletion mutant was used to exclude any effects of chromosomally encoded wild type RovA. Bacteria were grown to exponential growth phase at different temperatures and samples were taken for flow cytometry and Western blotting (Fig. 3.6). At temperatures up to 33°C almost all cells express $egfp_{LVA}$ in a RovA-dependent manner and at 35°C and 36°C approximately 75% of the population are eGFP-positive. However, at 37°C only about 20% of all cells are eGFP-positive, showing that even if a stabilized RovA is expressed under the control of a constitutive promoter, bistable *rovA* expression cannot be abolished at 37°C.

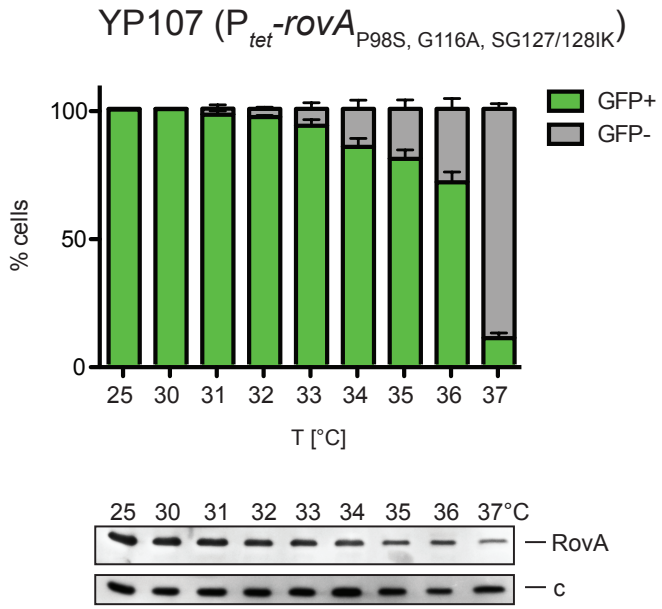

Fig. 3.6 *rovA* expression under control of the constitutive *tet*-promoter.
Y. pseudotuberculosis YP107 (Δ*rovA)* harboring plasmids pFS46 (P_{tet}-*rovA*$_{P98S,\ G116A,\ SG127/128IK}$) and pKH70 ($P_{rovA}$-*egfp*$_{LVA}$) was grown to exponential growth phase and samples were taken at indicated temperatures for flow cytometry and Western blot analysis. Upper panel shows quantification of eGFP-positive and eGFP-negative cells measured by flow cytometry. The data show the mean ± SEM of three independent experiments performed in triplicates. Lower panel shows a Western blot of chromosomally encoded RovA using a RovA specific antibody (c – loading control).

Besides the autoregulatory loop, the proteolysis and thermosensing domains of RovA, another regulatory component of the network controlling RovA synthesis was identified to affect heterogeneous expression of *rovA*. The transcriptional regulator RovM binds directly to the promoter region of *rovA* and represses *rovA* transcription (Heroven and Dersch, 2006). By using plasmid pKH70 a shift of bistable P_{rovA}-*egfp*$_{LVA}$ expression to higher temperatures could be determined in a Δ*rovM* mutant (Fig. 3.7). While the entire population express P_{rovA}-*egfp*$_{LVA}$ up to temperatures of 33°C, bistable expression was observed from 34°C to 36°C.

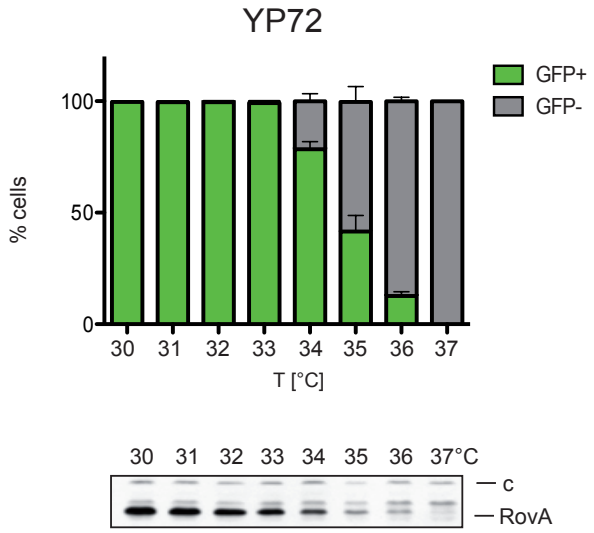

Fig. 3.7 Bistable expression of P_{rovA}-*egfp*$_{LVA}$ in a Δ*rovM* mutant.
Y. pseudotuberculosis YP72 (Δ*rovM)* harboring plasmid pKH70 (P_{rovA}-*egfp*$_{LVA}$) was grown to exponential growth phase and samples were taken at indicated temperatures for flow cytometry and Western blot analysis. Upper panel shows quantification of eGFP-positive and eGFP-negative cells measured by flow cytometry. The data show the mean ± SEM of three independet experiments performed in triplicates. Lower panel shows a Western blot of chromosomally encoded RovA using a RovA specific antibody (c – loading control; experiment was performed in cooperation with Nuss, A. M).

Based on these results and in order to increase the percentage of eGFP-positive cells at 37°C, *rovA*$_{P98S,\ G116A,\ SG127/128IK}$ was expressed under the control of a constitutive promoter in a Δ*rovM* mutant strain. Therefore, plasmid pFS46 (P_{tet}-*rovA*$_{P98S,\ G116A,\ SG127/128IK}$) and plasmid pKH70 ($P_{rovA}$-*egfp*$_{LVA}$) were transformed in strain YP72 (Δ*rovM*) and analyzed by flow cytometry and Western blot (Fig. 3.8). Only a slight increase of eGFP-positive cells could be detected at 35°C and 36°C in comparison to the P_{rovA}-*egfp*$_{LVA}$ expression in Δ*rovA* mutant, while the percentage of eGFP-positive cells is similar comparing the *rovA* deletion mutant with the *rovM* deletion mutant at 37°C (see Fig. 3.6).

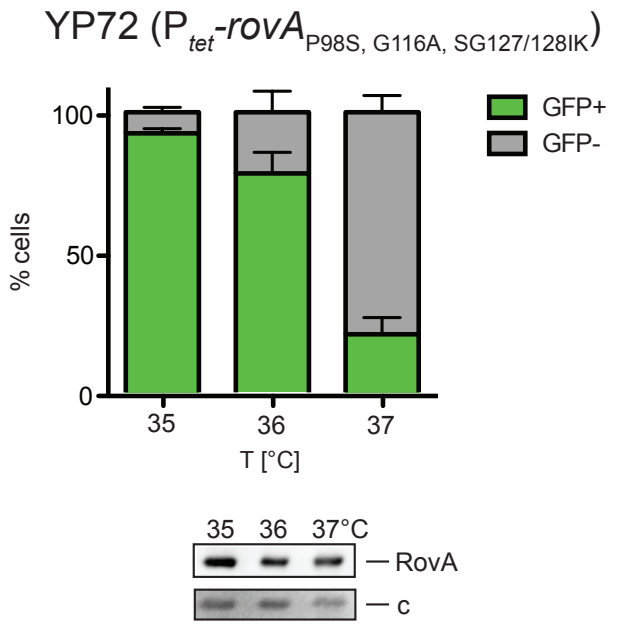

Fig. 3.8 RovA-dependent *egfp*$_{LVA}$ expression in a Δ*rovM* mutant under control of the constitutive *tet*-promoter.
Y. pseudotuberculosis YP72 (Δ*rovM)* harboring plasmids pFS46 (P$_{tet}$-*rovA*$_{P98S,\ G116A,\ SG127/128IK}$) and pKH70 (P$_{rovA}$-*egfp*$_{LVA}$) was grown to exponential growth phase and samples were taken at indicated temperatures for flow cytometry and Western blot analysis. Upper panel shows quantification of eGFP-positive and eGFP-negative cells measured by flow cytometry. The data show the mean ± SEM of three independent experiments performed in triplicates. Lower panel shows a Western blot of chromosomally encoded RovA using a RovA specific antibody (c – loading control).

In summary, the previous results show that bistability of RovA is very robust to perturbations and could not be abolished by mutations that stabilize RovA even if this RovA version is expressed constitutively in a *rovM* deletion mutant.

3.1.5 Stabilized RovA enhances *invA* expression at 37°C

Invasin was shown to be a direct target of RovA in *Y. pseudotuberculosis* (Nagel *et al.*, 2001). As a result of RovA-dependent regulation *invA* is expressed at 25°C, but not at 37°C (Nagel *et al*., 2001). Immunostainings of invasin of YPIII grown at 32°C revealed that RovA-positive cells carry more invasin on the cell surface than RovA-negative cells (Fig. S2, Nuss, A. M.).

Exchanges of the aminoacids P98S, G116A and SG127/128IK within the RovA protein result in expression of RovA at temperatures up to 37°C. To monitor if a stabilized RovA would also lead to expression of *invA* at host body temperatures (37°C), Western blotting of invasin was performed in *Y. pseudotuberculosis* YPIII (wt), YP269 (RovA$_{P98S}$), YP270 (RovA$_{G116A}$) and YP287 (RovA$_{P98S,\ G116A,\ SG127/128IK}$)

(Fig. 3.9). Neither in the wild type strain nor in the stabilized mutants YP269 ($RovA_{P98S}$) and YP270 ($RovA_{G116A}$) invasin was detectable at 37°C. Only in the most stabilized mutant YP287 ($RovA_{P98S,\ G116A,\ SG127/128IK}$) invasin could be detected. The amount of invasin correlates with the RovA-level at 37°C in the respective mutants, which illustrates that *invA* expression correlates with the amount of RovA (see Fig. 3.4, 3.5).

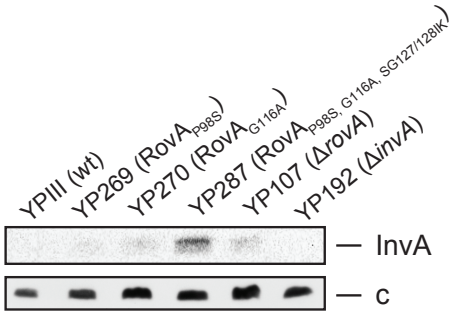

Fig. 3.9 *invA* expression at 37°C in RovA mutants expressing stabilized versions of RovA.
Y. pseudotuberculosis YPIII (wt), YP269 ($RovA_{P98S}$), YP270 ($RovA_{G116A}$) YP287 ($RovA_{P98S,\ G116A,\ SG127/128IK}$), YP107 (Δ*rovA*), and YP192 (Δ*invA*) were grown to exponential growth phase at 37°C and samples were taken for Western blotting. Whole cell extracts were prepared, separated on 12% SDS-polyacrylamide gels and chromosomally encoded InvA was analyzed with an InvA specific antibody (c – loading control).

3.2 Strain-specific differences in the bistable expression of *rovA*

To gain information whether bistable expression of *rovA* varies between different *Y. pseudotuberculosis* strains, bistable *rovA* expression was also investigated in the clinical isolate IP32953. Therefore, the bacteria carrying plasmid pKH70 (P_{rovA}-$egfp_{LVA}$) were grown to exponential growth phase at different temperatures and analyzed by flow cytometry and Western blot (Fig. 3.10). Bistable expression of P_{rovA}-$egfp_{LVA}$ could be observed from 34°C to 36°C. The amount of RovA within the entire population correlates with the flow cytometry data and shows a decrease of RovA amounts with increasing temperatures. Comparing RovA-dependent expression of $egfp_{LVA}$ in *Y. pseudotuberculosis* strains YPIII and IP32953 reveals expression of RovA at higher temperatures in strain IP32953 (see Fig. 3.1 B).

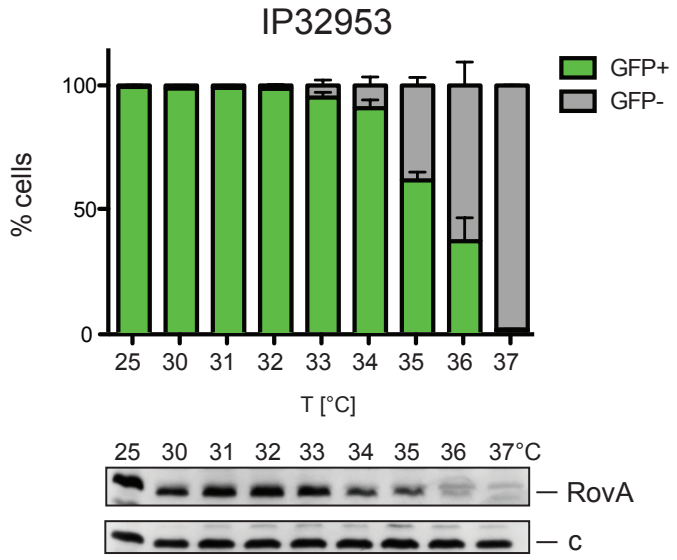

Fig. 3.10 Bistable expression of P_{rovA}-*egfp*$_{LVA}$ in *Y. pseudotuberculosis* IP32953.
Y. pseudotuberculosis IP32953 harboring plasmid pKH70 (P_{rovA}-*egfp*$_{LVA}$) was grown to exponential growth phase and samples were taken at indicated temperatures for flow cytometry and Western blot analysis. Upper panel shows quantification of eGFP-positive and eGFP-negative cells measured by flow cytometry. The data show the mean ± SEM of three independent experiments performed in duplicates or triplicates. Lower panel shows Western blots of chromosomally encoded RovA using a RovA specific antibody (c – loading control).

One main difference between the two isolates is the presence of a functional PhoP, which is the response regulator of the two-component system PhoP/PhoQ. While *Y. pseudotuberculosis* IP32953 encodes a functional PhoP, *Y. pseudotuberculosis* YPIII encodes only a truncated version of the *phoP* gene through a T160P amino acid substitution (Grabenstein *et al.*, 2004). In *Y. pestis* it was described that PhoP directly controls expression of *rovA* by repression of *rovA* transcription (Zhang *et al.*, 2011). Expression of *slyA,* the *rovA* homologue of *S. enterica* serovar Typhimurium, was shown to be activated by PhoP (Norte *et al*., 2003). In order to examine the role of PhoP on *rovA* expression in *Y. pseudotuberculosis* and unravel a possible implication in bistability of RovA, the two clinical isolates YPIII and IP32953 of *Y. pseudotuberculosis* were used for this investigation. Furthermore, isogenic *phoP* mutants of the two strains were analyzed: YP149, which is the *phoP*-positive derivative of YPIII, and YPIP6, which is the *phoP*-negative derivative of IP32953.

3.2.1 PhoP acts positively on *rovA* expression

In order to gain information on *rovA* expression dependent on PhoP, the promoter activity of a translational *rovA-lacZ* fusion (pCM33) was determined in the

Y. pseudotuberculosis strains YPIII (*phoP*$^-$) and IP32953 (*phoP*$^+$) and their respective *phoP*-positive and *phoP*-negative derivatives. The β-galactosidase activity was measured in the different strains during exponential growth (Fig. 3.11 A). At 25°C the β-galactosidase activity in the *phoP*-positive derivatives is significantly higher than in the *phoP*-negative derivatives. In contrast, at 37°C a basal expression of *rovA-lacZ* was observed in all strains with only a slight difference between the *phoP*-positive and *phoP*-negative derivatives of IP32953 and YPIII. Western blots are consistent with these data and show a higher amount of RovA in the *phoP*-positive derivatives compared to *phoP*-negative derivatives at 25°C (Fig. 3.11 B).

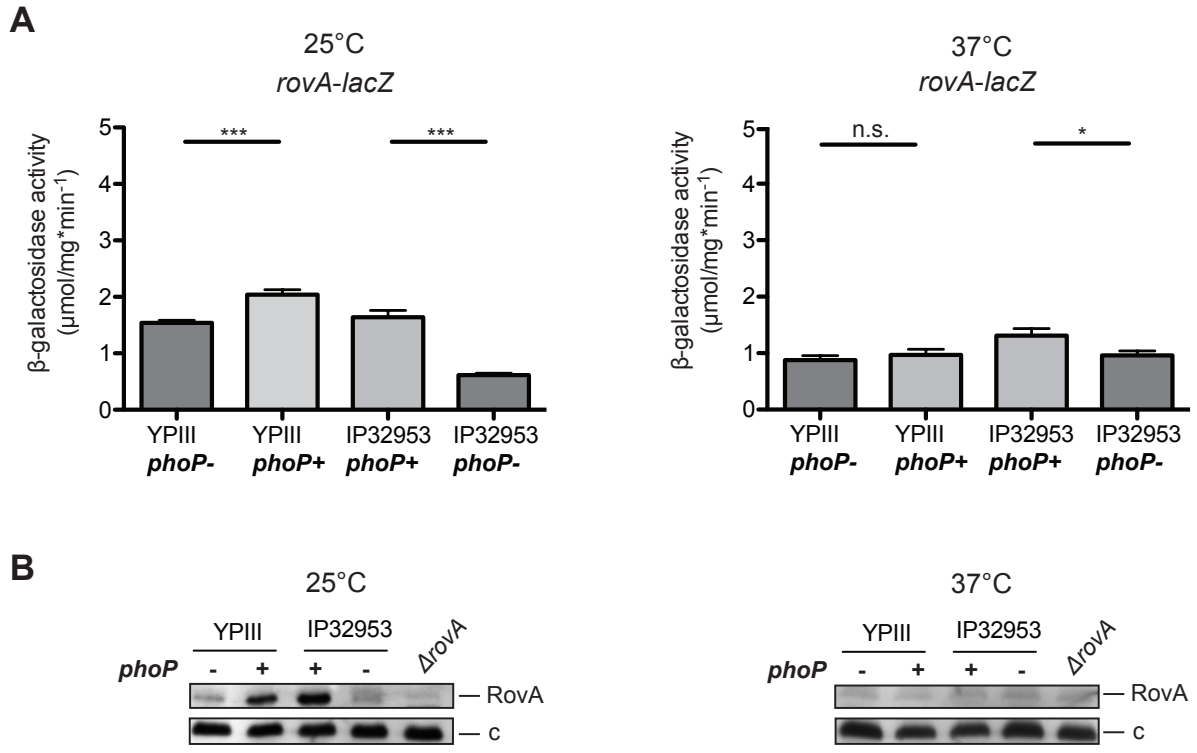

Fig. 3.11 PhoP regulates *rovA* expression positively in *Y. pseudotuberculosis*.
Y. pseudotuberculosis strains YPIII and IP32953 and their respective *phoP*-positive and *phoP*-negative derivatives were grown to exponential growth phase at 25°C or 37°C as indicated. **(A)** The β-galactosidase activity of a translational *rovA-lacZ* (pCM33) fusion was determined. The data represent the mean ± SEM of three independent experiments performed in triplicates. Data were analyzed by Student's t-test (*, P<0.05; **, P <0.01; ***, P <0.001; n.s. – not significant). **(B)** Whole cell extracts were prepared, separated on 15% SDS-polyacrylamide gels and analyzed by Western blotting with a RovA specific antibody. YP107 (*ΔrovA*) was used as negative control (c – loading control).

3.2.1.1 PhoP-dependent activation of *rovA* expression is mediated by RovM

Furthermore, it was analyzed whether PhoP controls *rovA* expression directly or indirectly. For this purpose, the regulatory network of RovA was examined. The LysR-type regulator RovM was shown to repress *rovA* expression directly by binding upstream of promoter P1 (Heroven and Dersch, 2006).

To investigate whether synthesis of RovM is PhoP-dependent, the RovM protein level was examined in the different *phoP*-positive and *phoP*-negative derivatives of YPIII and IP32953. To do so, the different strains were grown to exponential growth phase and samples were taken at 25°C and 37°C and analyzed by Western blotting (Fig. 3.12). At both temperatures increased RovM-levels were observed in the *phoP*-deficient strains in comparison to the *phoP*-positive strains. This indicates that the PhoP-mediated positive regulation of *rovA* is indirect and occurs via RovM. Additionally, RovM is more abundant in the IP32953 background, which leads to the assumption that other regulatory factors besides PhoP contribute to RovM regulation.

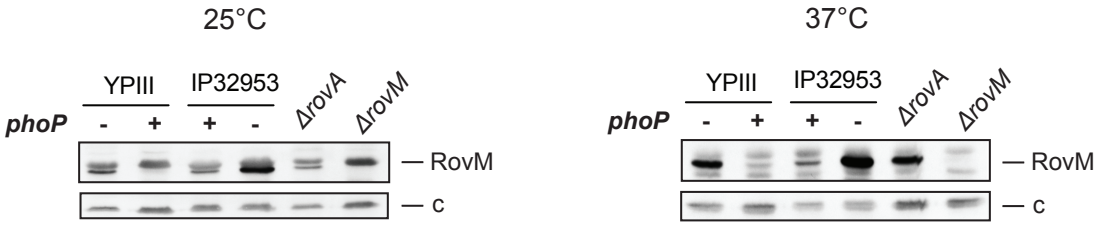

Fig. 3.12 Impact of PhoP on *rovA* expression is mediated through RovM.
The *Y. pseudotuberculosis* strains YPIII and IP32953 and their respective *phoP*-positive and *phoP*-negative derivative were grown to exponential growth phase at 25°C or 37°C as indicated and samples were taken for Western blotting using a specific RovM antibody. YP72 (Δ*rovM*) served as negative control (c – loading control).

3.2.1.2 Expression of *crp* and *csrA* is not affected by PhoP

Besides temperature, expression of *rovA* depends on the nutrient availability of the surrounding media (Heroven *et al*., 2012a; Nagel *et al*., 2001). In minimal media *rovA* is repressed, which is mediated by Crp and the Csr-system via RovM (see Fig. 1.6) (Heroven and Dersch, 2006; Heroven *et al*., 2012a). Since PhoP-dependent activation of *rovA* occurs via RovM, it is possible that the Csr-system or Crp is involved in this regulation, which was further investigated. In addition, it was recently shown, that *crp* is directly activated by PhoP in *Y. pestis* (Zhang *et al*., 2013).

In order to test whether PhoP acts on *crp*, the respective *phoP*-positive and *phoP*-negative derivatives of YPIII and IP32953 were grown to exponential growth phase at 25°C and 37°C and the β-galactosidase activity of a translational *crp-lacZ* fusion was determined (Fig. 3.13 A). No significant differences in the β-galactosidase activity were observed neither at 25°C nor at 37°C.

To confirm the reporter fusion experiment and exclude differences in the stability of Crp, Western blot analysis of Crp was performed (Fig. 3.13 B). Consistent with the data of the β-galactosidase assay, no differences between *phoP*-positive and *phoP*-negative strains could be detected, indicating that PhoP has no impact on Crp expression in *Y. pseudotuberculosis*.

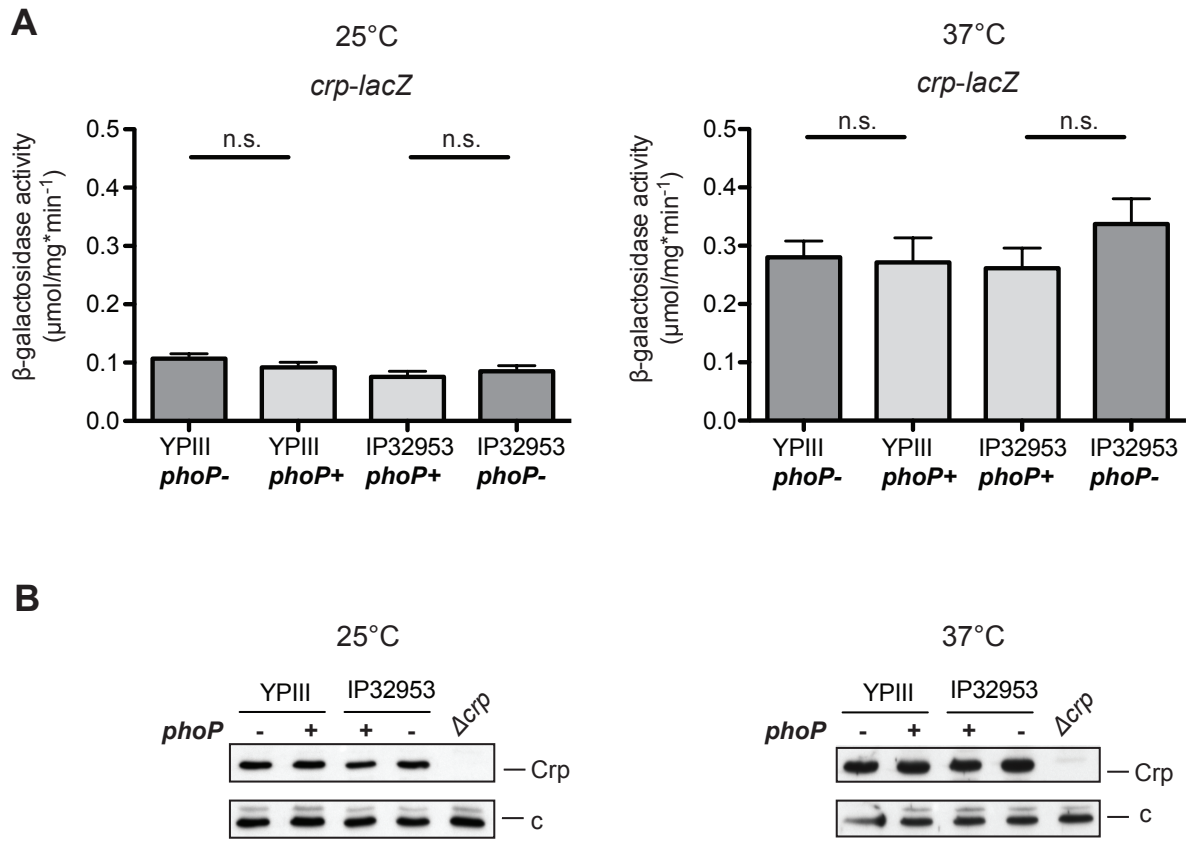

Fig. 3.13 Crp is not involved in PhoP-dependent regulation of *rovA*.
The *Y. pseudotuberculosis* strains YPIII and IP32953 and their respective *phoP*-positive and *phoP*-negative derivative were grown to exponential growth phase at 25°C or 37°C as indicated. **(A)** The β-galactosidase activity of a translational *crp-lacZ* (pAKH139) fusion was determined. The data represent the mean ± SEM of three independent experiments performed in triplicates. Data were analyzed by Student's t-test and do not differ statistically significant (n.s. – not significant). **(B)** Whole cell extracts were prepared, separated on 15% SDS-polyacrylamide gels and analyzed by Western blotting with a Crp specific antibody. YP89 (*Δcrp*) was used as negative control (c – loading control).

Furthermore, it was tested whether PhoP has an effect on *csrA* expression. To do so, the β-galactosidase activity of a translational *csrA-lacZ* fusion was determined in bacteria grown to exponential growth phase (Fig. 3.14). At 25°C and 37°C no significant differences could be detected, indicating that PhoP has no influence on *csrA* expression.

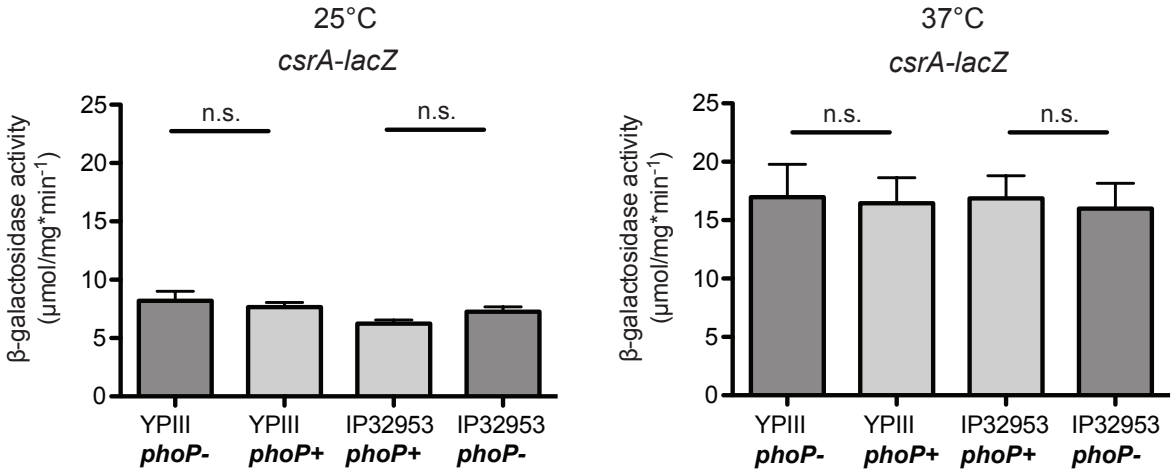

Fig. 3.14 Impact of PhoP on *csrA* expression in *Y. pseudotuberculosis*.
The *Y. pseudotuberculosis* strains YPIII and IP32953 and their respective *phoP*-positive and *phoP*-negative derivative were grown to exponential growth phase at 25°C or 37°C as indicated. The β-galactosidase activity of a translational *csrA-lacZ* (pKB63) fusion was determined. The data represent the mean ± SEM of three independent experiments performed in triplicates. Data were analyzed by Student's t-test (n.s. – not significant).

3.2.1.3 CsrC is involved in PhoP-dependent activation of *rovA* expression

An impact of PhoP on the Csr-system can still not be excluded, since the amount of free CsrA and activity of CsrA was not examined. CsrB and CsrC are small non-coding RNAs, which sequester CsrA from target mRNAs and thereby inhibit the function of CsrA (Heroven *et al*., 2008; Romeo *et al*., 2013). Increasing amounts of CsrB or CsrC would lead to decreased levels of active CsrA in the cell, although the expression of *csrA* does not change. Therefore expression analyses of *csrB* and *csrC* were performed in the different *phoP*-positive and *phoP*-negative derivatives (Fig. 3.15, Fig. 3.16).

Only low β-galactosidase activity of a *csrB-lacZ* fusion could be observed and revealed no differences between *phoP*-positive and *phoP*-negative derivatives at 25°C, but a slightly higher expression in the *phoP*-positive derivatives at 37°C (Fig. 3.15 A). While the activity of the β-galactosidase is similar at 25°C and 37°C in

Y. pseudotuberculosis YPIII, a temperature regulation of *csrB* could be observed in the IP32953 derivatives, which shows a four to five-fold induction at 25°C.

In addition to the expression analysis of the *csrB-lacZ* reporter fusion, transcript levels of CsrB were compared in the different *phoP*-positive and *phoP*-negative derivatives. For this purpose, total RNA of exponential grown YPIII and IP32953 was isolated and the CsrB transcript was quantified by Northern blotting (Fig. 3.15 B). Consistent with the results of the *csrB-lacZ* reporter gene fusion CsrB levels do not differ between *phoP*-positive and *phoP*-negative derivatives, neither at 25°C nor at 37°C. In contrast, the CsrB transcript is more abundant in IP32953 at 25°C compared to 37°C and shows the same temperature-dependency as the β-galactosidase activity of the *csrB-lacZ* reporter gene fusion (Fig. 3.15).

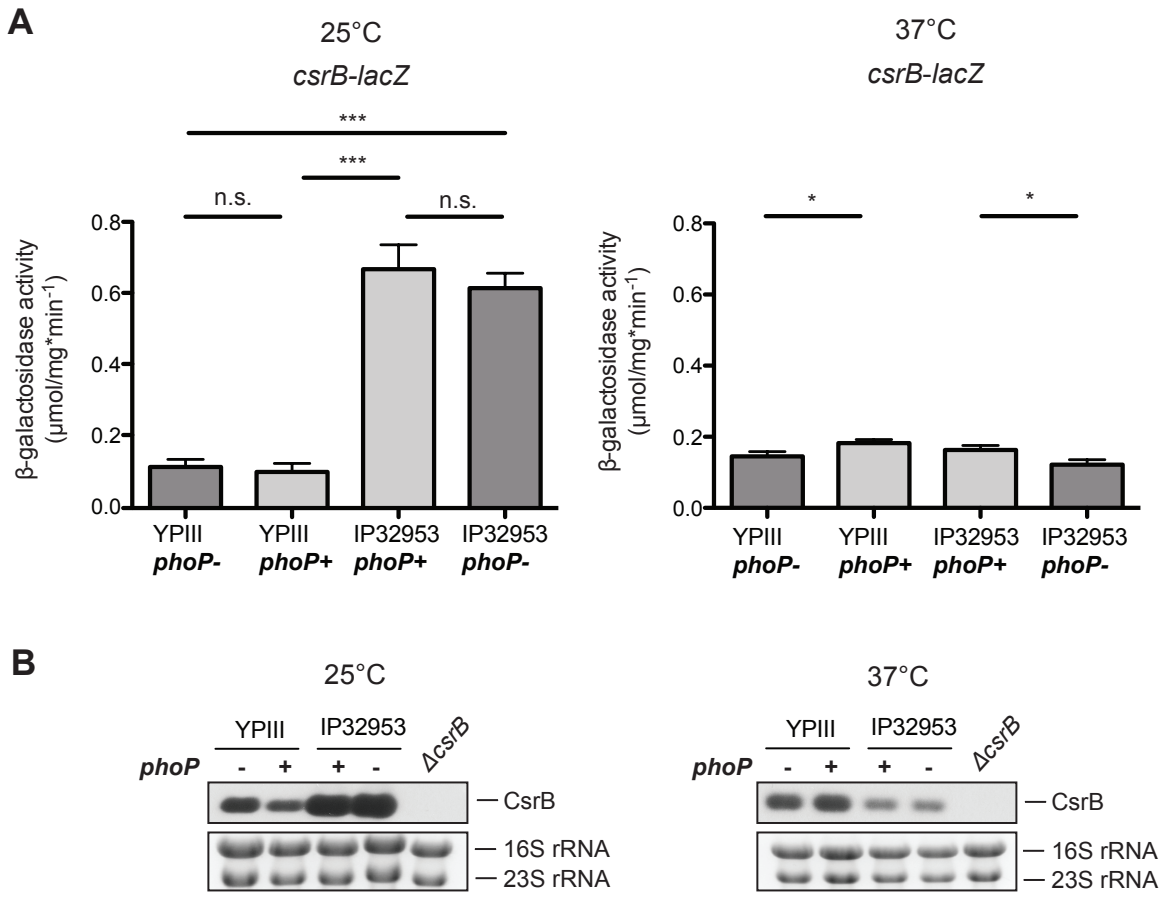

Fig. 3.15 PhoP-dependent expression of *csrB*.
The *Y. pseudotuberculosis* strains YPIII and IP32953 and their respective *phoP*-positive and *phoP*-negative derivative were grown to exponential growth phase at 25°C or 37°C as indicated. **(A)** The β-galactosidase activity of a *csrB-lacZ* (pAKH101) fusion was determined. The data represent the mean ± SEM of three independent experiments performed in triplicates. Data were analyzed by Student's t-test (*, P<0.05; **, P <0.01; ***, P <0.001; n.s. – not significant). **(B)** Total RNA was extracted, separated on 1.2% MOPS agarose gels and analyzed by Northern blotting with CsrB-specific probes. YP69 (*ΔcsrB*) was used as negative control, 16S rRNA and 23S rRNAs served as loading controls.

A comparison of the β-galactosidase activity of a *csrC-lacZ* fusion in the respective *phoP*-positive and *phoP*-negative derivatives revealed a significant increase at 25°C and 37°C in the *phoP*-positive derivatives (Fig. 3.16 A). The CsrC transcript levels confirm the data of the β-galactosidase assay; less CsrC is detectable in the derivatives harboring a truncated *phoP* (Fig. 3.16 B). Obviously, the β-galactosidase activity of YPIII (*phoP*$^-$) and IP32953 (*phoP*$^-$) is similar, while the amount of CsrC much higher in YPIII (*phoP*$^-$). This indicates that the stability of CsrC is different in the two clinical isolates.

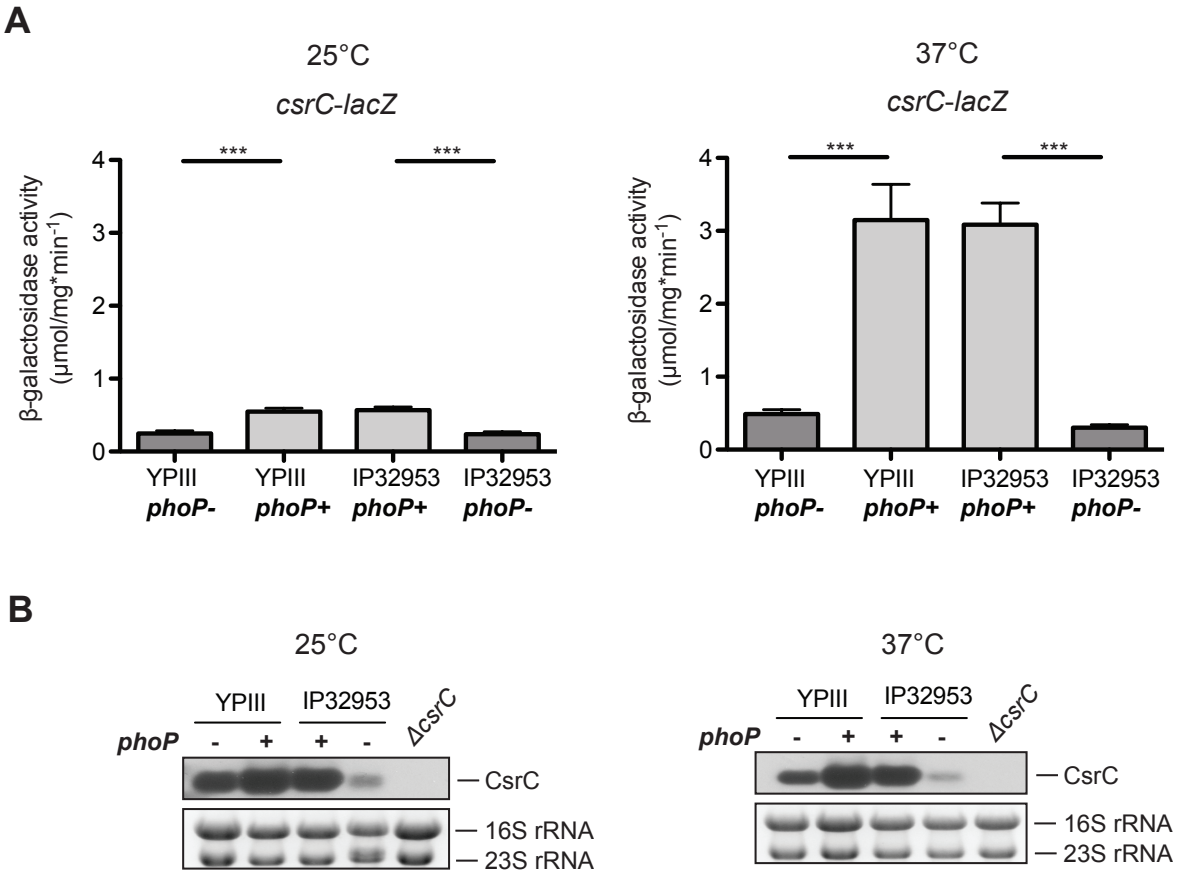

Fig. 3.16 PhoP activates *csrC* expression in *Y. pseudotuberculosis*.
The *Y. pseudotuberculosis* strains YPIII and IP32953 and their respective *phoP*-positive and *phoP*-negative derivative were grown to exponential growth phase at 25°C or 37°C. **(A)** The β-galactosidase activity of a *csrC-lacZ* (pAKH103) fusion was determined. The data represent the mean ± SEM of three independent experiments performed in triplicates. Data were analyzed by Student's t-test (*, P<0.05; **, P <0.01; ***, P <0.001). **(B)** Total RNA was extracted, separated on 1.2% MOPS agarose gels and analyzed by Northern blotting with CsrC-specific probes. YP126 (*ΔcsrC*) was used as negative control, 16S rRNA and 23S rRNA served as loading controls.

In summary, the data show that PhoP activates *rovA* expression via the CsrC-RovM regulatory cascade and does not affect *crp* and *csrA* expression.

3.2.1.4 PhoP binds directly to the regulatory region of *csrC*

The two-component system BarA/UvrY is known to directly control the expression of the small regulatory RNA *csrB*, while no transcriptional regulator of *csrC* was identified in *Y. pseudotuberculosis* so far (Heroven *et al*., 2008). Therefore, it was tested if PhoP directly controls *csrC* expression.

Previously, the promoter region of *csrC* was analyzed revealing the transcriptional start site (TSS) of *csrC* as well as the -35 and -10 region of the *csrC* promoter (Heroven *et al*., 2008). *In silico* analysis of the upstream region of *csrC* revealed two putative PhoP-binding sites 32 nucleotides and 94 nucleotides upstream of the TSS.

To test if PhoP binds to the upstream region of *csrC*, gel retardation assays were performed. For this purpose, three different fragments were analyzed. One fragment contains both putative PhoP-boxes (position +93 to -297 relative to the TSS (+1)). The two other fragments comprise only one of the two putative binding sites (position +93 to -76 and -55 to -297, respectively) (Fig. 3.17).

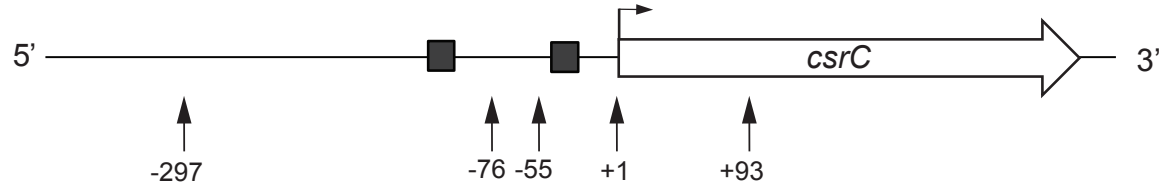

Fig. 3.17 Schematic overview of the *csrC* upstream region.
The transcriptional start site of *csrC* is indicated with +1, grey boxes represent the putative PhoP binding sites. The position of the fragments used for gel retardation assays are shown by vertical arrows with respect to the transcriptional start site of *csrC*.

Increasing amounts of purified His_6-PhoP protein were incubated with the different fragments of the *csrC* upstream region and *gyrA* as control fragment (Fig. 3.18). A retardation of the DNA-fragment containing both putative PhoP-boxes was observed, indicating the formation of a DNA-PhoP complex, whereas no binding was detectable to the negative control *gyrA* (Fig. 3.18 A). Additionally, a dissociation constant (K_d) of 1.7 µM was determined. In order to test whether *csrC* harbors one or two PhoP-binding sites, electrophoretic mobility shift assays were also performed with fragments containing either the first or the second putative PhoP-box. For both fragments a specific shift of *csrC* was observed, which indeed indicates the presence

of two PhoP-binding sites (Fig. 3.18 B, C). Determination of the K_d reveals a similar affinity of PhoP to both binding sites with about 3.3 µM for the first binding site and 3.9 µM for the second one. To validate this, a competitive electromobility shift assay was performed, in which both DNA-fragments with single binding sites were incubated simultaneously with PhoP (Fig. 3.18 D). In consistency with the K_d values, PhoP binds with the same affinity to both DNA-fragments .

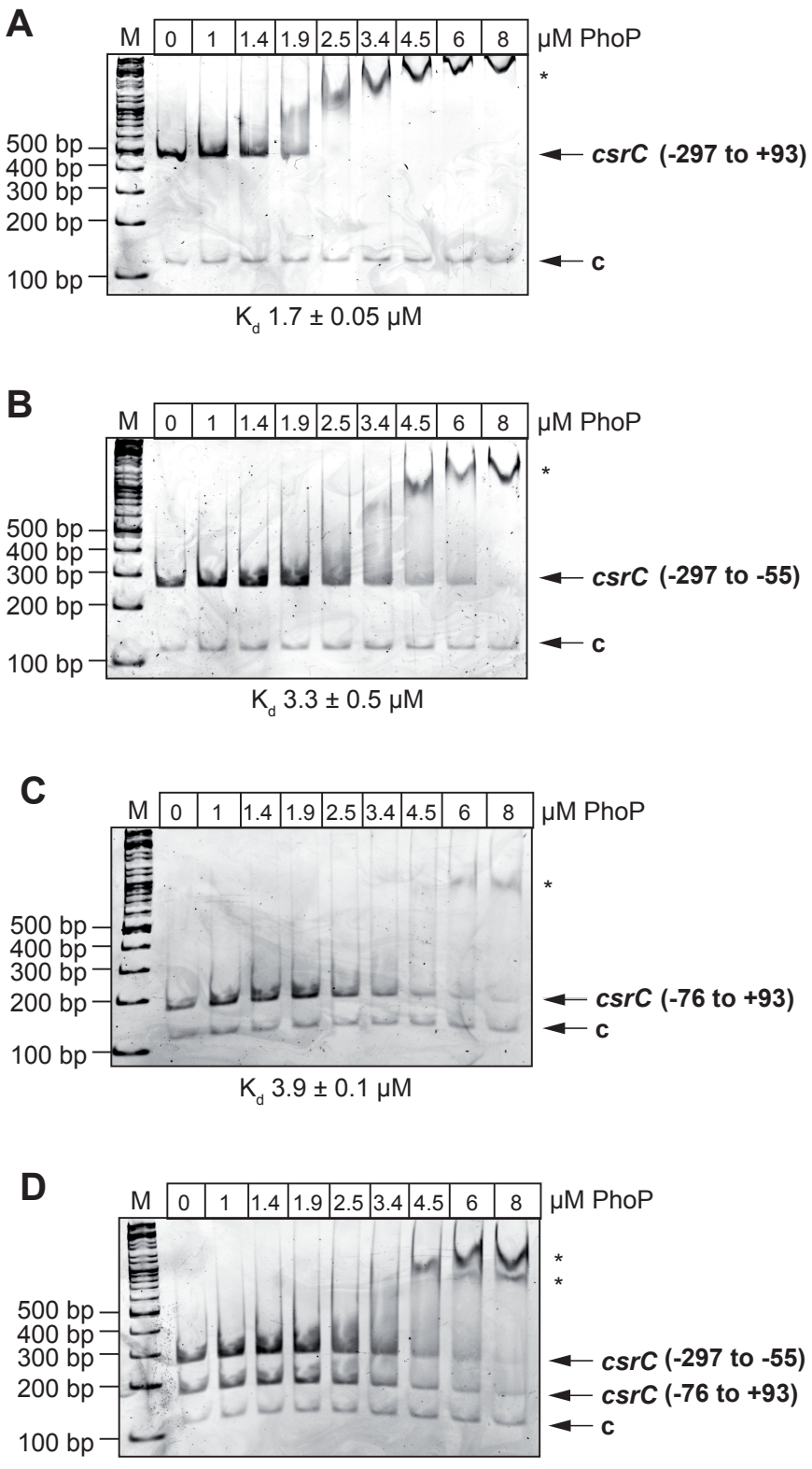

Fig. 3.18 PhoP binds to the regulatory region of *csrC*.
Increasing concentrations of purified His_6-PhoP were incubated with different fragments of the proximal region of *csrC* and separated on 5% polyacrylamide gels. The PhoP-DNA complexes are marked with an asterisk. *gyrA* was used as negative control (c). The *csrC* fragments were the following: **(A)** -297 to +93, containing both putative PhoP-boxes, **(B)** -297 to -55, containing the first putative PhoP-box and **(C)** -76 to +93, containing the second PhoP-box. The K_d values were determined densiometrically and show the mean ± SEM from three independent experiments. **(D)** Competitive assay with the *csrC* fragments from region -297 to -55 and -76 to +93.

To get further information about the precise binding sites of PhoP, DNaseI footprinting experiments were performed. For this purpose, increasing amounts of purified His_6-PhoP protein were incubated with the regulatory region of *csrC,* subsequently digested with DNaseI and separated on a 6% polyacrylamide gel (Fig. 3.19). Usually, binding of protein to the DNA results in a protection from the DNaseI digestion in the specific binding region. For both analyzed strands two protected regions are visible, reaching from position -112 to -85 and -39 to -19 for the sense strand and from position -112 to -85 and -49 to -18 for the anti-sense strand relative to the TSS (Fig. 3.19 A, B). Within the protected regions some nucleotides became hypersensitive against DNaseI, which is most probably caused by conformational changes of the DNA through binding of PhoP. The DNaseI footprinting reaction was repeated with the anti-sense strand after pre-incubation of PhoP with acetyl phosphate for 30 min (Fig. 3.19 C). Phosphorylation led to a more efficient binding of PhoP especially to the first binding site (position -49 to -18).

Taken together, the data reveal direct and specific binding of PhoP to two distinct sites of the *csrC* proximal region.

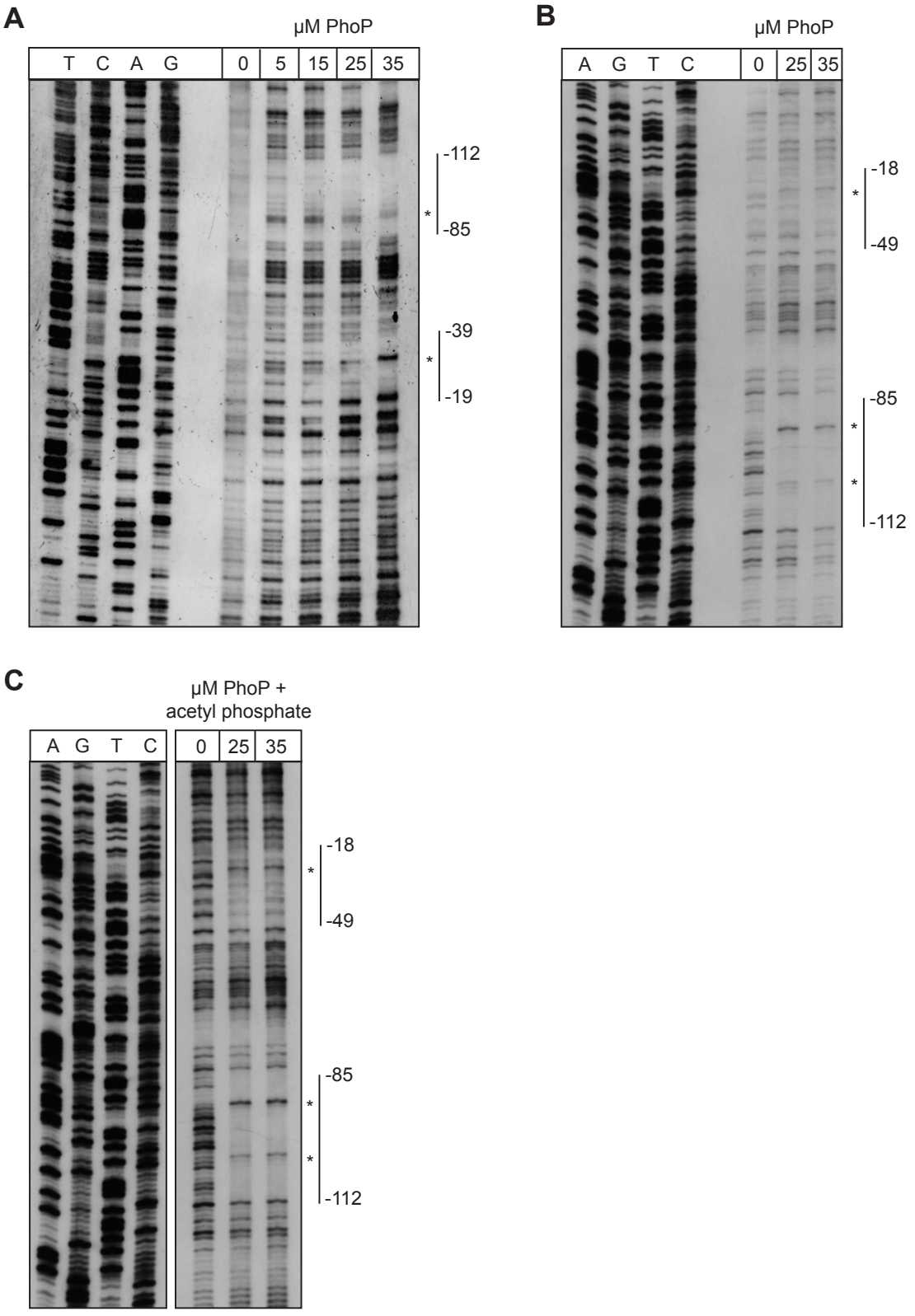

Fig. 3.19 DNase I footprint of PhoP with the regulatory region of *csrC*.
Increasing concentrations of purified His_6-PhoP were incubated with the proximal region of the sense **(A)** and anti-sense **(B)** strand of DIG-labeled *csrC*, digested with DNaseI and separated on 6% polyacrylamide gels. The DNaseI protected regions are marked with vertical bars, hypersensitive regions are indicated by asterisks. The numbers represent the nucleotide position upstream of *csrC,* the lanes T, C, A, G designate the Sanger sequencing reactions. **(C)** DNaseI footprinting reaction of the anti-sense strand after pre-incubation of PhoP with 20 mM acetyl phosphate for 30 min at 25°C.

3.2.1.5 PhoP-dependent synthesis of two CsrC transcripts

The TSS of *csrC* was already mapped 2008 by Heroven *et al*. in *Y. pseudotuberculosis* YPIII. Here, the TSS was investigated in the *phoP*-positive and *phoP*-negative derivatives of *Y. pseudotuberculosis* YPIII (Nuss and Schuster *et al*., 2014). The data confirmed the identified TSS, but an additional TSS was found 61 nt further upstream. Additionally, putative promoter sequences with PhoP binding sites located in close proximity were identified upstream of the two TSSs (Nuss and Schuster *et al*., 2014).

The two different TSSs led to the assumption that *csrC* is transcribed from two different promoters, leading to two distinct CsrC transcripts. In order to confirm this hypothesis, a high-resolution Northern blot was performed with the respective *phoP*-positive and *phoP*-negative derivatives of *Y. pseudotuberculosis* YPIII and IP32953 (Fig. 3.20). In fact, two CsrC transcripts were identified in the *phoP*-positive derivatives of YPIII and IP32953. In the *phoP*-negative derivative of *Y. pseudotuberculosis* YPIII only the shorter transcript is visible, while in the *phoP*-negative derivative of IP32953 no CsrC was detectable.

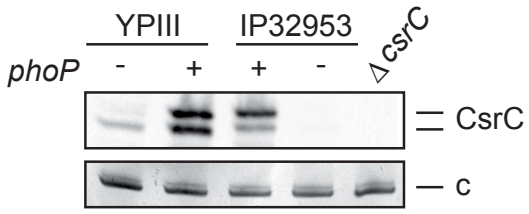

Fig. 3.20 High resolution Northern blot of CsrC.
The *Y. pseudotuberculosis* strains YPIII and IP32953 and their respective *phoP*-positive and *phoP*-negative derivative were grown to exponential growth phase at 25°C and samples were taken. RNA was extracted, separated on a high-resolution urea-polyacrylamide gel and analyzed by Northern blotting with CsrC specific probes. YP126 (*ΔcsrC*) was used as negative control (c – loading control).

3.2.1.6 An insertion of 20 nucleotides is responsible for a decreased CsrC transcript stability in *Y. pseudotuberculosis* IP32953

Previous results indicated a difference in the stability of CsrC in *Y. pseudotuberculosis* YPIII and IP32953 (see Fig. 3.16). Furthermore, a sequence alignment of *csrC* in different *Y. pestis* and *Y. pseudotuberculosis* strains revealed an additional 20 nucleotide stretch in *csrC* of *Y. pseudotuberculosis* IP32953, which is

not present in the other *Yersinia* strains and probably the result of two duplication events.

In order to prove the hypothesis that the stability of CsrC is reduced in *Y. pseudotuberculosis* IP32953 compared to YPIII, a CsrC stability assay was performed (Fig. 3.21). For this purpose, *csrC* of YPIII and IP32953 was inserted into strain YP285 (YP149 *ΔcsrC*), generating strains YP308 and YP307, respectively. *Y. pseudotuberculosis* YP285 harbors a functional *phoP* and accomplishes full expression of *csrC*. Moreover, the additional 20 nucleotides of *Y. pseudotuberculosis* IP32953 *csrC* were inserted into *csrC* of YPIII, yielding *Y. pseudotuberculosis* YP306. The different strains were grown to exponential growth phase at 25°C and transcription was blocked by the addition of rifampicin. At certain time points samples were taken and analyzed by Northern blotting. The blots revealed a clear reduction in $CsrC_{IP32953}$ stability. The half-life of $CsrC_{YPIII}$ is approximately 90 min, while $CsrC_{IP32953}$ has a half-life of only 42 min. The insertion of the 20 nucleotide stretch in strain YP306 harboring $csrC_{YPIII + 20\ nt\ IP32953}$ led to an enhanced degradation rate, which results in a half-life similar to $CsrC_{IP32953}$ of about 42 min.

To conclude, CsrC of *Y. pseudotuberculosis* IP32953 has a reduced stability compared to *Y. pseudotuberculosis* YPIII, which is caused by an insertion of 20 nucleotides in *Y. pseudotuberculosis* IP32953.

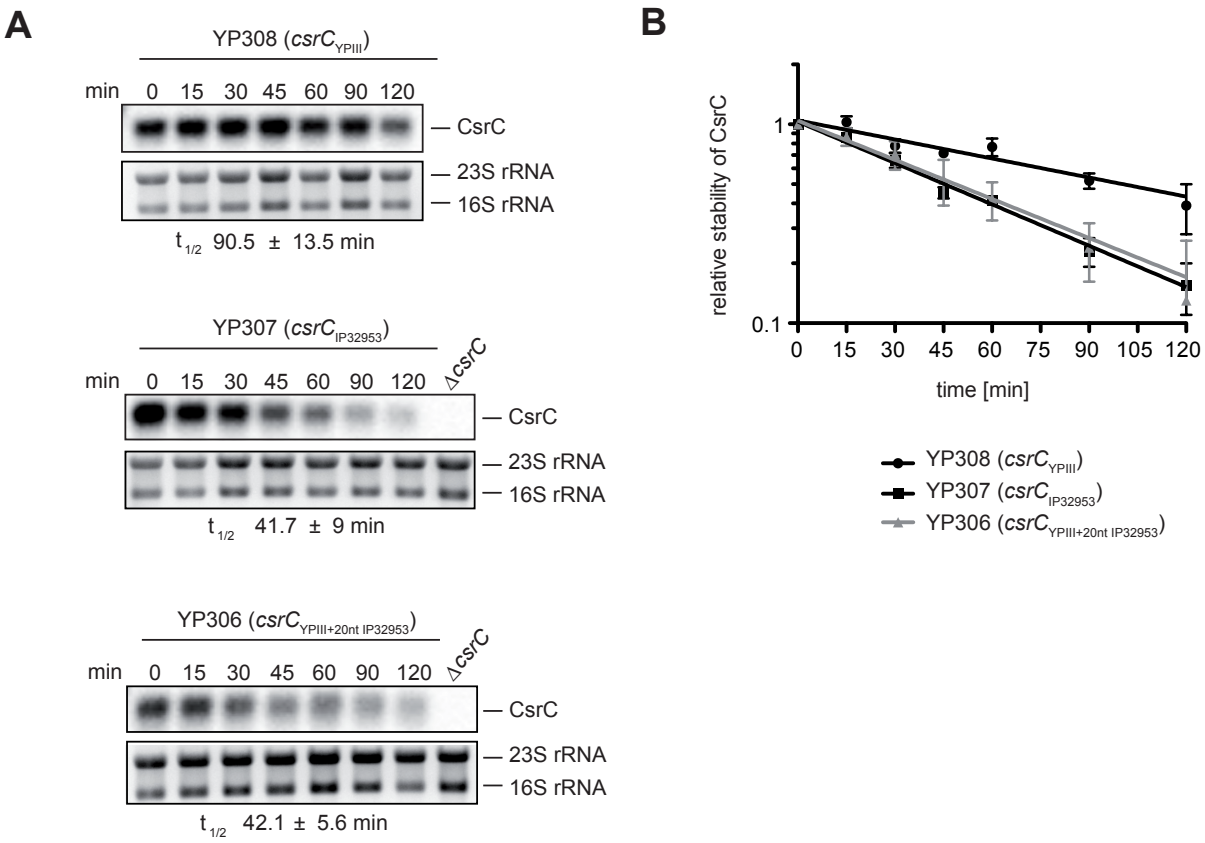

Fig. 3.21 RNA stability assay of CsrC.
(A) *Y. pseudotuberculosis* strains YP308 (*csrC*$_{YPIII}$), YP307 (*csrC*$_{IP32953}$) and YP306 (*csrC*$_{YPIII+20nt\ IP32953}$) were grown to exponential growth phase at 25°C and transcription was stopped by the addition of 2 mg/ml rifampicin. Samples were taken after 0, 15, 30, 45, 60, 90 and 120 min. RNA was extracted, separated on 1.2% MOPS agarose gels and Northern blotting was performed with CsrC-specific probes. YP126 (*ΔcsrC*) was used as negative control, 16S and 23S rRNAs served as loading controls. **(B)** The half-life of CsrC was measured in the strains YP308 (*csrC*$_{YPIII}$), YP307 (*csrC*$_{IP32953}$) and YP306 (*csrC*$_{YPIII+20nt\ IP32953}$). The data show the mean ± SEM from three independent experiments.

3.2.2 PhoP affects bistable *rovA* expression

To further investigate the effect of PhoP on bistable *rovA* expression in the different *Y. pseudotuberculosis* isolates YPIII and IP32953 and compare them with their respective isogenic *phoP*-positive and *phoP*-negative mutants, flow cytometry analysis and Western blots were performed at different temperatures. To do so, plasmid pKH70 (P$_{rovA}$-*egfp*$_{LVA}$) was transformed into the different strains and cells were grown to exponential growth phase. Comparing YPIII (*phoP*$^-$) and its cognate derivative YPIII (*phoP*$^+$) revealed RovA-dependent *egfp*$_{LVA}$ expression at higher temperatures in YPIII (*phoP*$^+$) (Fig. 3.22 A, B). A similar, but even more pronounced effect can be seen in the IP32953 strain (Fig. 3.22 C, D). *egfp*$_{LVA}$ is expressed at higher temperatures in the *phoP*-positive derivative of IP32953, while RovA-dependent *egfp*$_{LVA}$ expression is strongly diminished in IP32953 (*phoP*$^-$).

In summary, PhoP as new factor controlling bistable *rovA* expression independently of temperature could be identified.

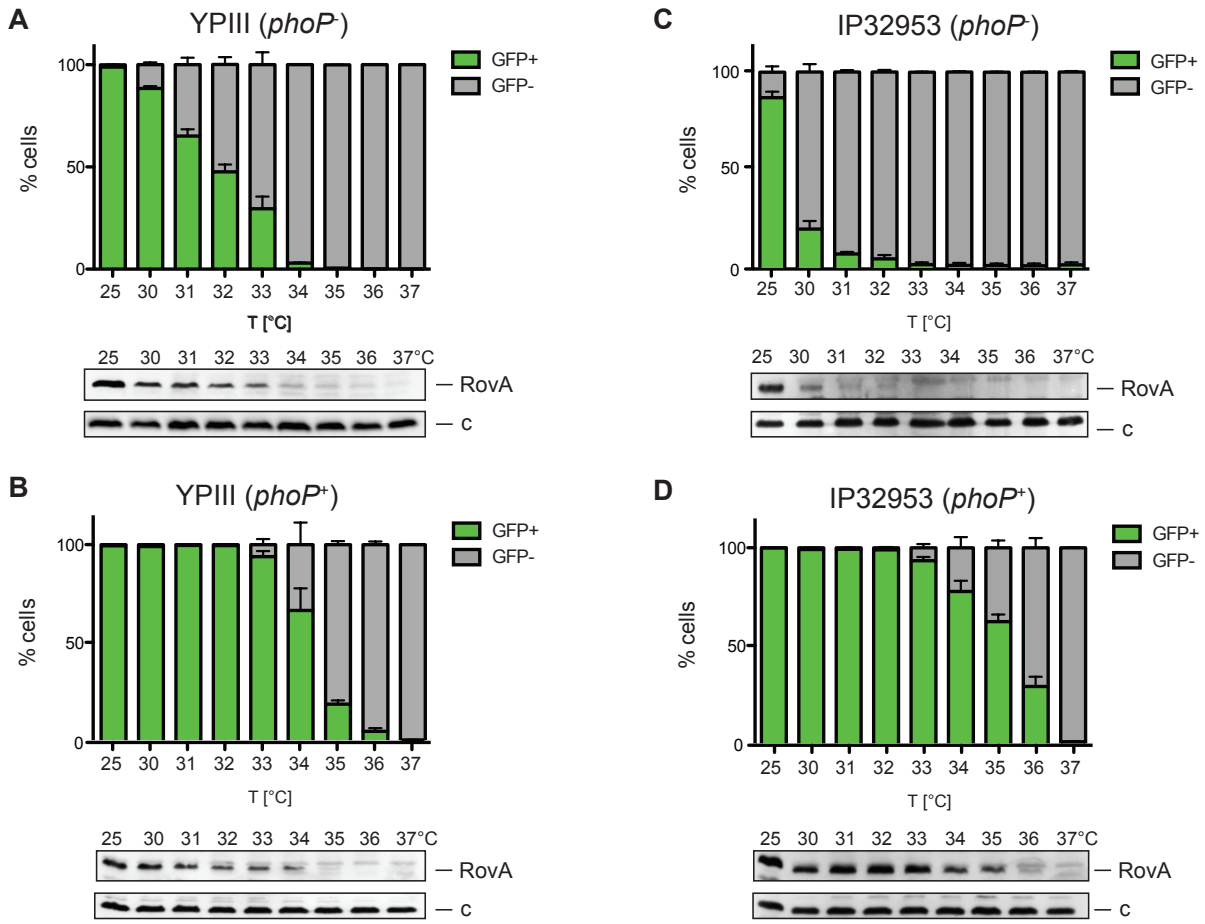

Fig. 3.22 PhoP-dependent P_{rovA}-*egfp*$_{LVA}$ expression.
Y. pseudotuberculosis YPIII (*phoP*$^-$) **(A)**, YPIII (*phoP*$^+$) **(B)**, IP32953 (*phoP*$^+$) **(C)**, IP32953 (*phoP*$^-$) **(D)** harboring plasmid pKH70 (P_{rovA}-*egfp*$_{LVA}$) were grown to exponential growth phase and samples were taken at indicated temperatures for flow cytometry and Western blot analysis. Upper panels show quantification of eGFP-positive and eGFP-negative cells measured by flow cytometry. The data show the mean ± SEM of three independent experiments performed in duplicates or triplicates. Lower panels show Western blots of chromosomally encoded RovA using a RovA specific antibody (c – loading control).

3.3 Analysis of bistable *rovA* expression in the mouse model

Since no expression of *rovA* could be observed in *Y. pseudotuberculosis* YPIII at 37°C under *in vitro* conditions, it was tested whether *rovA* is actually expressed in the host and if this expression is heterogeneous. Previously, it was reported that *invA* is expressed three days post infection (Pisano *et al*., 2012), which indicates that *rovA* might be also active during infection. The mouse model was used to characterize the expression of *rovA* under *in vivo* conditions.

3.3.1 Expression of P_{tet}-*mCherry* is suitable for investigations in combination with P_{rovA}-*egfp*$_{LVA}$

In order to analyze *rovA* expression in infected organs and to detect bacteria within colonized tissue an adequate reporter system had to be constructed. For this purpose plasmid pFS48, for constitutive expression of *mCherry* under the P_{tet} promoter, was constructed and tested for *mCherry* expression at different temperatures. No temperature-dependent expression of P_{tet}-*mCherry* was observed (Fig. 3.23 A, B). P_{tet}-*mCherry* was expressed within the entire population and the fluorescence intensity was very high under all tested conditions. Additionally, expression of P_{tet}-*mCherry* should not affect RovA-dependent *egfp*$_{LVA}$ expression. The constitutive expression of mCherry might be energy consuming and could influence the expression pattern of P_{rovA}-*egfp*$_{LVA}$. Also an interference of emission and/or excitation spectra of mCherry and eGFP could affect bistable P_{rovA}-*egfp*$_{LVA}$ expression. Therefore, bistable *rovA* expression was investigated in *Y. pseudotuberculosis* YPIII harboring the two plasmids pKH70 (P_{rovA}-*egfp*$_{LVA}$) and pFS48 (P_{tet}-*mCherry*) (Fig. 3.23 C, D). Flow cytometry revealed that bistability of RovA is not affected by constitutive *mCherry* expression. Two distinct subpopulation can be observed between 30°C and 34°C, similar to *Y. pseudotuberculosis* YPIII harboring just pKH70 (P_{rovA}-*egfp*$_{LVA}$) (Fig. 3.23 C, Fig 3.1 B). Also the RovA protein amount correlates with RovA-dependent *egfp*$_{LVA}$ pattern (Fig 3.23 D). Therefore, the combination of pFS48 (P_{tet}-*mCherry*) and pKH70 (P_{rovA}-*egfp*$_{LVA}$) seems to be suitable for further studies of RovA bistability in the mouse model.

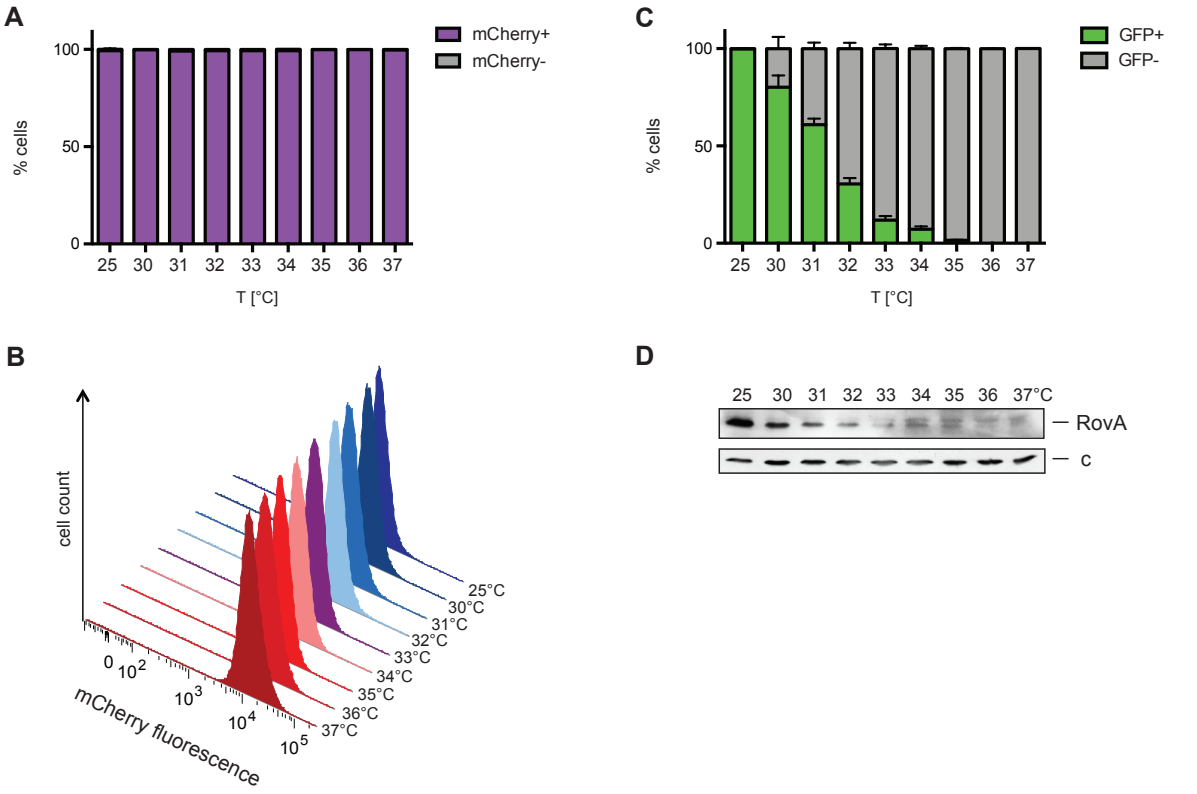

Fig. 3.23 Constitutively expressed *mCherry* has no influence on RovA-dependent expression of eGFP$_{LVA}$.
Y. pseudotuberculosis YPIII harboring plasmids pKH70 (P$_{rovA}$-*egfp*$_{LVA}$) and pFS48 (P$_{tet}$-*mCherry*) was grown to exponential growth phase and samples were taken at different temperatures for flow cytometry and Western blotting. **(A)** Quantification of mCherry-positive and mCherry-negative cells at indicated temperatures measured by flow cytometry. The data show the mean ± SEM of one experiment performed in triplicates. **(B)** Intensity of mCherry fluorescence at different temperatures is shown in a histogram. All cells express *mCherry* with a high intensity. **(C)** Quantification of eGFP-positive and eGFP-negative cells at indicated temperatures measured by flow cytometry. The data show the mean ± SEM of one experiment performed in triplicates. **(D)** Whole cell extracts were prepared, separated on 15% SDS-polyacrylamide gels and RovA expressed from the chromosomal *rovA* gene was analyzed by Western blotting with a RovA specific antibody (c – loading control).

3.3.2 Expression of *rovA in vivo*

In order to test if *rovA* is expressed *in vivo,* cryosections of infected tissue samples were prepared. Cryosections do not only allow quantification of *rovA* expressing cells, but further enable the analysis of the precise localization of RovA positive cells within tissues. Besides the expression of wild type *rovA* on single cell level in different organs, potential differences of bacteria expressing the different stabilized versions of RovA were investigated. For this purpose BALB/c mice were infected orally with 2x10^8 bacteria of *Y. pseudotuberculosis* YPIII (wt) or YP287 (RovA$_{P98S, G116A, SG127/128IK}$) carrying plasmids pKH70 (P$_{rovA}$-*egfp*$_{LVA}$) and pFS48 (P$_{tet}$-*mCherry*). Additionally, *Y. pseudotuberculosis* YPIII harboring only plasmid pFS48 (P$_{tet}$-*mCherry*) served as negative control to exclude unspecific green fluorescence.

Caecum and Peyer's patches were analyzed three days post infection (Fig. 3.24, Fig. 3.25). Bacterial cells were visualized by red fluorescence due to constitutive expression of P_{tet}-*mCherry*.

In the cryosections of the Peyer's patches only very few eGFP-positive cells were identified within red fluorescent microcolonies as shown in figure 3.24. Green fluorescence was specific for eGFP, as no background fluorescence could be observed for *Y. pseudotuberculosis* YPIII harboring only pFS48 (P_{tet}-*mCherry*) (Fig. 3.24). This reveals that RovA-dependent *egfp*$_{LVA}$ expression indeed occurs during Peyer's patch colonization. Moreover, no obvious differences in the amount or localization of eGFP-positive cells were observed between *Y. pseudotuberculosis* YPIII (wt) and YP287 ($RovA_{P98S, G116A, SG127/128IK}$).

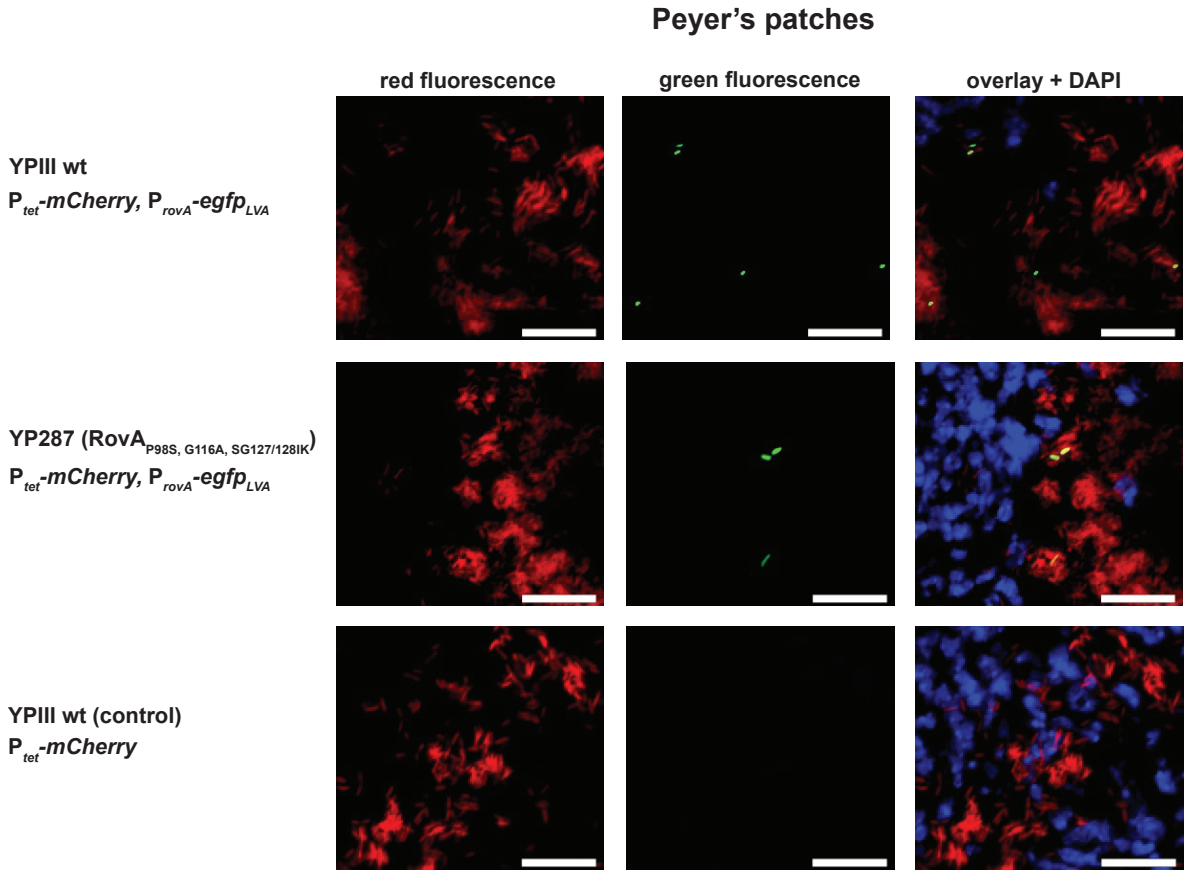

Fig. 3.24 Heterogeneous expression of P_{rovA}-*egfp*$_{LVA}$ in Peyer's patches.
BALB/c mice were orally infected with $2x10^8$ bacteria of either *Y. pseudotuberculosis* YPIII wild type (wt) or YP287 ($RovA_{P98S, G116A, SG127/128IK}$) harboring plasmids pFS48 (P_{tet}-*mCherry*) and pKH70 (P_{rovA}-*egfp*$_{LVA}$). *Y. pseudotuberculosis* YPIII wt harboring only plasmid pFS48 (P_{tet}-*mCherry*) served as a control. Three days post infection mice were sacrificed and Peyer's patches were isolated. Cryosections of 6-8 µm were prepared and imaged with a fluorescence microscope. Bacteria were visualized by *mCherry* expression. Green fluorescence indicates bacteria expressing P_{rovA}-*egfp*$_{LVA}$. DAPI was used for cell nuclei staining. Three mice were analyzed and a representative image is shown. White bars indicate 20 µm.

Bacteria expressing eGFP under the control of RovA were also identified in the caecum three days post infection (Fig. 3.25). While only few eGFP-positive cells were visible in the caecum of mice infected with *Y. pseudotuberculosis* YPIII (wt), a considerably higher amount was detectable in YP287 ($RovA_{P98S,\ G116A,\ SG127/128IK}$) infected tissue. eGFP-positive bacteria seem to be randomly distributed within microcolonies without any obvious spatial preference.

In order to exclude loss of reporter plasmids during infection, bacteria from infected tissues were plated on LB-agar with or without antibiotics. As a result, no plasmid loss was detected (Fig. S3).

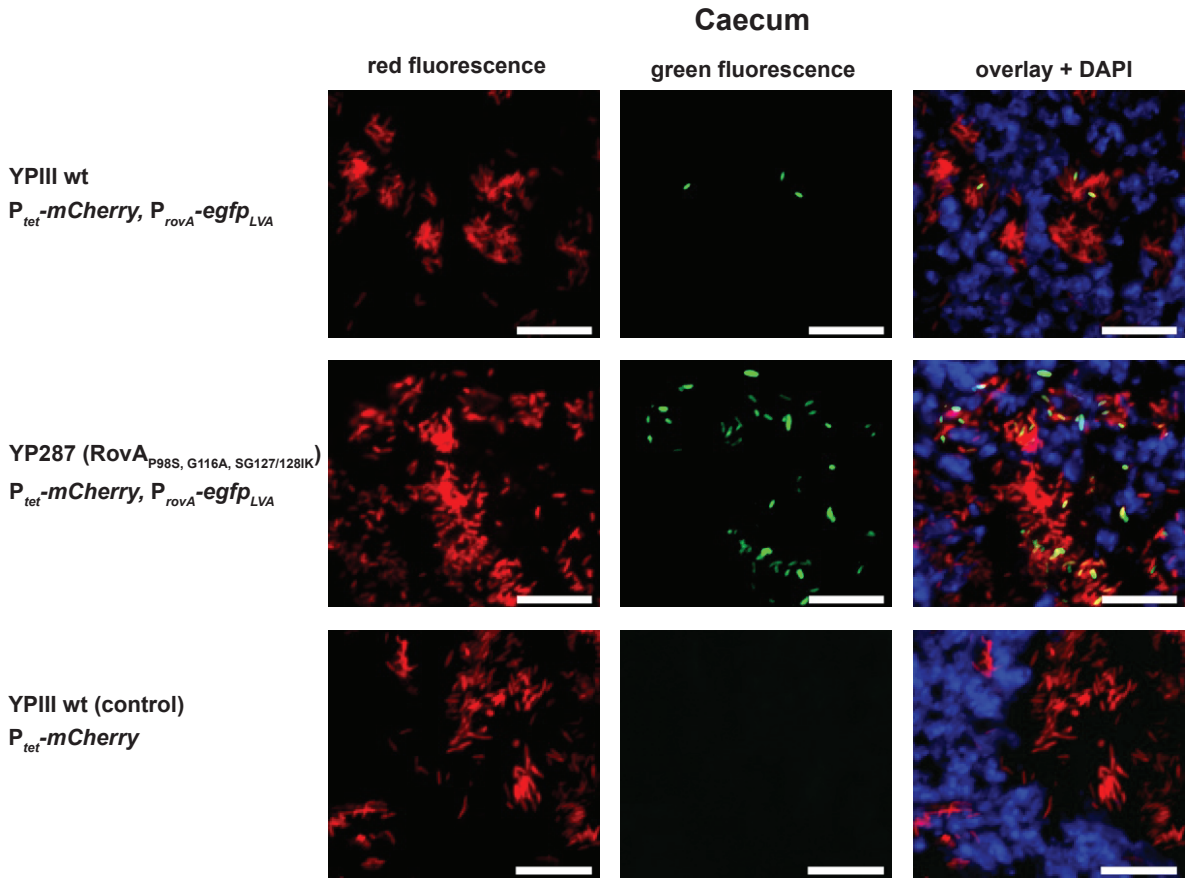

Fig. 3.25 Heterogeneous expression of P_{rovA}-*egfp*$_{LVA}$ in the caecum.
BALB/c mice were orally infected with $2x10^8$ bacteria of either *Y. pseudotuberculosis* YPIII wild type (wt) or YP287 ($RovA_{P98S,\ G116A,\ SG127/128IK}$) harboring plasmids pFS48 (P_{tet}-*mCherry*) and pKH70 (P_{rovA}-*egfp*$_{LVA}$). As control served *Y. pseudotuberculosis* YPIII (wt) harboring only plasmid pFS48 (P_{tet}-*mCherry*). Three days post infection mice were sacrificed and the caecum was isolated. Cryosections of 6-8 µm were prepared and imaged with a fluorescence microscope. Bacteria were visualized by *mCherry* expression. Green fluorescence indicates bacteria expressing P_{rovA}-*egfp*$_{LVA}$. DAPI was used for staining the cell nuclei. Three mice were analyzed and a representative image is shown. White bars indicate 20 µm.

Microscopic observation of the bacteria indicated that more bacteria expressing P_{rovA}-$egfp_{LVA}$ are located in the caecum of mice infected with *Y. pseudotuberculosis* YP287 ($RovA_{P98S,\ G116A,\ SG127/128IK}$) than with YPIII (wt) (Fig. 3.26). In Peyer's patches of *Y. pseudotuberculosis* YPIII (wt) as well as YP287 ($RovA_{P98S,\ G116A,\ SG127/128IK}$) infected mice only very few eGFP-positive cells were found. In the caecum of mice infected with *Y. pseudotuberculosis* YP287 ($RovA_{P98S,\ G116A,\ SG127/128IK}$) approx. 4% of all bacteria express $egfp_{LVA}$ in a RovA-dependent manner, while only 0.5% are found in *Y. pseudotuberculosis* YPIII (wt). This reveals a significantly increase of eGFP-positive cells of about eight-fold through stabilization of RovA.

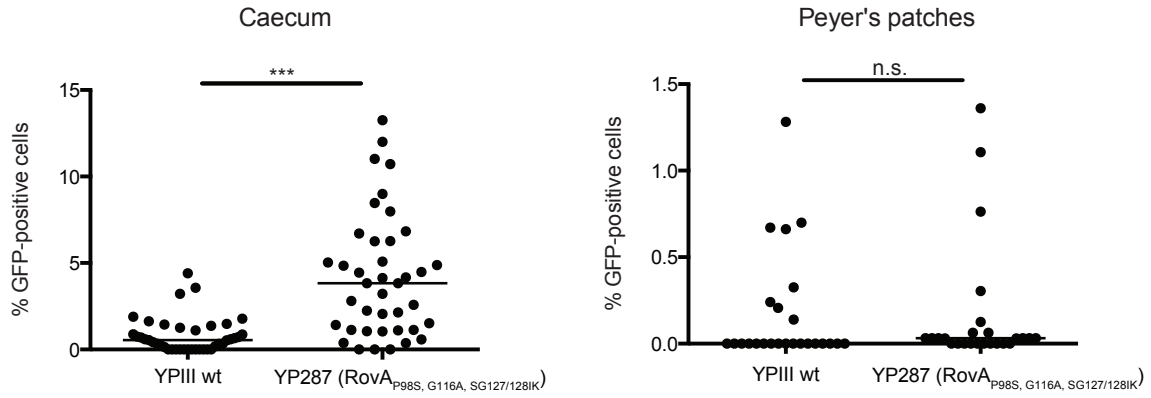

Fig. 3.26 Relative amount of P_{rovA}-$egfp_{LVA}$ expressing cells in caecum and Peyer's patches.
The amount of GFP-positive cells was counted and divided by the amount of all cells, which were visualized by red fluorescence through *mCherry* expression. Each dot represents the ratio of eGFP to mCherry-positive cells in one picture. Three to 23 pictures were analyzed per mouse; three mice were analyzed. The bar indicates the median of the data. Statistics were performed by Student's t-test with ***, P <0.001, n.s. - not significant.

In summary, the results show that bistable *rovA* expression occurs in caecum and Peyer's patches of *Y. pseudotuberculosis* YPIII (wt) and YP287 ($RovA_{P98S,\ G116A,\ SG127/128IK}$) three days post infection. Furthermore, stabilization of RovA leads to an increase of *rovA*-expressing bacteria in the caecum.

3.3.3 Bistable *rovA* expression and its role for virulence

One major goal of this study was to investigate the role of bistable *rovA* expression on virulence. It was previously shown that a *rovA* knock-out mutant in *Y. enterocolitica* is highly attenuated in virulence and the LD_{50} is significantly higher than in the wild type (Revell and Miller, 2002). In *Y. pseudotuberculosis* the *rovA*

deletion mutant does not colonize mice as efficiently as the wild type and dissemination to deeper organs such as liver and spleen is diminished (Heroven and Dersch, 2006). However, the impact of bistable expression and effect of the expression of stabilized variants of RovA on the virulence of *Y. pseudotuberculosis* remains unclear.

The substitutions of amino acid P98S, G116A and SG127/128IK within the RovA protein led to alterations in the bistable expression of *rovA in vitro*. To assess whether the modifications of RovA affect also bacterial pathogenesis, survival and organ burden experiments of *Y. pseudotuberculosis* YP269 ($RovA_{P98S}$), YP270 ($RovA_{G116A}$), YP287 ($RovA_{P98S, G116A, SG127/128IK}$) expressing different stabilized variants of RovA as well as *Y. pseudotuberculosis* YPIII wild type and YP107 (Δ*rovA*) were investigated in the mouse model.

For the survival experiment mice were orally infected with $2x10^8$ bacteria and survival, bodyweight and general appearance, such as rough fur, were monitored up to 15 days and the date of death was recorded (Fig. 3.27). All mice infected with *Y. pseudotuberculosis* YPIII (wt) developed severe symptoms of disease and succumbed to infection five to eight days post infection. In contrast, mice infected with YP107 (Δ*rovA*) as well as the stabilized mutants YP269 ($RovA_{P98S}$), YP270 ($RovA_{G116A}$) and YP287 ($RovA_{P98S, G116A, SG127/128IK}$) remained healthier and differed significantly from those infected with the YPIII wild type. Only about 50% of YP107 (Δ*rovA*), YP270 ($RovA_{G116A}$) and YP287 ($RovA_{P98S, G116A, SG127/128IK}$) infected mice displayed symptoms of disease and succumbed to infection, while the remaining mice developed only mild symptoms and regained weight after seven to ten days post infection. More than 60% of mice challenged with YP269 ($RovA_{P98S}$) succumbed within eleven days post infection and developed severe symptoms similar to the wild type.

Taken together, tight control of the bistable expression of *rovA* seems to be crucial for full virulence of *Y. pseudotuberculosis.* The stabilization of RovA, which results in an increase of RovA positive bacteria, had a similar effect on YPIII virulence as the complete loss of RovA.

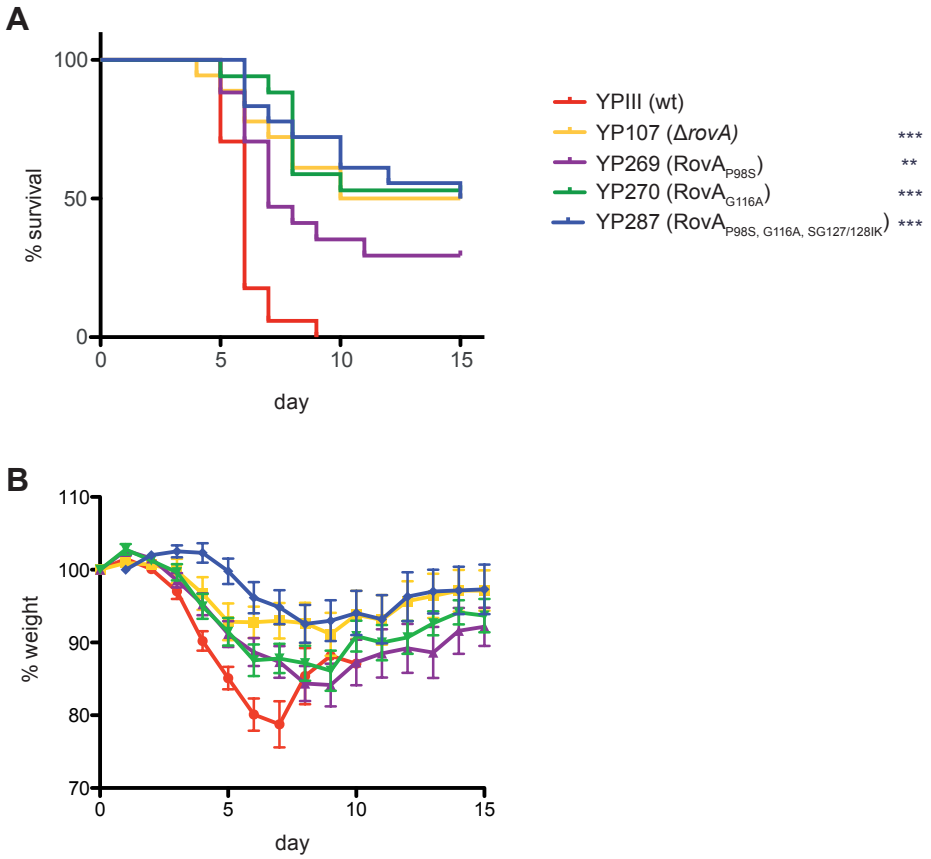

Fig. 3.27 Influence of RovA on the survival of BALB/c mice infected with *Y. pseudotuberculosis*.
BALB/c mice (n=17-18/strain) were orally infected with $2x10^8$ bacteria of *Y. pseudotuberculosis* YPIII wild type (red line), YP107 (Δ*rovA*, yellow line) as well as different stabilized RovA mutant strains; YP269 ($RovA_{P98S}$, purple line), YP270 ($RovA_{G116A}$, green line), YP287 ($RovA_{P98S, G116A, SG127/128IK}$, blue line). Survival **(A)** and bodyweight **(B)** were monitored up to 15 days post infection. Data were analyzed with log-rank (Mantel-Cox) test and show statistically significant differences between the wild type and mutant strains with **, P <0.01; ***, P <0.001.

3.3.4 Organ colonization is attenuated in the different *rovA* mutants

To determine the effect of stabilized RovA during the course of infection and identify differences in the bacterial load of the organs, colonization properties of the mutants were investigated. Therefore mice were orally infected with $2x10^8$ CFU of *Y. pseudotuberculosis* YPIII wild type (wt), YP107 (Δ*rovA*), YP269 ($RovA_{P98S}$), YP270 ($RovA_{G116A}$) or YP287 ($RovA_{P98S, G116A, SG127/128IK}$) and Peyer's patches, caecum, mesenteric lymph nodes (MLNs), liver and spleen were isolated one, three and five days post infection. The organs were homogenized, plated on LB and the CFUs were calculated per gram of tissue (Fig. 3.28, 3.29, 3.30).

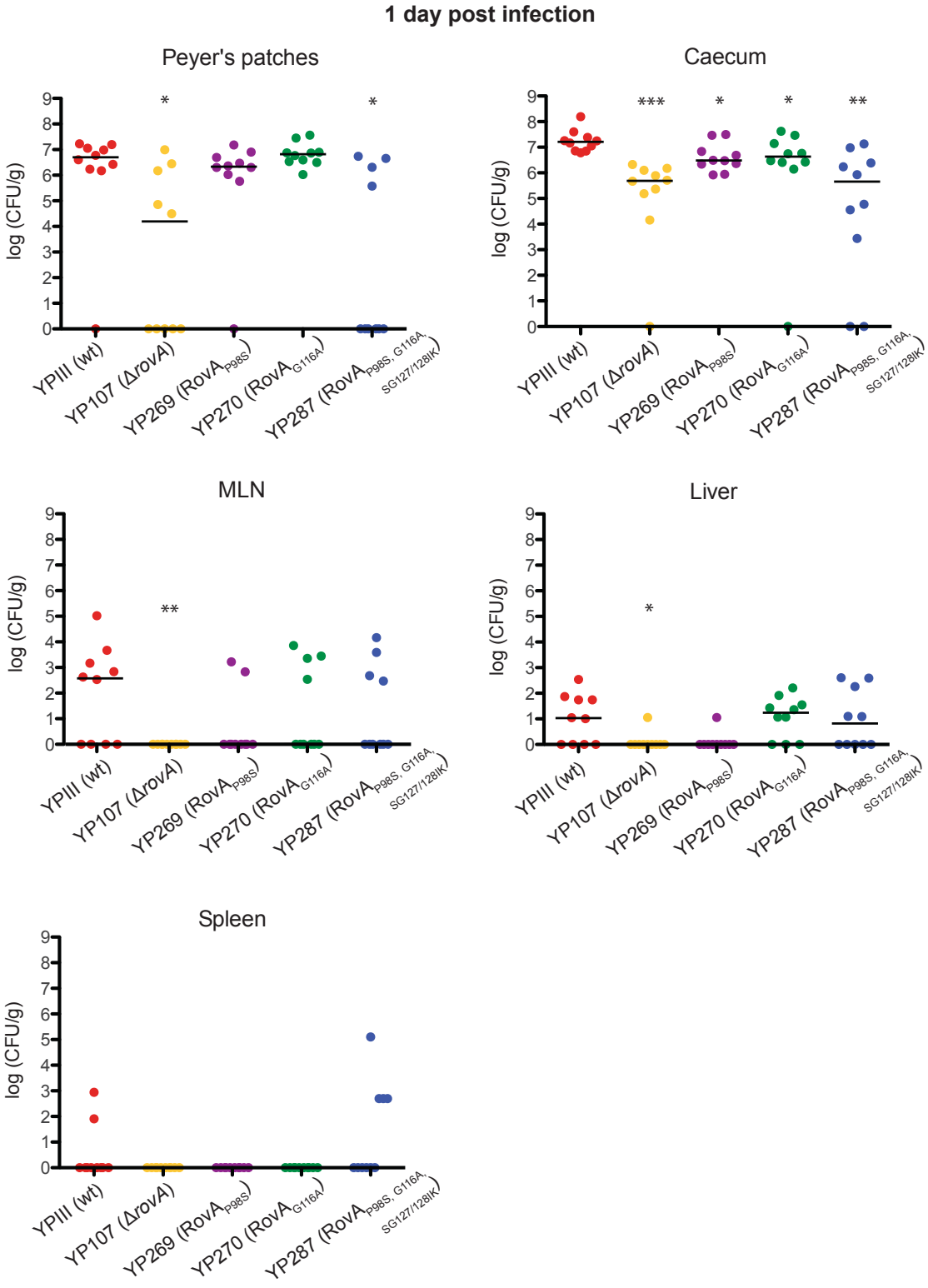

Fig. 3.28 Organ colonization of BALB/c mice one day after infection with *Y. pseudotuberculosis*.
BALB/c mice (n=10/strain) were orally infected with $2x10^8$ bacteria of *Y. pseudotuberculosis* YPIII wild type (wt), YP107 (Δ*rovA*) as well as YP269 ($RovA_{P98S}$), YP270 ($RovA_{G116A}$) and YP287 ($RovA_{P98S, G116A, SG127/128IK}$). One day post infection the number of bacteria in Peyer's patches, caecum, MLNs, liver and spleen were determined by plating. The dots represent the CFU per gram tissue of one mouse; lines illustrate the medians. Data were analyzed with Mann-Whitney test and show statistically significant differences between the wild type and mutant strains with *, $P<0.05$; **, $P<0.01$; ***, $P<0.001$.

One day post infection Peyer's patches are highly colonized by *Y. pseudotuberculosis* YPIII (wt), YP269 ($RovA_{P98S}$) and YP270 ($RovA_{G116A}$), while a significantly lower bacterial load was detectable in mice infected with YP107 (Δ*rovA*) and YP287 ($RovA_{P98S,\ G116A,\ SG127/128IK}$) (Fig. 3.28). All tested mutants were significantly impaired in colonization of the caecum, while the strongest attenuation was observed for YP107 (Δ*rovA*) and YP287 ($RovA_{P98S,\ G116A,\ SG127/128IK}$). At day one post infection only few bacteria could be recovered from MLNs, liver and spleen.

Three days post infection differences in the organ colonization between *Y. pseudotuberculosis* YPIII (wt) and the RovA mutants were pronounced (Fig. 3.29). Strain YP107 (Δ*rovA*) is attenuated in host invasion, replication within Peyer's patches and dissemination to deeper organs. The bacterial load in the organs of mice infected with strain YP287 expressing the most stabilized RovA variant is comparable to the Δ*rovA* mutant; Peyer's patches, caecum, MLNs and spleen show a significantly lower colonization than the wild type. All tested mutants affect the colonization of MLNs as a significantly lower bacterial load was determined in all strains in comparison to the wild type.

Consistent with the survival experiment, stabilization of RovA has a similar negative effect on host colonization efficiency as the deletion of *rovA*.

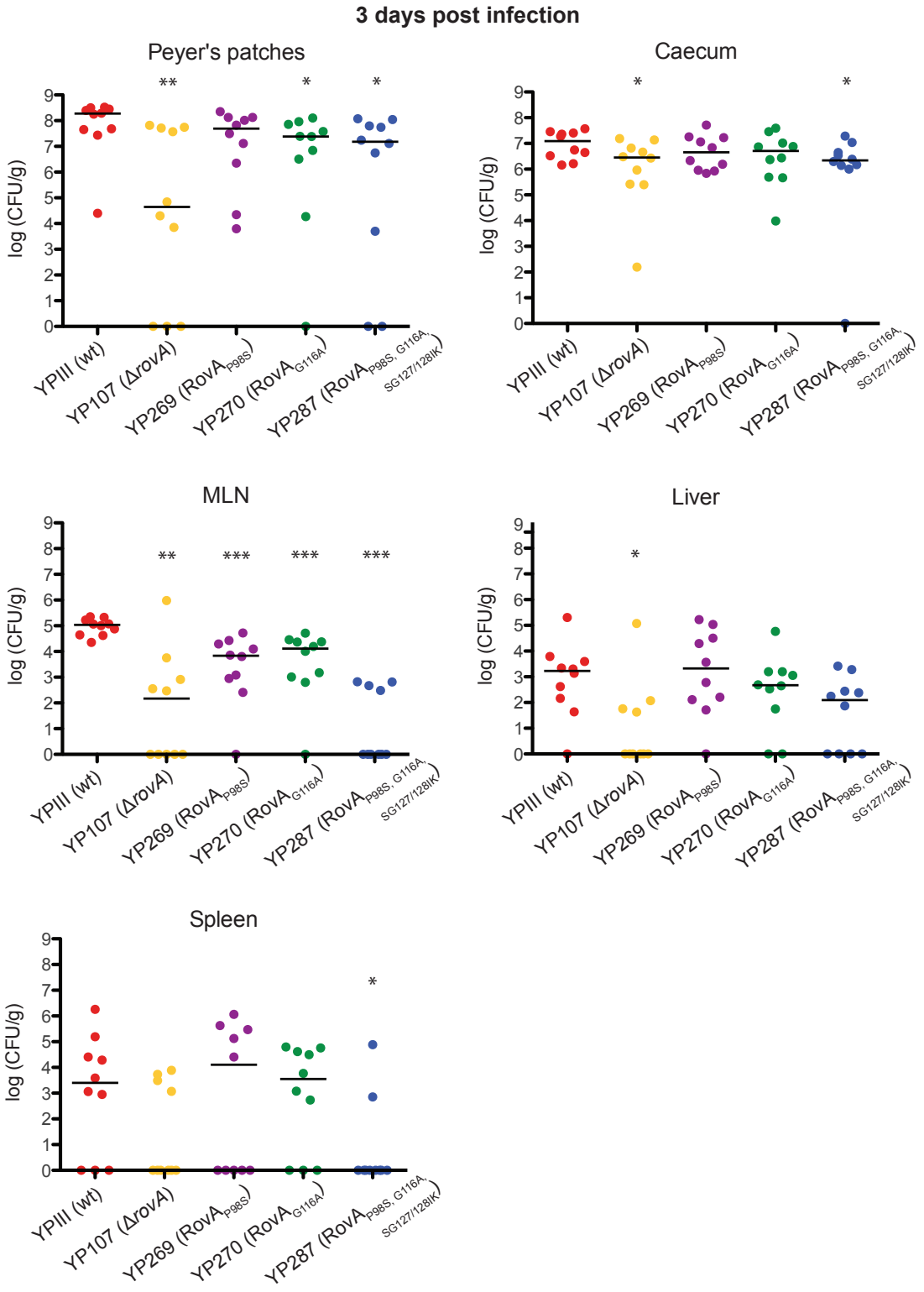

Fig. 3.29 Organ colonization of BALB/c mice three days after infection with *Y. pseudotuberculosis*.
BALB/c mice (n=10/strain) were orally infected with 2x10^8 CFU of *Y. pseudotuberculosis* YPIII wild type (wt), YP107 (Δ*rovA*) as well as YP269 (RovA$_{P98S}$), YP270 (RovA$_{G116A}$) and YP287 (RovA$_{P98S, G116A, SG127/128IK}$). Three days post infection the number of bacteria in Peyer's patches, caecum, MLNs, liver and spleen were determined by plating. The dots represent the CFU per gram tissue of one mouse; lines illustrate the medians. Data were analysed with Mann-Whitney test and show statistically significant differences between the wild type and mutant strains with *, P<0.05; **, P <0.01; ***, P <0.001.

At day five post infection differences in the colonization are no longer visible (Fig. 3.30). Only Peyer's patches and spleen show a lower bacterial load of YP107 (Δ*rovA*) than YPIII (wt). This indicates that the negative impact of a *rovA* knock-out mutant and stabilized RovA mutants is eliminated after several days of infection and most likely delayed compared to the wild type. Interestingly, although no differences in the colonization were detectable five days post infection; the survival rates differed significantly between the strains.

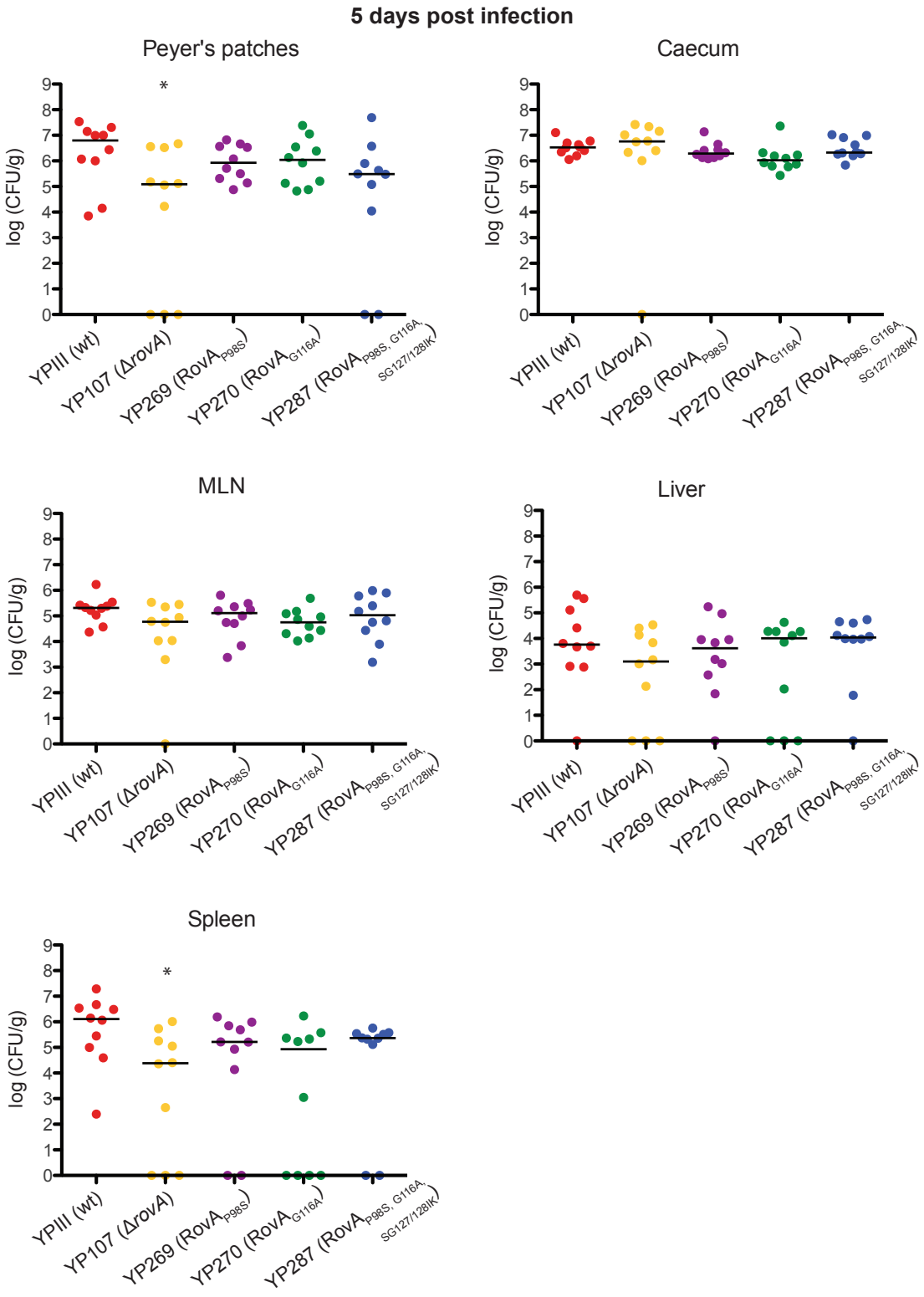

Fig. 3.30 Organ colonization of BALB/c mice five days after infection with *Y. pseudotuberculosis*.
BALB/c mice (n=10/strain) were orally infected with $2x10^8$ CFU of *Y. pseudotuberculosis* YPIII wild type (wt), YP107 (Δ*rovA*) as well as YP269 ($RovA_{P98S}$), YP270 ($RovA_{G116A}$) and YP287 ($RovA_{P98S, G116A, SG127/128IK}$). Five days post infection the number of bacteria in Peyer's patches, caecum, MLNs, liver and spleen were determined by plating. The dots represent the CFU per gram tissue of one mouse; lines illustrate the medians. Data were analysed with Mann-Whitney test and show statistically significant differences between the wild type and mutant strains with *, $P<0.05$; **, $P<0.01$; ***, $P<0.001$.

4 Discussion

Pathogenic bacteria are often confronted with fast changing environmental conditions, e.g. switching between environmental lifestyles and host colonization. In this process, bacteria have to rapidly adapt their gene expression pattern in order to be competitive with other microorganisms, to avoid recognition by the host immune system, to optimize their fitness and to save energy expenses (Straley and Perry, 1995). To this purpose, several mechanisms on transcriptional, post-transcriptional, translational and post-translational level have been evolved to rapidly regulate gene expression. However, pre-adaptation of a subset of the population to certain conditions might be even more advantageous in order to survive under sudden changes and environmental uncertainty, increasing the fitness of a species. This pre-adaption is accomplished via phenotypic heterogeneity. Phenotypic heterogeneity is a widespread phenomenon in bacteria that describes two or more cell types within one population and can arise through epigenetic changes and certain gene regulatory circuits. A special type of phenotypic heterogeneity is bistability, which is characterized by the bifurcation of one bacterial population into distinct subpopulations only by changes on transcriptional level without any mutations or DNA-rearrangements (Dubnau and Losick, 2006). A well-known example of bistability is described for sporulation in *B. subtilis*. Under nutrient-limiting conditions, Spo0A, the master regulator of sporulation, is activated by phosphorylation via a phosphorelay (Errington, 1993). The phosphorylation of Spo0A as well as the transcription of *spo0A* are under positive auto-regulatory control and were shown to be responsible for the heterogeneous phenotype in a sporulating culture (Strauch *et al*., 1992; Veening *et al*., 2005). The benefit of bistability is survival of a population during harsh conditions (bet-hedging) and an increased fitness of a population by divison of labor (Veening *et al*., 2008a).

In this study the bistable expression of the virulence regulator RovA of *Y. pseudotuberculosis* was examined. The mechanisms underlying *rovA* bistability as well as factors involved in formation of bistability were analysed. Moreover, the contribution of bistable *rovA* expression to virulence was investigated.

4.1 Bistability of RovA is characterized by a temperature-inducible switch

Temperature is one of the most important signals pathogenic bacteria monitor in order to adjust their virulence gene expression patterns. Therefore, it is not surprising that thermosensors on DNA, RNA and protein level evolved to sense temperature fluctuations via conformational changes (Klinkert and Narberhaus, 2009; Steinmann and Dersch, 2013). The nucleoid-associated protein H-NS was found to act on DNA topology, thereby affecting temperature-dependent transcription of target genes: expression of *virF* of *Shigella flexneri* is inhibited by DNA-bending at temperatures up to 32°C. At temperatures below 32°C H-NS interacts with two H-NS binding sites within the *virF* promoter and prevents transcription initiation. At higher temperatures the bent DNA opens up and as a result the transcriptional activator FIS can bind and activate *virF* transcription (Falconi *et al.*, 1998; Prosseda *et al*., 2004). Temperature-dependent expression of the DNA-binding protein LcrF of *Y. pseudotuberculosis* is regulated on RNA level (Böhme *et al.*, 2012; Hoe *et al*., 1992; Skurnik and Toivanen, 1992). At moderate temperature, the intergenic region of the polycistronic *yscW-lcrF* mRNA forms secondary structures that prevent binding of ribosomes through masking the ribosomal binding site. At host body temperature (37°C) the secondary structure melts and binding of ribosomes is enabled (Böhme *et al.*, 2012). Moreover, the transcriptional repressor TlpA of *S. enterica* serovar Typhimurium was shown to be a protein thermometer that forms coiled-coil homodimers at moderate temperatures, while a temperature increase to 37°C leads to a dissociation into non-functional monomers (Hurme *et al.*, 1997). Also RovA of *Y. pseudotuberculosis* was shown to act as a thermosensor by altering its conformation (Herbst *et al*., 2009). At host body temperature (37°C) the DNA-binding capacity of RovA is reduced. In this process, amino acids of the central DNA-binding domain are exposed, which are recognized by Lon and Clp proteases, leading to enhanced degradation of RovA (Herbst *et al*., 2009). Expression of *rovA* was further shown to be regulated by a positive and a negative feedback loop as well as cooperative binding (Heroven *et al.*, 2004). Additionally, it was described previously that DNA-binding and proteolysis are temperature-dependent (Herbst *et al*., 2009; Quade *et al.*, 2012).

In this study it was demonstrated that *rovA* is bistably expressed in a temperature-dependent manner. At moderate temperature the DNA-binding affinity of RovA is

high, while the degradation rate is low. As a consequence *rovA* is expressed in all cells within the entire bacterial population. A shift to 37°C decreases the DNA-binding affinity and enhances proteolysis reducing the overall amount of active RovA in the bacteria. Experiments following RovA expression in the population on single cell level demonstrated bistable *rovA* expression within a certain temperature range (30°C to 33°C). This led to the formation of RovA-positive and RovA-negative subpopulations. A mathematical modeling approach was used to describe the parameters involved in the establishment of bistable *rovA* expression and is given by a differential equation for the temporal change of RovA concentration in response to temperature (Fig. S4, Müller, J.; Münch, R.). The developed mathematical model predicted that the molecular determinants underlying the formation of two subpopulations at intermediate temperature are mainly the positive feedback loop and non-linear response of cooperative binding, which lead to an enormous increase of RovA amount in the cell and thereby reaching a critical threshold, which results in expression of *rovA*. A second important determinant for the establishment of bistable *rovA* expression is proteolysis, which leads to a fast degradation of RovA in the cell and thereby to a RovA-negative population. Thus, the modeling predicts two subpopulations with either high or low *rovA* expression dependent on the temperature.

Until now, no other temperature-tunable bistable switch was described in bacteria. The bistable expression of other regulators is mostly dependent on the growth phase or on the nutrient availability of the surrounding medium. For instance, expression of virulence genes of *Vibrio cholerae*, encoding the toxin-coregulated pilus and the cholera toxin, were shown to be bistable during entry into stationary phase (Nielsen *et al*., 2010). Phenotypic heterogeneity was also reported for *Salmonella* in host tissues through the formation of non-replicating persister cells, which are more tolerant to antibiotic treatment (Claudi *et al*., 2014; Helaine *et al*., 2014). This form of pathogen specialization indicates the importance of phenotypic heterogeneity also for virulence and demonstrates new challenges in disease control.

4.2 Autoregulation, proteolysis and DNA-binding contribute to bistable *rovA* expression

Time-lapse microscopy, which monitored the switching process of cells from the “ON” (*rovA* expression) to the “OFF” (no *rovA* expression) state and vice versa, revealed hysteresis of bistable *rovA* expression. In this process, bacterial cells tend to remain in the same state as the ancestor cell (Ninfa and Mayo, 2004; Veening *et al.*, 2008a). Hysteresis of bistable *rovA* expression was also confirmed by temperature up- and downshifts in bioreactor experiments (Nuss, A. M.; Bücker, R., unpublished data). Switching of the bacteria from the “ON” to the “OFF” state after a rapid temperature shift from 25°C to 37°C was fast, after three to four hours all bacteria were in the “OFF” state. The reverse switch was slow and even after eighteen hours at 25°C still one third of the bacterial population remained in the “OFF” state (Nuss, A. M.; Bücker, R., unpublished data). The mathematical model can be used to explain the mechanisms causing hysteresis. The model predicts that the net production rate of RovA in the cell tends to be zero at 37°C (Müller J.; Münch R., unpublished data). This explains the very slow “ON” switch after a temperature downshift, as possibly only stochastic fluctuations in basal gene expression are the main trigger for production of critical RovA amounts until a threshold is reached, which in turn lead to an “ON” switch. The rapid “OFF” switch is caused by an immediate stop of *rovA* transcription due to conformational changes of the RovA protein, which lead to reduced DNA-binding affinity and increased degradation of RovA (Herbst *et al*., 2009). A decreased production rate in combination with enhanced proteolysis seems to be the main effector for the fast “OFF” switch.

In order to get information about the molecular mechanisms underlying bistable *rovA* expression and confirm the prediction of the mathematical model that proteolysis is crucial for bistable *rovA* expression, mutations were introduced in the *rovA* gene leading to RovA variants with amino acid exchanges of P98S, G116A and SG127/128IK. These amino acid substitutions lead to stabilized RovA variants with enhanced DNA-binding affinity at 37°C and decreased proteolysis at 37°C. Data of this study demonstrated that in the mutants, expressing stabilized RovA variants, bistable *rovA* expression shifted to higher temperatures and occurs in a broader temperature range. Still, a stabilization of RovA due to exchange of the amino acids P98S, G116A and SG127/128IK do not lead to abrogation of bistability. As predicted

in the mathematical model, only extremely high or low degradation and production rates are able to abolish bistable *rovA* expression (Müller J.; Münch R., unpublished data). This indicates that bistable *rovA* expression is very robust to perturbations and the introduced amino acid exchanges of P98S, G116A and SG127/128IK are not sufficient to totally block proteolysis of RovA.

Furthermore, the mathematical model predicted that the positive feedback loop is the main requirement for the formation of bistable *rovA* expression (Müller J.; Münch R., unpublished data). To investigate experimentally the impact of the autoregulatory loops on bistable *rovA* expression, stabilized $RovA_{P98S,\ G166A,\ SG127/128IK}$ was expressed under the control of a constitutive promoter. The data demonstrated that the autoregulation has a high impact on bistable expression of *rovA,* but also show that bistable *rovA* expression can still be observed, especially at higher temperatures (34°C to 37°C). At host body temperature (37°C) only approximately 20% of the population are RovA-positive. The bistable expression of *rovA* even under the control of a constitutive promoter is caused by the remaining proteolysis of RovA, which is enhanced at 37°C. Moreover, expression of *lon* is temperature-dependent. At 37°C, significantly higher amounts of Lon protease are present compared to 25°C (Herbst *et al.*, 2009). Apart from temperature-dependent proteolysis of RovA, it is possible that the synthesis of RovA is temperature-dependent through so far unknown factors.

The influence of the autoregulatory loop was also described in other bistable systems, which are not temperature regulated, e.g. ComK of *B. subtilis*. The transcriptional regulator ComK is responsible for the appearance of bistability during competence development (Smits *et al.*, 2005). By un-coupling the expression of *comK* from positive autoregulation with an inducible promoter, bifurcation into two subpopulations was fully abolished (Smits *et al*., 2005). This confirms that bistability of RovA is not only caused by the autoregulatory loop, but also by proteolysis or additional unknown factors.

4.3 Fine-tuning of the RovA bistable switch by environmental factors

The bistable expression of *rovA* was demonstrated to be mainly promoted by proteolysis and autoregulation, which are both temperature-dependent. Besides

temperature, also nutrients, pH and ion concentrations are crucial signals pathogenic bacteria sense in order to adapt their gene expression pattern. The two-component system PhoP/PhoQ is one of the main transduction systems involved in virulence of many pathogenic bacteria like *Salmonella*, *Mycobacterium* and *Yersinia* and senses low Mg^{2+}-concentrations, antimicrobial peptides and acidic pH (Grabenstein *et al*., 2004; Miller *et al*., 1989; Pérez *et al.*, 2001). Data of the present study reveals a connection of PhoP with the virulence regulator RovA. The analysis of different *phoP*-positive and *phoP*-negative *Y. pseudotuberculosis* strains demonstrated that PhoP activates *rovA* expression through the non-coding RNA CsrC. PhoP positively affects *csrC* expression by direct binding to two distinct binding sites within the regulatory region of *csrC*, identifying the first transcriptional regulator of *csrC* in *Y. pseudotuberculosis*. So far, only factors indirectly controlling *csrC* expression were described. For instance, Crp positively regulates CsrC by acting indirectly via the other Csr-type regulatory RNA CsrB, which occurs mainly through counter-regulation of the two non-coding RNAs, and a CsrB-independent mechanism (Heroven *et al*., 2012a). Moreover, Hfq indirectly activates *csrC* expression on transcriptional level, while the *Yersinia* modulator protein YmoA stabilizes CsrC (Böhme, K., PhD thesis). In other bacterial species e.g. *E. coli* or *Salmonella,* both small regulatory RNAs are regulated by the BarA/UvrY or BarA/SirA two-component system, respectively, whereas in *Yersinia* only *csrB* is regulated by BarA/UvrY (Chavez *et al.*, 2010; Heroven *et al*., 2008; Martínez *et al.*, 2014). For *V. cholerae* three non-coding RNAs are described, which are all controlled by the homologues two-component system VarS/VarA and redundantly expressed (Lenz *et al.*, 2005). However, the small regulatory RNAs RsmY and RsmZ are differentially expressed in *Pseudomonas aeruginosa*. Both RNAs are activated by the two-component system GacA/GacS, which is homologous to the BarA/UvrY system, but the output of this activation depends on the incoming signal. While RetS activates both RNAs via the two-component system, HptB activates only *rsmY* via GacA/GacS through another distinct signalling pathway (Bordi *et al*., 2010). Nevertheless, all known non-coding RNAs of the Csr-system, except CsrC of *Yersinia*, are regulated by the BarA/UvrY system (Heroven *et al*., 2012b). The involvement of two independent signalling systems promotes a better fine-tuning of the regulation of virulence factors. The inducing signal for BarA/UvrY is unknown in *Yersinia*, but in *E. coli* and *S. enterica* serovar Typhimurium BarA is activated by formate, acetate and other short-chain

fatty acids (Chavez *et al*., 2010; Lawhon *et al*., 2002). These activating metabolites are produced by commensal bacteria and are present in the gastrointestinal tract, where they probably serve as energy source for *Yersinia* and other bacteria. Signals to activate the two-component system PhoP/PhoQ are low Mg^{2+}- and Ca^{2+}-concentrations, acidic pH as well as antimicrobial peptides, characteristics of professional phagocytes (Groisman, 2001; Groisman and Mouslim, 2006; Véscovi *et al*., 1996). Activated PhoP promotes survival and replication in macrophages by activating e.g. Mg^{2+}-transport systems as described for *Salmonella* and *Yersinia* (Li *et al*., 2008; Tao *et al*., 1995; Zhou *et al*., 2005). As demonstrated in this study, PhoP enhances expression of *rovA* and this might play a role in survival in macrophages. Moreover, Crp is involved in the regulation of the Csr-system in *Y. pseudotuberculosis,* which adapts the bacterial metabolism to different sugars (Heroven *et al*., 2012a). In the presence of glucose, a reduction of Crp and cAMP levels leads to the inhibition of the catabolism of alternative sugars, while under glucose-limiting conditions a Crp-cAMP-complex binds to target DNA and induces expression of catabolic pathways of other sugars (Saier, 1998). The different signals that are received by the Csr-system demonstrate the high complexity of this system and, as it was shown for PhoP, play a role in a fine-tuned bistable expression of *rovA,* which may contribute to the adaption to different niches within the host.

Furthermore, this study revealed a reduced stability of CsrC of *Y. pseudotuberculosis* IP32953 compared to *Y. pseudotuberculosis* YPIII. Responsible for this is the insertion of a 20 nucleotides stretch in *Y. pseudotuberculosis* IP32953, which renders the transcript more susceptible for degradation by RNases. A decreased stability of CsrC in *Y. pseudotuberculosis* IP32953 leads to a lower transcript level in comparison to *Y. pseudotuberculosis* YPIII, while the presence of PhoP in *Y. pseudotuberculosis* IP32953 results in a higher expression of *csrC* than in strain YPIII. In *Y. pseudotuberculosis* IP32953 PhoP is crucial for strong *rovA* expression, while PhoP is dispensable in *Y. pseudotuberculosis* YPIII for full *rovA* expression. The enhanced stability of CsrC in *Y. pseudotuberculosis* YPIII probably compensates the lack of PhoP and leads to a similar amount of RovA at 25°C in both strains. Moreover, in the present study it was demonstrated that two CsrC transcripts are synthesized dependent on PhoP. While the shorter transcript version is also produced in the absence of PhoP, but highly induced in the presence of PhoP, the expression of the longer transcript is strongly dependent on PhoP. Structure analysis

of the two CsrC transcripts using Mfold revealed no differences in the overall structure of CsrC, but an additional hairpin in the longer transcript (Nuss and Schuster *et al.*, 2014). The hairpin does not harbour any further GGA-motifs, which are preferably bound by CsrA. Thereby, an impact on CsrA by sequestration due to this additional hairpin is unlikely. Based on these data, a model for PhoP-dependent regulation of *csrC* is shown in figure 4.1.

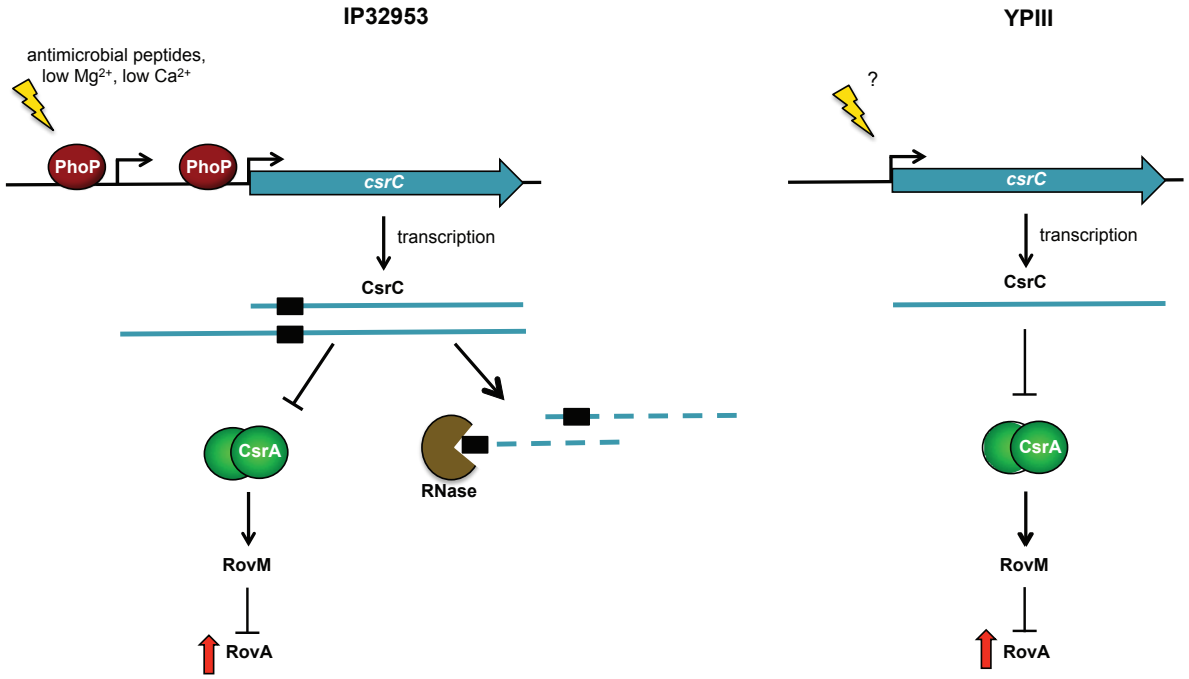

Fig. 4.1 Model of PhoP-dependent regulation of *csrC* in *Y. pseudotuberculosis* and strain-specific differences.
In *Y. pseudotuberculosis* IP32953 PhoP binds to two distinct binding sites in the promoter region of *csrC* and thereby activates expression of *csrC*. This leads to the synthesis of two CsrC transcripts, a shorter and an extended version. A 20 nucleotides stretch (indicated as black box) is responsible for a fast degradation of CsrC by RNases. *Y. pseudotuberculosis* YPIII carries a non-functional PhoP, thus *csrC* expression cannot be activated by PhoP. A so far unknown mechanism leads to transcription of *csrC*, which results in the synthesis of only the shorter CsrC transcript. Since *Y. pseudotuberculosis* YPIII does not harbor the 20 nucleotides stretch, CsrC is less susceptible to degradation. In both *Y. pseudotuberculosis* strains CsrC inhibits CsrA activity, which in turn results in lower RovM-levels and increased RovA synthesis.

As PhoP promotes survival and replication in macrophages (Grabenstein *et al.*, 2004; Oyston *et al.*, 2000) and controls the expression of the virulence regulator RovA, it is intriguing to analyse whether PhoP affects virulence of *Y. pseudotuberculosis*. Several studies regarding the influence of PhoP on virulence have been undertaken. A *phoP* mutant of *Y. pestis* strain GB has a reduced ability to survive in macrophages and is 75-fold less virulent in mice (Oyston *et al.*, 2000). Strikingly, the *phoP* mutant

of *Y. pestis* strain CO92 is not attenuated in virulence in mice, even if the survival in macrophages was decreased (Bozue *et al*., 2011). For a *phoP* mutant in *Y. pseudotuberculosis* 32777 a 100-fold decreased virulence in a murine oral infection model was reported (Grabenstein *et al*., 2004). Pisano *et al.* (2014) investigated the impact of PhoP in the same *Y. pseudotuberculosis* strains, YPIII and IP32953, that were also analyzed in this study. Consistent with previous results, survival in macrophages was significantly decreased in the isogenic *phoP* mutants of each strain. However, only a slight increase of the lethality was observed with mice infected with *Y. pseudotuberculosis* YPIII *phoP*$^{+}$ but not with IP32953. Overall, only a low impact of PhoP on virulence and organ colonization by the two strains was detected (Pisano *et al*., 2014).

4.4 Bistable expression of *rovA* during infection

Expression of *rovA* was previously shown to be temperature-dependent and repressed at 37°C (Herbst *et al.*, 2009; Nagel *et al.*, 2001). Flow cytometry data of this study also revealed that *rovA* expression is “OFF” in the whole population under *in vitro* conditions. Hence, it was questionable whether RovA-positive populations exist during the course of *Yersinia* infection. The presented data indeed demonstrated expression of *rovA* in the caecum and Peyer’s patches during acute infection. Around 0.5% of the bacterial population is RovA-positive in the caecum, while only very few RovA-positive bacteria were found in the Peyer’s patches. Temperature-independent factors such as nutrients, ion concentration, pH and oxygen concentration most likely contribute to expression of *rovA* *in vivo*. For instance, RovM was reported to repress *rovA* expression under nutrient-limiting conditions (Heroven and Dersch, 2006), which lead to an abrogation of bistable *rovA* expression. Moreover, it was shown in this study that bistable *rovA* expression shifts to a higher temperature range in the absence of RovM. As the gastrointestinal tract is nutrient-rich, a de-repression of *rovA* expression in the gut might lead to the formation of a small subpopulation of RovA-positive cells. Furthermore, it was demonstrated that *Y. pseudotuberculosis* secretes a factor during stationary phase, which was shown to enhance stability of RovA at 37°C (Herbst, K., PhD thesis; Mendonca, C., PhD thesis). A comparison of the *in vivo* and *in vitro* transcriptome of *Y. pseudotuberculosis* YPIII by RNA-seq at different growth phases revealed that the

expression pattern *in vivo* correlates best with gene expression during stationary phase (Nuss, A. M., unpublished data). Therefore, it is likely that this factor is produced *in vivo* leading to stabilization of RovA and consequently to a subpopulation of RovA-positive cells during infection.

Initial colonization of the host by enteropathogenic *Yersinia* occurs through the interaction of invasin with β_1-integrins on M-cells and further colonization of the underlying Peyer's patches (Clark *et al*., 1998). In a recent study it was described that invasion of the Peyer's patches is clonal by one single bacterium (Oellerich *et al.*, 2007). By infecting mice with a mixture of green and red fluorescing bacteria it was further demonstrated that a microcolony in liver and spleen is either green or red indicating a clonal formation of microcolonies (Oellerich *et al.*, 2007). As a consequence, formation of either RovA-positive or RovA-negative subpopulations most likely occurs after the invasion of the Peyer's patches in a growing microcolony and is not the result of heterogenous *rovA* expression within a bacterial population prior to invasion.

Phenotypic hetereogeneity plays an important role for virulence of pathogenic bacteria. Recently, another heterogeneous expression of virulence-associated genes was described for *Y. pseudotuberculosis* in the spleen of infected mice (Davis *et al.*, 2015). Exterior bacteria of a microcolony express *hmp*, which encodes a nitric oxide dioxygenase, while interior bacteria are *hmp*-negative. Exterior bacteria are surrounded by neutrophils, which release reactive nitrogen species as nitric oxide that can be detoxified by the nitric oxide dioxygenase. Moreover, bacteria located most peripherally are in direct contract to host cells and express *yopE* to prevent phagocytosis by neutrophils (Davis *et al*., 2015). This indicates that peripheral and interior bacteria of a microcolony respond to different signals dependent on their microenvironment (Davis *et al*., 2015). In contrast, cryo-sections of infected organs performed in this study demonstrated that single RovA-positive cells were randomly distributed among the RovA-negative population without any preferred site in the periphery or centre of a microcolony. Thus, a reaction to different microenvironments or host cell contact is rather unlikely.

The finding that *rovA* is expressed in the caecum leads to the hypothesis that it might help *Yersinia* to re-infect the host specifically from this organ during persistent infections. In this context, the bacteria would need to express *rovA* in order to

activate *invA* expression. In accordance with these observations, Fahlgren *et al.* (2014) identified the caecum as primary colonization site of *Y. pseudotuberculosis* during persistence. By using a sublethal infection dose, bacterial colonization of the caecum and in rare cases of Peyer's patches could be detected in infected but asymptomatic mice, indicating a persistent infection. As *Y. pseudotuberculosis* infections occur via the faecal-oral route, persistence in the gastro-intestinal tract is advantageous, because bacteria can spread by faecal shedding (Avican *et al*., 2015; Fahlgren *et al*., 2014). Therefore, expression of *rovA* in a subpopulation of cells might prepare a subset of the bacteria for better survival within the gut and enhance re-infection and/or shedding, which would support infection of a new host. Moreover, *in vivo* RNA-seq of bacteria during colonization of the caecum at early and persistent infection stages revealed a distinct transcriptional pattern (Avican *et al.*, 2015). The transcriptome during the persistent stage resembles the pattern observed at 26°C under *in vitro* conditions. While genes of the T3SS were down-regulated, an up-regulation of flagella genes, *invA* as well as *rovA* was monitored (Avican *et al*., 2015). In the persistent stage of infection, temperature is no longer the main environmental signal to adjust gene expression. More likely, low oxygen concentrations as well as oxidative and acidic stress seem to be crucial signals, as related genes were significantly up-regulated (Avican *et al.*, 2015). Bacteria in the persistent stage are often surrounded by polymorphonuclear neutrophils, which may trigger the activation of genes involved in protection against oxidative and acidic stress as well as limited oxygen concentrations (Avican *et al.*, 2015; Fahlgren *et al*., 2014). Therefore, it is conceivable that bistable expression of *rovA* not only contributes to *invA* expression to mediate re-infection of the host, but is further involved in the regulation of genes important to ensure survival during persistence.

Interestingly, the central regulator of biofilm formation CsgD in *S. enterica* serovar Typhimurium, which was shown to be bistably expressed, seems also important for persistence in the environment (Grantcharova *et al.,* 2010; MacKenzie *et al.,* 2015). In a liquid culture grown under biofilm-inducing conditions, the population bifurcates into aggregated and planktonic cells due to the differential expression of *csgD* (Grantcharova *et al.*, 2010). It is assumed, that the planktonic cells are primed for host cell invasion, while the multicellular aggregates prepare persistence outside the host (MacKenzie *et al.*, 2015). A similar mechanism is feasible for bistable expression of *rovA.* A small subset of RovA-positive cells might already prepare the

bacteria for the persistent infection stage, while the majority of cells, the RovA-negative subpopulation, expresses genes important for the defense of the host immune system during the acute infection phase such as the T3SS. Future experiments are directed to test whether *rovA* is expressed in a bistable manner during the persistent stage of infection and is indeed involved in the establishment of long-term infections.

Besides host mammalian colonization, bistable expression of *rovA* could also contribute to survival in invertebrates. It is well-known that *Y. pestis* colonizes insects such as the flea, which serves as a transmission vector to infect the human host (Perry and Fetherston, 1997). For instance, in *Y. pestis* expression of *phoP,* which activates the CsrA-RovM-RovA cascade is up-regulated in fleas during transition to warm-blooded hosts, which is believed to prepare the bacteria against attacks of the human immune system (Vadyvaloo *et al*., 2010). Also the enteropathogenic *Yersinia* species are able to colonize insects like flies (Rahuma *et al*., 2005; Zurek *et al*., 2000, 2001). Some of the *Y. enterocolitica* and *Y. pseudotuberculosis* strains carry a *tc* (toxin complex) gene cluster on a *tc* pathogenicity island (Fuchs *et al*., 2008). Tc proteins were first identified in the Gram-negative bacterium *Photorhabdus luminescens* and reported to have an insecticidal activity (Bowen and Ensign, 1998). For *Y. pseudotuberculosis* IP32953 an insecticidal activity was demonstrated against *Manduca sexta* larvae (Pinheiro and Ellar, 2007). So far, not much is known about the expression pattern and regulation of genes involved in colonization of insects by *Y. pseudotuberculosis*. However, it is likely that the temperature-dependent bistable expression of RovA is not only advantageous during shifts between a free-living lifestyle and the mammalian host, but could additionally favour the colonization of insects.

4.5 Tightly adjusted bistable *rovA* expression is crucial for virulence

The major aim of this study was directed to investigate the physiological relevance of bistable *rovA* expression for virulence. Mouse infection experiments clearly demonstrated that precise RovA-levels seem to be very crucial for full virulence of *Y. pseudotuberculosis* in mice. *Y. pseudotuberculosis* YPIII mutants which express a stabilized version of RovA, resulting in formation of larger RovA-positive

subpopulations especially at 37°C, were strongly attenuated in the mouse infection model. These mutants were impaired in colonization of Peyer's patches, caecum and MLNs. Especially the initial colonization of the *Y. pseudotuberculosis* YPIII Δ*rovA* mutant and mutants, which express the stabilized RovA variants, seems to be delayed in mice. At day five post-infection the differences in the bacterial load between the wild type and the mutants during the initial colonization were almost diminished. In the PhD thesis of R. Geyer it was demonstrated that a *Y. pseudotuberculosis* YPIII Δ*invA* mutant is also delayed in colonizing mice, which indicates that the attenuated colonization in the *Y. pseudotuberculosis* YPIII Δ*rovA* mutant arise due to the lack of induction of *invA* expression by RovA.

This study further revealed that higher amounts of invasin are produced at 37°C in the mutant strain expressing the stabilized $RovA_{P98S,\ G116A,\ SG127/128IK}$ variant. Invasin is important for the initial invasion of host cells, but is not expressed in the wild type at later infection stages (Nagel *et al*., 2001). Furthermore, invasin is highly immunogenic and leads to recognition by the host-immune system. It interacts with β_1-integrins on host cells and induces the release of cytokines and activation of NF-κB during uptake by the host cell (Grassl *et al*., 2003; Kampik *et al*., 2000; Schulte *et al.*, 2000). Recently, it was also shown that invasin induces formation of neutrophil extracellular traps in *Y. pseudotuberculosis* strains lacking the T3SS (Gillenius and Urban, 2015). These findings support the hypothesis that expression of *invA* in an increased portion of cells at later infection stages due to the stabilization of RovA might lead to a stronger reaction of the immune system, which could promote a faster elimination from infected medium. In order to prove this hypothesis, the production of cytokines and innate/adaptive immune cell dynamics should be analysed in future experiments.

Besides *invA*, it was described that RovA also affects central metabolic pathways in *Y. pseudotuberculosis*. Fluxome analysis of a *Y. pseudotuberculosis* YPIII Δ*rovA* mutant for instance revealed an increased pyruvate secretion during growth on glucose (Bücker *et al*., 2014). Moreover, the flux through the acetyl-CoA-tricarboxylic acid cycle was reduced in a *Y. pseudotuberculosis* YPIII Δ*rovA* mutant, which is caused by the lack of carbon in the core metabolism through the increased pyruvate secretion (Bücker *et al*., 2014). Moreover, a *Y. pseudotuberculosis* YPIII Δ*rovA* mutant was shown to be able to grow on nucleosides and the genes *nupC1* and

nupC2 encoding for nucleoside transporter, are up-regulated (Bücker *et al*., 2014; Heroven, AK., unpublished data). It is feasible that some RovA-positive cells are important to prepare the population to survive in a future environment, e.g. by up-regulation of nucleoside transporters, while an increased portion of this subpopulation of RovA-positive cells might be disadvantageous and therefore leads to an attenuation in virulence. Hence, a tight regulation of bistable *rovA* expression is crucial for virulence of *Y. pseudotuberculosis*.

4.6 Model of bistable *rovA* expression during infection

This study revealed for the first time expression of the virulence regulator RovA in a small subpopulation of *Y. pseudotuberculosis* in the Peyer's patches and the caecum during infection. According to the current data, a hypothetical model of bistable *rovA* expression at different infection stages was developed (Fig. 4.2). *Y. pseudotuberculosis,* adapted to the external environment and entering the host via contaminated food or water, is flagellated and expresses RovA, which activates *invA* expression. Invasin promotes uptake into M-cells and transcytosis to Peyer's patches. The temperature shift from environmental to host body temperature leads to changes in the expression pattern. After clonal invasion of the Peyer's patches a growing microcolony consists of two subpopulations with either high or low *rovA* expression. The majority of cells are in a RovA "OFF" state, in which consequently *invA* expression is turned off and the pathogen is less immunogenic. During persistence of *Y. pseudotuberculosis* in the caecum, the expression pattern changes again, whereby signals as nutrients, pH, ions and oxygen might be important. The signals are for instance sensed by the two-component systems BarA/UvrY and PhoP/PhoQ. Two different subpopulations can be found with either high (RovA "ON") or low (RovA "OFF") *rovA* expression. Cells in the RovA "ON" state are well prepared to re-infect the host or infect new host by shedding into faeces.

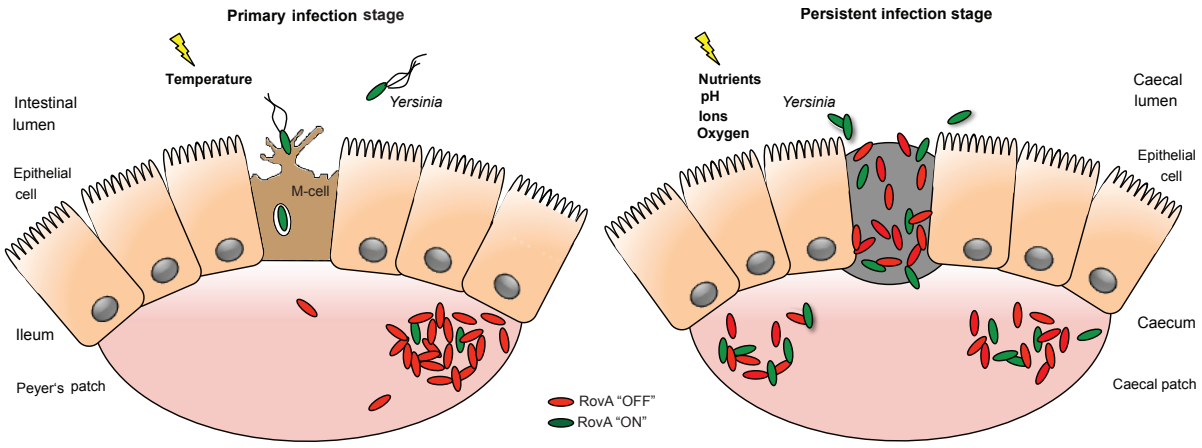

Fig. 4.2 Hypothetical model of bistable *rovA* expression at different infection stages.
During primary infection bacteria adapted to the external environment are RovA-positive (RovA "ON") and express early-stage virulence factors as invasin, which promotes interaction with β_1-integrins on M-cells and transcytosis through the M-cells to underlying Peyer's patches. Temperature is the main inducing signal to change the expression pattern. While in the Peyer's patches most cells are RovA-negative (RovA "OFF") and express genes important for the later phase of infection as genes encoding for the T3SS, some cells still express *rovA* (RovA "ON"). At the persistent infection stage factors as nutrients, pH, limited oxygen and ions are signals to change the expression pattern again leading to two subpopulations, which are either RovA "ON" or RovA "OFF". Expression of *rovA* contributes to re-infection and spreading to new hosts by shedding into faeces.

5 Outlook

The present study demonstrated that *rovA* of the enteric pathogen *Y. pseudotuberculosis* is expressed in a bistable manner during infection. Although most bacteria do not express the virulence regulator RovA during infection, a small subpopulation of RovA-positive bacteria were found in Peyer's patches and caecum at day three post-infection. In order to clarify whether *rovA* is bistable expressed in MLNs, liver and spleen or if it is restricted to gut-associated tissues, expression analyses should be also performed in these organs. However, it is likely that at early infection stages the bacterial load in the systemic organs might be too low to observe bistable *rovA* expression. To overcome this problem an alternative infection route, e.g. intravenous injection could be chosen. To elucidate the benefit of bistable *rovA* expression and the generation of two different subpopulations, it is important to gain more information about the amount of *rovA*-expressing cells at different infection stages, e.g. at one, three, five and seven days after infection. Since an impact of RovA during persistence is assumed, investigations concerning bistable *rovA* expression after a long infection period are required to prove the hypothesis. This could also reveal if *rovA* is more induced expressed during the persistent infection state.

Additionally, it was shown that bistable *rovA* expression is advantageous for pathogenesis of *Y. pseudotuberculosis* during infection of mice. A *Y. pseudotuberculosis* YPIII Δ*rovA* mutant and mutants expressing stabilized RovA variants are significantly attenuated in virulence. To test if invasin overexpression in the stabilized RovA variants is the main cause of the attenuation, *invA* should be deleted in those mutants and compared to the respective *invA*$^{+}$ strains. In this context, intravenous injections should be performed to avoid differences during primary host colonization due to InvA-mediated M-cell invasion. In order to address the question if the host immune response is altered as a consequence of stabilized RovA, immune response analyses and cytokine production assays should be performed. Moreover, a mutant, that constitutively expresses *rovA* at host body temperature (37°C) should be constructed and analysed *in vivo* in regard to survival and organ colonization of mice. This mutant could be compared to a strain, which

constitutively expresses *invA* in order to prove whether invasin is exclusively responsible for the phenotype or if other factors are involved.

In order to gain information on the biological function of bistable *rovA* expression, genes, which are differentially expressed in RovA-positive and RovA-negative cells, should be analysed in more detail. For this approach, transcriptome or proteome analyses, combined with previous cell sorting, could be performed to dissect the genes/proteins, which are differentially expressed in the RovA-positive and RovA-negative subpopulation. As the amount of RovA-positive cells might be too low in *Y. pseudotuberculosis* YPIII wild type, RNA-sequencing analyses of a Δ*rovA* mutant and a strain constitutively expressing *rovA,* could be compared to the wild type and might reveal differences in host and pathogen responses.

6 Summary

The enteropathogen *Yersinia pseudotuberculosis* switches routinely between a free-living lifestyle and host colonization. The bacterium is thereby confronted with different environmental challenges, such as nutrient fluctuations, responses of the host immune system, and the necessity of host cell invasion. The bistable expression of important regulators is an advantageous mechanism, evolved in order to survive rapid changes of environmental conditions. RovA of *Y. pseudotuberculosis* is a protein thermosensor regulating early-phase virulence genes, such as invasin. Due to conformational changes, the regulator recognizes temperature shifts, which occur when invading a host. RovA was shown to be expressed in a temperature-dependent bistable manner in *Y. pseudotuberculosis* leading to RovA “ON” and RovA “OFF” subpopulations within a certain temperature range.

In the present study, the mechanisms leading to the establishment of bistable expression of *rovA* and its role during infection were investigated. Time-lapse microscopy was employed to examine the dynamics of the switching-process of bistable *rovA* expression, revealing hysteresis, a memory-like behaviour of cells. The analysis of different RovA mutants demonstrated that the thermosensing capacity and proteolysis of RovA are important for accurate bistable *rovA* expression. Besides temperature-dependent factors influencing bistable *rovA* expression, PhoP of the two-component system PhoP/PhoQ was found to affect bistable *rovA* expression. PhoP, which responds to low Mg^{2+}-concentrations and antimicrobial peptides, was discovered to indirectly activate *rovA* expression through direct interaction with the non-coding RNA CsrC of the carbon-storage regulator system and connects two regulatory networks. Thus, the first direct activator of *csrC* transcription in *Y. pseudotuberculosis* was identified in this study.

Furthermore, this work uncovered the existence of RovA-positive and RovA-negative subpopulations in murine Peyer’s patches and murine caecum during the infection of mice. Moreover, it was demonstrated that mutants expressing stabilized variants of RovA are clearly attenuated in virulence similar to a *rovA* deletion mutant.

In summary, this study reveals that bistable *rovA* expression is very robust to perturbations and that precise RovA-levels are crucial for *Y. pseudotuberculosis* to achieve full virulence.

References

Achtman, M., Zurth, K., Morelli, G., Torrea, G., Guiyoule, A., and Carniel, E. (1999). *Yersinia pestis*, the cause of plague, is a recently emerged clone of *Yersinia pseudotuberculosis*. Proc. Natl. Acad. Sci. U. S. A. *96*, 14043–14048.

Ackermann, M. (2015). A functional perspective on phenotypic heterogeneity in microorganisms. Nat. Rev. Microbiol. *13*, 497–508.

Ackermann, M., Stecher, B., Freed, N.E., Songhet, P., Hardt, W.-D., and Doebeli, M. (2008). Self-destructive cooperation mediated by phenotypic noise. Nature *454*, 987–990.

Alekshun, M.N., Levy, S.B., Mealy, T.R., Seaton, B.A., and Head, J.F. (2001). The crystal structure of MarR, a regulator of multiple antibiotic resistance, at 2.3 A resolution. Nat. Struct. Biol. *8*, 710–714.

Altier, C., Suyemoto, M., and Lawhon, S.D. (2000). Regulation of *Salmonella enterica* serovar typhimurium invasion genes by CsrA. Infect. Immun. *68*, 6790–6797.

Andersen, J.B., Sternberg, C., Poulsen, L.K., Bjorn, S.P., Givskov, M., and Molin, S. (1998). New unstable variants of green fluorescent protein for studies of transient gene expression in bacteria. Appl. Environ. Microbiol. *64*, 2240–2246.

Ariza, R.R., Cohen, S.P., Bachhawat, N., Levy, S.B., and Demple, B. (1994). Repressor mutations in the *marRAB* operon that activate oxidative stress genes and multiple antibiotic resistance in *Escherichia coli*. J. Bacteriol. *176*, 143–148.

Arnoldini, M., Vizcarra, I.A., Peña-Miller, R., Stocker, N., Diard, M., Vogel, V., Beardmore, R.E., Hardt, W.-D., and Ackermann, M. (2014). Bistable expression of virulence genes in *Salmonella* leads to the formation of an antibiotic-tolerant subpopulation. PLoS Biol. *12*, e1001928.

Avican, K., Fahlgren, A., Huss, M., Heroven, A.K., Beckstette, M., Dersch, P., and Fällman, M. (2015). Reprogramming of *Yersinia* from virulent to persistent mode revealed by complex in vivo RNA-seq analysis. PLoS Pathog. *11*, e1004600.

Azizi, A., Kumar, A., Diaz-Mitoma, F., and Mestecky, J. (2010). Enhancing oral vaccine potency by targeting intestinal M cells. PLoS Pathog. *6*, e1001147.

Babitzke, P., Baker, C.S., and Romeo, T. (2009). Regulation of translation initiation by RNA binding proteins. Annu. Rev. Microbiol. *63*, 27–44.

Balligand, G., Laroche, Y., and Cornelis, G. (1985). Genetic analysis of virulence plasmid from a serogroup 9 *Yersinia enterocolitica* strain: role of outer membrane protein P1 in resistance to human serum and autoagglutination. Infect. Immun. *48*, 782–786.

Bergmiller, T., and Ackermann, M. (2011). Pole age affects cell size and the timing of cell division in *Methylobacterium extorquens* AM1. J. Bacteriol. *193*, 5216–5221.

Black, D.S., and Bliska, J.B. (2000). The RhoGAP activity of the *Yersinia pseudotuberculosis* cytotoxin YopE is required for antiphagocytic function and virulence. Mol. Microbiol. *37*, 515–527.

Bliska, J.B., and Falkow, S. (1992). Bacterial resistance to complement killing mediated by the Ail protein of *Yersinia enterocolitica.* Proc. Natl. Acad. Sci. U. S. A. *89*, 3561–3565.

Böhme, K., Steinmann, R., Kortmann, J., Seekircher, S., Heroven, A.K., Berger, E., Pisano, F., Thiermann, T., Wolf-Watz, H., Narberhaus, F., et al. (2012). Concerted actions of a thermo-labile regulator and a unique intergenic RNA thermosensor control *Yersinia* virulence. PLoS Pathog. *8*, e1002518.

Bölin, I., Norlander, L., and Wolf-Watz, H. (1982). Temperature-inducible outer membrane protein of *Yersinia pseudotuberculosis* and *Yersinia enterocolitica* is associated with the virulence plasmid. Infect. Immun. *37*, 506–512.

Bordi, C., Lamy, M.-C., Ventre, I., Termine, E., Hachani, A., Fillet, S., Roche, B., Bleves, S., Méjean, V., Lazdunski, A., et al. (2010). Regulatory RNAs and the HptB/RetS signalling pathways fine-tune *Pseudomonas aeruginosa* pathogenesis. Mol. Microbiol. *76*, 1427–1443.

Bottone, E.J. (1997). *Yersinia enterocolitica*: the charisma continues. Clin. Microbiol. Rev. *10*, 257–276.

Bowen, D., and Ensign, J. (1998). Purification and characterization of a high-molecular-weight insecticidal protein complex produced by the entomopathogenic bacterium *Photorhabdus luminescens*. Appl. Environ. Microbiol. *64*, 3029–3035.

Bozue, J., Mou, S., Moody, K.L., Cote, C.K., Trevino, S., Fritz, D., and Worsham, P. (2011). The role of the *phoPQ* operon in the pathogenesis of the fully virulent CO92 strain of *Yersinia pestis* and the IP32953 strain of *Yersinia pseudotuberculosis*. Microb. Pathog. *50*, 314–321.

Bücker, R., Heroven, A.K., Becker, J., Dersch, P., and Wittmann, C. (2014). The pyruvate-tricarboxylic acid cycle node: a focal point of virulence control in the enteric pathogen *Yersinia pseudotuberculosis*. J. Biol. Chem. *289*, 30114–30132.

Burghout, P., Beckers, F., de Wit, E., van Boxtel, R., Cornelis, G.R., Tommassen, J., and Koster, M. (2004). Role of the pilot protein YscW in the biogenesis of the YscC secretin in *Yersinia enterocolitica*. J. Bacteriol. *186*, 5366–5375.

Cahn, F.H., and Fox, M.S. (1968). Fractionation of Transformable Bacteria from Competent Cultures of *Bacillus subtilis* on Renografin Gradients. J. Bacteriol. *95*, 867–875.

Carniel, E., Guiyoule, A., Guilvout, I., and Mercereau-Puijalon, O. (1992). Molecular cloning, iron-regulation and mutagenesis of the *irp2* gene encoding HMWP2, a protein specific for the highly pathogenic *Yersinia*. Mol. Microbiol. *6*, 379–388.

Casadaban, M.J., and Cohen, S.N. (1980). Analysis of gene control signals by DNA fusion and cloning in *Escherichia coli*. J. Mol. Biol. *138*, 179–207.

Casadesús, J., and Low, D. (2006). Epigenetic gene regulation in the bacterial world. Microbiol. Mol. Biol. Rev. *70*, 830–856.

Casadesús, J., and Low, D. a (2013). Programmed heterogeneity: epigenetic mechanisms in bacteria. J. Biol. Chem. *288*, 13929–13935.

Casjens, S.R., and Hendrix, R.W. (2015). Bacteriophage lambda: Early pioneer and still relevant. Virology *479-480*, 310–330.

Cathelyn, J.S., Crosby, S.D., Lathem, W.W., Goldman, W.E., and Miller, V.L. (2006). RovA, a global regulator of *Yersinia pestis*, specifically required for bubonic plague. Proc. Natl. Acad. Sci. U. S. A. *103*, 13514–13519.

Chain, P.S.G., Carniel, E., Larimer, F.W., Lamerdin, J., Stoutland, P.O., Regala, W.M., Georgescu, A.M., Vergez, L.M., Land, M.L., Motin, V.L., et al. (2004). Insights into the evolution of *Yersinia pestis* through whole-genome comparison with *Yersinia pseudotuberculosis*. Proc. Natl. Acad. Sci. U. S. A. *101*, 13826–13831.

Chavez, R.G., Alvarez, A.F., Romeo, T., and Georgellis, D. (2010). The physiological stimulus for the BarA sensor kinase. J. Bacteriol. *192*, 2009–2012.

Chen, P.E., Cook, C., Stewart, A.C., Nagarajan, N., Sommer, D.D., Pop, M., Thomason, B., Thomason, M.P.K., Lentz, S., Nolan, N., et al. (2010). Genomic characterization of the *Yersinia* genus. Genome Biol. *11*, R1.

China, B., Sory, M.P., N'Guyen, B.T., De Bruyere, M., and Cornelis, G.R. (1993). Role of the YadA protein in prevention of opsonization of *Yersinia enterocolitica* by C3b molecules. Infect. Immun. *61*, 3129–3136.

Clark, M.A., Hirst, B.H., and Jepson, M.A. (1998). M-cell surface beta1 integrin expression and invasin-mediated targeting of *Yersinia pseudotuberculosis* to mouse Peyer's patch M cells. Infect. Immun. *66*, 1237–1243.

Claudi, B., Spröte, P., Chirkova, A., Personnic, N., Zankl, J., Schürmann, N., Schmidt, A., and Bumann, D. (2014). Phenotypic variation of *Salmonella* in host tissues delays eradication by antimicrobial chemotherapy. Cell *158*, 722–733.

Cohen, S.P., Hächler, H., and Levy, S.B. (1993). Genetic and functional analysis of the multiple antibiotic resistance (*mar*) locus in *Escherichia coli*. J. Bacteriol. *175*, 1484–1492.

Cornelis, G.R. (2002). *Yersinia* type III secretion: send in the effectors. J. Cell Biol. *158*, 401–408.

Cornelis, G.R., Boland, A., Boyd, A.P., Geuijen, C., Iriarte, M., Neyt, C., Sory, M.P., and Stainier, I. (1998). The virulence plasmid of *Yersinia*, an antihost genome. Microbiol. Mol. Biol. Rev. *62*, 1315–1352.

Cossart, P., and Sansonetti, P.J. (2004). Bacterial invasion: the paradigms of enteroinvasive pathogens. Science *304*, 242–248.

Cozy, L.M., Phillips, A.M., Calvo, R.A., Bate, A.R., Hsueh, Y.-H., Bonneau, R., Eichenberger, P., and Kearns, D.B. (2012). SlrA/SinR/SlrR inhibits motility gene expression upstream of a hypersensitive and hysteretic switch at the level of σ(D) in *Bacillus subtilis*. Mol. Microbiol. *83*, 1210–1228.

Crasnier, M. (1996). Cyclic AMP and catabolite repression. Res. Microbiol. *147*, 479–482.

Davis, K.M., Mohammadi, S., and Isberg, R.R. (2015). Community behavior and spatial regulation within a bacterial microcolony in deep tissue sites serves to protect against host attack. Cell Host Microbe *17*, 21–31.

Deacon, A.G., Hay, A., and Duncan, J. (2003). Septicemia due to *Yersinia pseudotuberculosis*--a case report. Clin. Microbiol. Infect. *9*, 1118–1119.

Dersch, P., and Isberg, R.R. (1999). A region of the *Yersinia pseudotuberculosis* invasin protein enhances integrin-mediated uptake into mammalian cells and promotes self-association. EMBO J. *18*, 1199–1213.

Dewoody, R.S., Merritt, P.M., and Marketon, M.M. (2013). Regulation of the *Yersinia* type III secretion system: traffic control. Front. Cell. Infect. Microbiol. *3*, 4.

Diard, M., Garcia, V., Maier, L., Remus-Emsermann, M.N.P., Regoes, R.R., Ackermann, M., and Hardt, W.-D. (2013). Stabilization of cooperative virulence by the expression of an avirulent phenotype. Nature *494*, 353–356.

Dolan, K.T., Duguid, E.M., and He, C. (2011). Crystal structures of SlyA protein, a master virulence regulator of *Salmonella*, in free and DNA-bound states. J. Biol. Chem. *286*, 22178–22185.

Dubey, A.K. (2005). RNA sequence and secondary structure participate in high-affinity CsrA-RNA interaction. RNA *11*, 1579–1587.

Dubey, A.K., Baker, C.S., Suzuki, K., Jones, A.D., Pandit, P., Romeo, T., and Babitzke, P. (2003). CsrA regulates translation of the *Escherichia coli* carbon starvation gene, *cstA*, by blocking ribosome access to the *cstA* transcript. J. Bacteriol. *185*, 4450–4460.

Dubnau, D., and Losick, R. (2006). Bistability in bacteria. Mol. Microbiol. *61*, 564–572.

Elowitz, M.B., Levine, A.J., Siggia, E.D., and Swain, P.S. (2002). Stochastic gene expression in a single cell. Science *297*, 1183–1186.

Errington, J. (1993). *Bacillus subtilis* sporulation: regulation of gene expression and control of morphogenesis. Microbiol. Rev. *57*, 1–33.

Fahlgren, A., Avican, K., Westermark, L., Nordfelth, R., and Fällman, M. (2014). Colonization of cecum is important for development of persistent infection by *Yersinia pseudotuberculosis*. Infect. Immun. *82*, 3471–3482.

Falconi, M., Colonna, B., Prosseda, G., Micheli, G., and Gualerzi, C.O. (1998). Thermoregulation of *Shigella* and *Escherichia coli* EIEC pathogenicity. A temperature-dependent structural transition of DNA modulates accessibility of *virF* promoter to transcriptional repressor H-NS. EMBO J. *17*, 7033–7043.

Ferrell, J.E. (1999). *Xenopus* oocyte maturation: new lessons from a good egg. Bioessays *21*, 833–842.

Ferrell, J.E. (2002). Self-perpetuating states in signal transduction: positive feedback, double-negative feedback and bistability. Curr. Opin. Cell Biol. *14*, 140–148.

Fredriksson-Ahomaa, M., Stolle, A., Siitonen, A., and Korkeala, H. (2006). Sporadic human *Yersinia enterocolitica* infections caused by bioserotype 4/O : 3 originate mainly from pigs. J. Med. Microbiol. *55*, 747–749.

Fuchs, T.M., Bresolin, G., Marcinowski, L., Schachtner, J., and Scherer, S. (2008). Insecticidal genes of *Yersinia* spp.: taxonomical distribution, contribution to toxicity towards *Manduca sexta* and *Galleria mellonella*, and evolution. BMC Microbiol. *8*, 214.

Galán, J.E., and Curtiss, R. (1989). Virulence and vaccine potential of *phoP* mutants of *Salmonella typhimurium*. Microb. Pathog. *6*, 433–443.

Galindo, C.L., Rosenzweig, J.A., Kirtley, M.L., and Chopra, A.K. (2011). Pathogenesis of *Y. enterocolitica* and *Y. pseudotuberculosis* in Human Yersinosis. J. Pathog. *2011*, 182051.

Gamba, P., Jonker, M.J., and Hamoen, L.W. (2015). A Novel Feedback Loop That Controls Bimodal Expression of Genetic Competence. PLoS Genet. *11*, e1005047.

García Véscovi, E., Soncini, F.C., and Groisman, E.A. (1996). Mg^{2+} as an extracellular signal: environmental regulation of *Salmonella* virulence. Cell *84*, 165–174.

George, A.M., and Levy, S.B. (1983). Amplifiable resistance to tetracycline, chloramphenicol, and other antibiotics in *Escherichia coli*: involvement of a non-plasmid-determined efflux of tetracycline. J. Bacteriol. *155*, 531–540.

Geyer, R. (2014). Analysis of the molecular function of invasin-like proteins of *Yersinia pseudotuberculosis* and their role in pathogenesis. Hannover Medical School.

Gillenius, E., and Urban, C.F. (2015). The adhesive protein invasin of *Yersinia pseudotuberculosis* induces neutrophil extracellular traps via β1 integrins. Microbes Infect. *17*, 327–336.

Grabenstein, J.P., Marceau, M., Pujol, C., Simonet, M., and Bliska, J.B. (2004). The response regulator PhoP of *Yersinia pseudotuberculosis* is important for replication in macrophages and for virulence. Infect. Immun. *72*, 4973–4984.

Grantcharova, N., Peters, V., Monteiro, C., Zakikhany, K., and Römling, U. (2010). Bistable expression of CsgD in biofilm development of *Salmonella enterica* serovar typhimurium. J. Bacteriol. *192*, 456–466.

Grassl, G.A., Bohn, E., Müller, Y., Bühler, O.T., and Autenrieth, I.B. (2003a). Interaction of *Yersinia enterocolitica* with epithelial cells: invasin beyond invasion. Int. J. Med. Microbiol. *293*, 41–54.

Grassl, G.A., Kracht, M., Wiedemann, A., Hoffmann, E., Aepfelbacher, M., von Eichel-Streiber, C., Bohn, E., and Autenrieth, I.B. (2003b). Activation of NF-kappaB

and IL-8 by *Yersinia enterocolitica* invasin protein is conferred by engagement of Rac1 and MAP kinase cascades. Cell. Microbiol. *5*, 957–971.

Graumann, P.L. (2006). Different genetic programmes within identical bacteria under identical conditions: the phenomenon of bistability greatly modifies our view on bacterial populations. Mol. Microbiol. *61*, 560–563.

Groisman, E.A. (2001). The pleiotropic two-component regulatory system PhoP-PhoQ. J. Bacteriol. *183*, 1835–1842.

Groisman, E.A., and Mouslim, C. (2006). Sensing by bacterial regulatory systems in host and non-host environments. Nat. Rev. Microbiol. *4*, 705–709.

Grützkau, A., Hanski, C., Hahn, H., and Riecken, E.O. (1990). Involvement of M cells in the bacterial invasion of Peyer's patches: a common mechanism shared by *Yersinia enterocolitica* and other enteroinvasive bacteria. Gut *31*, 1011–1015.

Gunn, J.S., and Miller, S.I. (1996). PhoP-PhoQ activates transcription of *pmrAB*, encoding a two-component regulatory system involved in *Salmonella typhimurium* antimicrobial peptide resistance. J. Bacteriol. *178*, 6857–6864.

Guo, L., Lim, K.B., Poduje, C.M., Daniel, M., Gunn, J.S., Hackett, M., and Miller, S.I. (1998). Lipid A Acylation and Bacterial Resistance against Vertebrate Antimicrobial Peptides. Cell *95*, 189–198.

Gutiérrez, P., Li, Y., Osborne, M.J., Pomerantseva, E., Liu, Q., and Gehring, K. (2005). Solution structure of the carbon storage regulator protein CsrA from *Escherichia coli*. J. Bacteriol. *187*, 3496–3501.

Hadden, C., and Nester, E.W. (1968). Purification of competent cells in the *Bacillus subtilis* transformation system. J. Bacteriol. *95*, 876–885.

Heesemann, Jã¼. (1987). Chromosomal-encoded siderophores are required for mouse virulence of enteropathogenic *Yersinia* species. FEMS Microbiol. Lett. *48*, 229–233.

Heise, T., and Dersch, P. (2006). Identification of a domain in *Yersinia* virulence factor YadA that is crucial for extracellular matrix-specific cell adhesion and uptake. Proc. Natl. Acad. Sci. U. S. A. *103*, 3375–3380.

Helaine, S., Cheverton, A.M., Watson, K.G., Faure, L.M., Matthews, S.A., and Holden, D.W. (2014). Internalization of *Salmonella* by macrophages induces formation of nonreplicating persisters. Science *343*, 204–208.

Herbst, K., Bujara, M., Heroven, A.K., Opitz, W., Weichert, M., Zimmermann, A., and Dersch, P. (2009). Intrinsic thermal sensing controls proteolysis of *Yersinia* virulence regulator RovA. PLoS Pathog. *5*, e1000435.

Herbst, K. (2011). The temperature- and growth-dependent regulation of the global virulence regulator RovA from *Yersinia pseudotuberculosis*. Technische Universität Carolo-Wilhelmina Braunschweig.

Heroven, A.K., and Dersch, P. (2006). RovM, a novel LysR-type regulator of the virulence activator gene *rovA*, controls cell invasion, virulence and motility of *Yersinia pseudotuberculosis*. Mol. Microbiol. *62*, 1469–1483.

Heroven, A.K., Nagel, G., Tran, H.J., Parr, S., and Dersch, P. (2004). RovA is autoregulated and antagonizes H-NS-mediated silencing of invasin and *rovA* expression in *Yersinia pseudotuberculosis*. Mol. Microbiol. *53*, 871–888.

Heroven, A.K., Böhme, K., Rohde, M., and Dersch, P. (2008). A Csr-type regulatory system, including small non-coding RNAs, regulates the global virulence regulator RovA of *Yersinia pseudotuberculosis* through RovM. Mol. Microbiol. *68*, 1179–1195.

Heroven, A.K., Sest, M., Pisano, F., Scheb-Wetzel, M., Steinmann, R., Böhme, K., Klein, J., Münch, R., Schomburg, D., and Dersch, P. (2012a). Crp induces switching of the CsrB and CsrC RNAs in *Yersinia pseudotuberculosis* and links nutritional status to virulence. Front. Cell. Infect. Microbiol. *2*, 158.

Heroven, A.K., Böhme, K., and Dersch, P. (2012b). The Csr/Rsm system of *Yersinia* and related pathogens: a post-transcriptional strategy for managing virulence. RNA Biol. *9*, 379–391.

Hoe, N.P., Minion, F.C., and Goguen, J.D. (1992). Temperature sensing in *Yersinia pestis*: regulation of *yopE* transcription by lcrF. J. Bacteriol. *174*, 4275–4286.

Hoffmann, C., Pop, M., Leemhuis, J., Schirmer, J., Aktories, K., and Schmidt, G. (2004). The *Yersinia pseudotuberculosis* cytotoxic necrotizing factor (CNFY) selectively activates RhoA. J. Biol. Chem. *279*, 16026–16032.

Hu, Y., Lu, P., Wang, Y., Ding, L., Atkinson, S., and Chen, S. (2009). OmpR positively regulates urease expression to enhance acid survival of *Yersinia pseudotuberculosis*. Microbiology *155*, 2522–2531.

Hu, Y., Lu, P., Zhang, Y., Li, L., and Chen, S. (2010). Characterization of an aspartate-dependent acid survival system in *Yersinia pseudotuberculosis*. FEBS Lett. *584*, 2311–2314.

Hurme, R., Berndt, K.D., Normark, S.J., and Rhen, M. (1997). A proteinaceous gene regulatory thermometer in *Salmonella*. Cell *90*, 55–64.

Iriarte, M., and Cornelis, G.R. (1998). YopT, a new *Yersinia* Yop effector protein, affects the cytoskeleton of host cells. Mol. Microbiol. *29*, 915–929.

Isberg, R.R., and Leong, J.M. (1990). Multiple β1 chain integrins are receptors for invasin, a protein that promotes bacterial penetration into mammalian cells. Cell *60*, 861–871.

Isberg, R.R., Voorhis, D.L., and Falkow, S. (1987). Identification of invasin: a protein that allows enteric bacteria to penetrate cultured mammalian cells. Cell *50*, 769–778.

Ishizuka, H., Hanamura, A., Inada, T., and Aiba, H. (1994). Mechanism of the down-regulation of cAMP receptor protein by glucose in *Escherichia coli*: role of autoregulation of the *crp* gene. EMBO J. *13*, 3077–3082.

Joh, R.I., and Weitz, J.S. (2011). To lyse or not to lyse: transient-mediated stochastic fate determination in cells infected by bacteriophages. PLoS Comput. Biol. *7*, e1002006.

Kampik, D., Schulte, R., and Autenrieth, I.B. (2000). *Yersinia enterocolitica* invasin protein triggers differential production of interleukin-1, interleukin-8, monocyte chemoattractant protein 1, granulocyte-macrophage colony-stimulating factor, and tumor necrosis factor alpha in epithelial cells: implicatio. Infect. Immun. *68*, 2484–2492.

Kato, A., Tanabe, H., and Utsumi, R. (1999). Molecular characterization of the PhoP-PhoQ two-component system in *Escherichia coli* K-12: identification of extracellular Mg^{2+}-responsive promoters. J. Bacteriol. *181*, 5516–5520.

Kearns, D.B., and Losick, R. (2005). Cell population heterogeneity during growth of *Bacillus subtilis*. Genes Dev. *19*, 3083–3094.

Klinkert, B., and Narberhaus, F. (2009). Microbial thermosensors. Cell. Mol. Life Sci. *66*, 2661–2676.

Koornhof, H.J., Smego, R.A., and Nicol, M. (1999). Yersiniosis. II: The pathogenesis of *Yersinia* infections. Eur. J. Clin. Microbiol. Infect. Dis. *18*, 87–112.

Kovacikova, G., Lin, W., and Skorupski, K. (2004). Vibrio cholerae AphA uses a novel mechanism for virulence gene activation that involves interaction with the LysR-type regulator AphB at the *tcpPH* promoter. Mol. Microbiol. *53*, 129–142.

Kraehenbuhl, J.P., and Neutra, M.R. (2000). Epithelial M cells: differentiation and function. Annu. Rev. Cell Dev. Biol. *16*, 301–332.

Laemmli, U.K. (1970). Cleavage of structural proteins during the assembly of the head of bacteriophage T4. Nature *227*, 680–685.

Lawhon, S.D., Maurer, R., Suyemoto, M., and Altier, C. (2002). Intestinal short-chain fatty acids alter *Salmonella typhimurium* invasion gene expression and virulence through BarA/SirA. Mol. Microbiol. *46*, 1451–1464.

Lejona, S., Aguirre, A., Cabeza, M.L., García Véscovi, E., and Soncini, F.C. (2003). Molecular characterization of the Mg^{2+}-responsive PhoP-PhoQ regulon in *Salmonella enterica*. J. Bacteriol. *185*, 6287–6294.

Lenz, D.H., Miller, M.B., Zhu, J., Kulkarni, R. V, and Bassler, B.L. (2005). CsrA and three redundant small RNAs regulate quorum sensing in *Vibrio cholerae*. Mol. Microbiol. *58*, 1186–1202.

Lewis, K. (2007). Persister cells, dormancy and infectious disease. Nat. Rev. Microbiol. *5*, 48–56.

Li, Y., Gao, H., Qin, L., Li, B., Han, Y., Guo, Z., Song, Y., Zhai, J., Du, Z., Wang, X., et al. (2008). Identification and characterization of PhoP regulon members in *Yersinia pestis* biovar Microtus. BMC Genomics *9*, 143.

Libby, S.J., Goebel, W., Ludwig, A., Buchmeier, N., Bowe, F., Fang, F.C., Guiney, D.G., Songer, J.G., and Heffron, F. (1994). A cytolysin encoded by *Salmonella* is required for survival within macrophages. Proc. Natl. Acad. Sci. U. S. A. *91*, 489–493.

Lindler, L.E., Klempner, M.S., and Straley, S.C. (1990). *Yersinia pestis* pH 6 antigen: genetic, biochemical, and virulence characterization of a protein involved in the pathogenesis of bubonic plague. Infect. Immun. *58*, 2569–2577.

Liu, M.Y., Gui, G., Wei, B., Preston, J.F., Oakford, L., Yüksel, U., Giedroc, D.P., and Romeo, T. (1997). The RNA molecule CsrB binds to the global regulatory protein CsrA and antagonizes its activity in *Escherichia coli*. J. Biol. Chem. *272*, 17502–17510.

Lockman, H.A., Gillespie, R.A., Baker, B.D., and Shakhnovich, E. (2002). *Yersinia pseudotuberculosis* produces a cytotoxic necrotizing factor. Infect. Immun. *70*, 2708–2714.

Luong, T.T., Newell, S.W., and Lee, C.Y. (2003). Mgr, a novel global regulator in *Staphylococcus aureus*. J. Bacteriol. *185*, 3703–3710.

Lutz, R., and Bujard, H. (1997). Independent and tight regulation of transcriptional units in *Escherichia coli* via the LacR/O, the TetR/O and AraC/I1-I2 regulatory elements. Nucleic Acids Res. *25*, 1203–1210.

Maamar, H., and Dubnau, D. (2005). Bistability in the *Bacillus subtilis* K-state (competence) system requires a positive feedback loop. Mol. Microbiol. *56*, 615–624.

Macfarlane, E.L., Kwasnicka, A., and Hancock, R.E. (2000). Role of *Pseudomonas aeruginosa* PhoP-phoQ in resistance to antimicrobial cationic peptides and aminoglycosides. Microbiology *146 (Pt 1*, 2543–2554.

MacKenzie, K.D., Wang, Y., Shivak, D.J., Wong, C.S., Hoffman, L.J.L., Lam, S., Kröger, C., Cameron, A.D.S., Townsend, H.G.G., Köster, W., et al. (2015). Bistable expression of CsgD in *Salmonella enterica* serovar Typhimurium connects virulence to persistence. Infect. Immun. *83*, 2312–2326.

Manoil, C., and Beckwith, J. (1986). A genetic approach to analyzing membrane protein topology. Science (80-.). *233*, 1403–1408.

Marra, A., and Isberg, R.R. (1997). Invasin-dependent and invasin-independent pathways for translocation of *Yersinia pseudotuberculosis* across the Peyer's patch intestinal epithelium. Infect. Immun. *65*, 3412–3421.

Martínez, L.C., Martínez-Flores, I., Salgado, H., Fernández-Mora, M., Medina-Rivera, A., Puente, J.L., Collado-Vides, J., and Bustamante, V.H. (2014). In silico identification and experimental characterization of regulatory elements controlling the expression of the *Salmonella csrB* and *csrC* genes. J. Bacteriol. *196*, 325–336.

Mendonca, C. (2013). Environmental control of virulence by members of the SlyA/RovA regulator family. Hannover Medical School.

Miller, V.L., and Falkow, S. (1988). Evidence for two genetic loci in *Yersinia enterocolitica* that can promote invasion of epithelial cells. Infect. Immun. *56*, 1242–1248.

Miller, S.I., Kukral, A.M., and Mekalanos, J.J. (1989). A two-component regulatory system (phoP phoQ) controls *Salmonella typhimurium* virulence. Proc. Natl. Acad. Sci. U. S. A. *86*, 5054–5058.

Minagawa, S., Ogasawara, H., Kato, A., Yamamoto, K., Eguchi, Y., Oshima, T., Mori, H., Ishihama, A., and Utsumi, R. (2003). Identification and molecular characterization of the Mg^{2+} stimulon of *Escherichia coli.* J. Bacteriol. *185*, 3696–3702.

Moss, J.E., Fisher, P.E., Vick, B., Groisman, E.A., and Zychlinsky, A. (2000). The regulatory protein PhoP controls susceptibility to the host inflammatory response in *Shigella flexneri*. Cell. Microbiol. *2*, 443–452.

Moyed, H.S., and Bertrand, K.P. (1983). *hipA*, a newly recognized gene of *Escherichia coli* K-12 that affects frequency of persistence after inhibition of murein synthesis. J. Bacteriol. *155*, 768–775.

Nagel, G., Lahrz, A., and Dersch, P. (2001). Environmental control of invasin expression in *Yersinia pseudotuberculosis* is mediated by regulation of RovA, a transcriptional activator of the SlyA/Hor family. Mol. Microbiol. *41*, 1249–1269.

Naktin, J., and Beavis, K.G. (1999). *Yersinia enterocolitica* and *Yersinia pseudotuberculosis*. Clin. Lab. Med. *19*, 523–536, vi.

Nasser, W., Shevchik, V.E., and Hugouvieux-Cotte-Pattat, N. (1999). Analysis of three clustered polygalacturonase genes in *Erwinia chrysanthemi* 3937 revealed an anti-repressor function for the PecS regulator. Mol. Microbiol. *34*, 641–650.

Nielsen, A.T., Dolganov, N. a, Rasmussen, T., Otto, G., Miller, M.C., Felt, S. a, Torreilles, S., and Schoolnik, G.K. (2010). A bistable switch and anatomical site control *Vibrio cholerae* virulence gene expression in the intestine. PLoS Pathog. *6*, e1001102.

Ninfa, A.J., and Mayo, A.E. (2004). Hysteresis vs. graded responses: the connections make all the difference. Sci. STKE *2004*, pe20.

Norte, V.A., Stapleton, M.R., and Green, J. (2003). PhoP-responsive expression of the *Salmonella enterica* serovar typhimurium slyA gene. J. Bacteriol. *185*, 3508–3514.

Nuss, A.M., Schuster, F., Kathrin Heroven, A., Heine, W., Pisano, F., and Dersch, P. (2014). A direct link between the global regulator PhoP and the Csr regulon in *Y. pseudotuberculosis* through the small regulatory RNA CsrC. RNA Biol. *11*, 580–593.

O Cróinín, T., and Backert, S. (2012). Host epithelial cell invasion by *Campylobacter jejuni*: trigger or zipper mechanism? Front. Cell. Infect. Microbiol. *2*, 25.

Oellerich, M.F., Jacobi, C.A., Freund, S., Niedung, K., Bach, A., Heesemann, J., and Trülzsch, K. (2007). *Yersinia enterocolitica* infection of mice reveals clonal invasion and abscess formation. Infect. Immun. *75*, 3802–3811.

Oelschlaeger, T.A. (2001). Adhesins as invasins. Int. J. Med. Microbiol. *291*, 7–14.

Oyston, P.C., Dorrell, N., Williams, K., Li, S.R., Green, M., Titball, R.W., and Wren, B.W. (2000). The response regulator PhoP is important for survival under conditions of macrophage-induced stress and virulence in *Yersinia pestis*. Infect. Immun. *68*, 3419–3425.

Ozbudak, E.M., Thattai, M., Kurtser, I., Grossman, A.D., and van Oudenaarden, A. (2002). Regulation of noise in the expression of a single gene. Nat. Genet. *31*, 69–73.

Von Pawel-Rammingen, U., Telepnev, M. V, Schmidt, G., Aktories, K., Wolf-Watz, H., and Rosqvist, R. (2000). GAP activity of the *Yersinia* YopE cytotoxin specifically targets the Rho pathway: a mechanism for disruption of actin microfilament structure. Mol. Microbiol. *36*, 737–748.

Pepe, J.C., and Miller, V.L. (1993). *Yersinia enterocolitica* invasin: a primary role in the initiation of infection. Proc. Natl. Acad. Sci. U. S. A. *90*, 6473–6477.

Perera, I.C., and Grove, A. (2010). Urate is a ligand for the transcriptional regulator PecS. J. Mol. Biol. *402*, 539–551.

Perera, I.C., Lee, Y.-H., Wilkinson, S.P., and Grove, A. (2009). Mechanism for attenuation of DNA binding by MarR family transcriptional regulators by small molecule ligands. J. Mol. Biol. *390*, 1019–1029.

Pérez, E., Samper, S., Bordas, Y., Guilhot, C., Gicquel, B., and Martín, C. (2001). An essential role for *phoP* in *Mycobacterium tuberculosis* virulence. Mol. Microbiol. *41*, 179–187.

Pérez-Rueda, E., and Collado-Vides, J. (2001). Common history at the origin of the position-function correlation in transcriptional regulators in archaea and bacteria. J. Mol. Evol. *53*, 172–179.

Pernestig, A.-K., Georgellis, D., Romeo, T., Suzuki, K., Tomenius, H., Normark, S., and Melefors, O. (2003). The *Escherichia coli* BarA-UvrY two-component system is needed for efficient switching between glycolytic and gluconeogenic carbon sources. J. Bacteriol. *185*, 843–853.

Perry, R.D., and Fetherston, J.D. (1997). *Yersinia pestis*--etiologic agent of plague. Clin. Microbiol. Rev. *10*, 35–66.

Pinheiro, V.B., and Ellar, D.J. (2007). Expression and insecticidal activity of *Yersinia pseudotuberculosis* and *Photorhabdus luminescens* toxin complex proteins. Cell. Microbiol. *9*, 2372–2380.

Pisano, F., Kochut, A., Uliczka, F., Geyer, R., Stolz, T., Thiermann, T., Rohde, M., and Dersch, P. (2012). In vivo-induced InvA-like autotransporters Ifp and InvC of *Yersinia pseudotuberculosis* promote interactions with intestinal epithelial cells and contribute to virulence. Infect. Immun. *80*, 1050–1064.

Pisano, F., Heine, W., Rosenheinrich, M., Schweer, J., Nuss, A.M., and Dersch, P. (2014). Influence of PhoP and intra-species variations on virulence of *Yersinia pseudotuberculosis* during the natural oral infection route. PLoS One *9*, e103541.

Praillet, T., Nasser, W., Robert-Baudouy, J., and Reverchon, S. (1996). Purification and functional characterization of PecS, a regulator of virulence-factor synthesis in *Erwinia chrysanthemi*. Mol. Microbiol. *20*, 391–402.

Prosseda, G., Falconi, M., Giangrossi, M., Gualerzi, C.O., Micheli, G., and Colonna, B. (2004). The *virF* promoter in *Shigella*: more than just a curved DNA stretch. Mol. Microbiol. *51*, 523–537.

Quade, N., Mendonca, C., Herbst, K., Heroven, A.K., Ritter, C., Heinz, D.W., and Dersch, P. (2012). Structural basis for intrinsic thermosensing by the master virulence regulator RovA of *Yersinia*. J. Biol. Chem. *287*, 35796–35803.

Rahuma, N., Ghenghesh, K.S., Ben Aissa, R., and Elamaari, A. (2005). Carriage by the housefly (*Musca domestica*) of multiple-antibiotic-resistant bacteria that are potentially pathogenic to humans, in hospital and other urban environments in Misurata, Libya. Ann. Trop. Med. Parasitol. *99*, 795–802.

Reimmann, C., Valverde, C., Kay, E., and Haas, D. (2005). Posttranscriptional repression of GacS/GacA-controlled genes by the RNA-binding protein RsmE acting together with RsmA in the biocontrol strain *Pseudomonas fluorescens* CHA0. J. Bacteriol. *187*, 276–285.

Reuven, P., and Eldar, A. (2011). Macromotives and microbehaviors: the social dimension of bacterial phenotypic variability. Curr. Opin. Genet. Dev. *21*, 759–767.

Revell, P.A., and Miller, V.L. (2002). A chromosomally encoded regulator is required for expression of the *Yersinia enterocolitica inv* gene and for virulence. Mol. Microbiol. *35*, 677–685.

Reverchon, S., Nasser, W., and Robert-Baudouy, J. (1994). *pecS*: a locus controlling pectinase, cellulase and blue pigment production in *Erwinia chrysanthemi*. Mol. Microbiol. *11*, 1127–1139.

Reverchon, S., Rouanet, C., Expert, D., and Nasser, W. (2002). Characterization of indigoidine biosynthetic genes in *Erwinia chrysanthemi* and role of this blue pigment in pathogenicity. J. Bacteriol. *184*, 654–665.

Roland, K.L., Martin, L.E., Esther, C.R., and Spitznagel, J.K. (1993). Spontaneous *pmrA* mutants of *Salmonella typhimurium* LT2 define a new two-component regulatory system with a possible role in virulence. J. Bacteriol. *175*, 4154–4164.

Romeo, T. (1998). Global regulation by the small RNA-binding protein CsrA and the non-coding RNA molecule CsrB. Mol. Microbiol. *29*, 1321–1330.

Romeo, T., Gong, M., Liu, M.Y., and Brun-Zinkernagel, A.M. (1993). Identification and molecular characterization of *csrA*, a pleiotropic gene from *Escherichia coli* that affects glycogen biosynthesis, gluconeogenesis, cell size, and surface properties. J. Bacteriol. *175*, 4744–4755.

Romeo, T., Vakulskas, C.A., and Babitzke, P. (2013). Post-transcriptional regulation on a global scale: form and function of Csr/Rsm systems. Environ. Microbiol. *15*, 313–324.

Rosner, B.M., Stark, K., and Werber, D. (2010). Epidemiology of reported *Yersinia enterocolitica* infections in Germany, 2001-2008. BMC Public Health *10*, 337.

Rossez, Y., Wolfson, E.B., Holmes, A., Gally, D.L., and Holden, N.J. (2015). Bacterial flagella: twist and stick, or dodge across the kingdoms. PLoS Pathog. *11*, e1004483.

Rotem, E., Loinger, A., Ronin, I., Levin-Reisman, I., Gabay, C., Shoresh, N., Biham, O., and Balaban, N.Q. (2010). Regulation of phenotypic variability by a threshold-based mechanism underlies bacterial persistence. Proc. Natl. Acad. Sci. U. S. A. *107*, 12541–12546.

Rouvroit, C.L., Sluiters, C., and Cornelis, G.R. (1992). Role of the transcriptional activator, VirF, and temperature in the expression of the pYV plasmid genes of *Yersinia enterocolitica*. Mol. Microbiol. *6*, 395–409.

Ruckdeschel, K., Roggenkamp, A., Schubert, S., and Heesemann, J. (1996). Differential contribution of *Yersinia enterocolitica* virulence factors to evasion of microbicidal action of neutrophils. Infect. Immun. *64*, 724–733.

Saier, M.H. Multiple mechanisms controlling carbon metabolism in bacteria. Biotechnol. Bioeng. *58*, 170–174.

Sansonetti, P. (2002). Host-pathogen interactions: the seduction of molecular cross talk. Gut *50 Suppl 3*, III2–III8.

Savin, C., Martin, L., Bouchier, C., Filali, S., Chenau, J., Zhou, Z., Becher, F., Fukushima, H., Thomson, N.R., Scholz, H.C., et al. (2014). The *Yersinia pseudotuberculosis* complex: characterization and delineation of a new species, *Yersinia wautersii*. Int. J. Med. Microbiol. *304*, 452–463.

Schesser, K., Spiik, A.K., Dukuzumuremyi, J.M., Neurath, M.F., Pettersson, S., and Wolf-Watz, H. (1998). The *yopJ* locus is required for *Yersinia*-mediated inhibition of NF-kappaB activation and cytokine expression: YopJ contains a eukaryotic SH2-like domain that is essential for its repressive activity. Mol. Microbiol. *28*, 1067–1079.

Schulte, R. (2000). *Yersinia enterocolitica* invasin protein triggers IL-8 production in epithelial cells via activation of Rel p65-p65 homodimers. FASEB J. *14*, 1471–1484.

Schweer, J., Kulkarni, D., Kochut, A., Pezoldt, J., Pisano, F., Pils, M.C., Genth, H., Huehn, J., and Dersch, P. (2013). The cytotoxic necrotizing factor of *Yersinia pseudotuberculosis* (CNFY) enhances inflammation and Yop delivery during infection by activation of Rho GTPases. PLoS Pathog. *9*, e1003746.

Simon, R., Priefer, U., and Pühler, A. (1983). A Broad Host Range Mobilization System for In Vivo Genetic Engineering: Transposon Mutagenesis in Gram Negative Bacteria. Bio/Technology *1*, 784–791.

Van Sinderen, D., Luttinger, A., Kong, L., Dubnau, D., Venema, G., and Hamoen, L. (1995). *comK* encodes the competence transcription factor, the key regulatory protein for competence development in *Bacillus subtilis*. Mol. Microbiol. *15*, 455–462.

Skorupski, K., and Taylor, R.K. (1999). A new level in the *Vibrio cholerae* ToxR virulence cascade: AphA is required for transcriptional activation of the *tcpPH* operon. Mol. Microbiol. *31*, 763–771.

Skurnik, M., and Toivanen, P. (1992). LcrF is the temperature-regulated activator of the *yadA* gene of *Yersinia enterocolitica* and *Yersinia pseudotuberculosis*. J. Bacteriol. *174*, 2047–2051.

Skurnik, M., Bölin, I., Heikkinen, H., Piha, S., and Wolf-Watz, H. (1984). Virulence plasmid-associated autoagglutination in *Yersinia* spp. J. Bacteriol. *158*, 1033–1036.

Smego, R.A., Frean, J., and Koornhof, H.J. (1999). Yersiniosis I: microbiological and clinicoepidemiological aspects of plague and non-plague *Yersinia* infections. Eur. J. Clin. Microbiol. Infect. Dis. *18*, 1–15.

Smits, W.K., Eschevins, C.C., Susanna, K.A., Bron, S., Kuipers, O.P., and Hamoen, L.W. (2005). Stripping *Bacillus*: ComK auto-stimulation is responsible for the bistable response in competence development. Mol. Microbiol. *56*, 604–614.

Smits, W.K., Kuipers, O.P., and Veening, J.-W. (2006). Phenotypic variation in bacteria: the role of feedback regulation. Nat. Rev. Microbiol. *4*, 259–271.

Soncini, F.C., Véscovi, E.G., and Groisman, E.A. (1995). Transcriptional autoregulation of the *Salmonella typhimurium phoPQ* operon. J. Bacteriol. *177*, 4364–4371.

Stapleton, M.R., Norte, V.A., Read, R.C., and Green, J. (2002). Interaction of the *Salmonella typhimurium* transcription and virulence factor SlyA with target DNA and identification of members of the SlyA regulon. J. Biol. Chem. *277*, 17630–17637.

Steinmann, R., and Dersch, P. (2013). Thermosensing to adjust bacterial virulence in a fluctuating environment. Future Microbiol. *8*, 85–105.

Straley, S.C., and Perry, R.D. (1995). Environmental modulation of gene expression and pathogenesis in *Yersinia*. Trends Microbiol. *3*, 310–317.

Strauch, M., Trach, K., Day, J., and Hoch, J. (1992). SpoOA activates and represses its own synthesis by binding at its dual promoters. Biochimie *74*, 619–626.

Studier, F.W., and Moffatt, B.A. (1986). Use of bacteriophage T7 RNA polymerase to direct selective high-level expression of cloned genes. J. Mol. Biol. *189*, 113–130.

Sturm, A., Heinemann, M., Arnoldini, M., Benecke, A., Ackermann, M., Benz, M., Dormann, J., and Hardt, W.-D. (2011). The cost of virulence: retarded growth of *Salmonella* Typhimurium cells expressing type III secretion system 1. PLoS Pathog. *7*, e1002143.

Sulavik, M.C., Gambino, L.F., and Miller, P.F. (1995). The MarR repressor of the multiple antibiotic resistance (*mar*) operon in *Escherichia coli*: prototypic member of a family of bacterial regulatory proteins involved in sensing phenolic compounds. Mol. Med. *1*, 436–446.

Suzuki, K., Wang, X., Weilbacher, T., Pernestig, A.-K., Melefors, O., Georgellis, D., Babitzke, P., and Romeo, T. (2002). Regulatory circuitry of the CsrA/CsrB and BarA/UvrY systems of *Escherichia coli*. J. Bacteriol. *184*, 5130–5140.

Tao, T., Snavely, M.D., Farr, S.G., and Maguire, M.E. (1995). Magnesium transport in *Salmonella typhimurium: mgtA* encodes a P-type ATPase and is regulated by Mg^{2+} in a manner similar to that of the *mgtB* P-type ATPase. J. Bacteriol. *177*, 2654–2662.

Taylor, R.K., Miller, V.L., Furlong, D.B., and Mekalanos, J.J. (1987). Use of *phoA* gene fusions to identify a pilus colonization factor coordinately regulated with cholera toxin. Proc. Natl. Acad. Sci. U. S. A. *84*, 2833–2837.

Tran, H.J., Heroven, A.K., Winkler, L., Spreter, T., Beatrix, B., and Dersch, P. (2005). Analysis of RovA, a transcriptional regulator of *Yersinia pseudotuberculosis* virulence

that acts through antirepression and direct transcriptional activation. J. Biol. Chem. *280*, 42423–42432.

Treille, G.-F., and Yersin, A. (1894). La peste bubonique à Hong Kong.

Uliczka, F., Pisano, F., Schaake, J., Stolz, T., Rohde, M., Fruth, A., Strauch, E., Skurnik, M., Batzilla, J., Rakin, A., et al. (2011). Unique cell adhesion and invasion properties of *Yersinia enterocolitica* O:3, the most frequent cause of human Yersiniosis. PLoS Pathog. *7*, e1002117.

Vadyvaloo, V., Jarrett, C., Sturdevant, D.E., Sebbane, F., and Hinnebusch, B.J. (2010). Transit through the flea vector induces a pretransmission innate immunity resistance phenotype in *Yersinia pestis*. PLoS Pathog. *6*, e1000783.

Vakulskas, C.A., Potts, A.H., Babitzke, P., Ahmer, B.M.M., and Romeo, T. (2015). Regulation of bacterial virulence by Csr (Rsm) systems. Microbiol. Mol. Biol. Rev. *79*, 193–224.

Veening, J.-W., Hamoen, L.W., and Kuipers, O.P. (2005). Phosphatases modulate the bistable sporulation gene expression pattern in *Bacillus subtilis*. Mol. Microbiol. *56*, 1481–1494.

Veening, J.-W., Smits, W.K., and Kuipers, O.P. (2008a). Bistability, epigenetics, and bet-hedging in bacteria. Annu. Rev. Microbiol. *62*, 193–210.

Veening, J.-W., Igoshin, O.A., Eijlander, R.T., Nijland, R., Hamoen, L.W., and Kuipers, O.P. (2008b). Transient heterogeneity in extracellular protease production by *Bacillus subtilis*. Mol. Syst. Biol. *4*, 184.

Véscovi, E.G., Soncini, F.C., and Groisman, E.A. (1996). Mg^{2+} as an Extracellular Signal: Environmental Regulation of *Salmonella* Virulence. Cell *84*, 165–174.

Véscovi, E.G., Ayala, Y.M., Di Cera, E., and Groisman, E.A. (1997). Characterization of the bacterial sensor protein PhoQ. Evidence for distinct binding sites for Mg^{2+} and Ca^{2+}. J. Biol. Chem. *272*, 1440–1443.

White, D., Hart, M.E., and Romeo, T. (1996). Phylogenetic distribution of the global regulatory gene *csrA* among eubacteria. Gene *182*, 221–223.

Wilkinson, S.P., and Grove, A. (2004). HucR, a novel uric acid-responsive member of the MarR family of transcriptional regulators from *Deinococcus radiodurans*. J. Biol. Chem. *279*, 51442–51450.

Wilkinson, S.P., and Grove, A. (2006). Ligand-responsive transcriptional regulation by members of the MarR family of winged helix proteins. Curr. Issues Mol. Biol. *8*, 51–62.

Zhang, Y., Gao, H., Wang, L., Xiao, X., Tan, Y., Guo, Z., Zhou, D., and Yang, R. (2011). Molecular characterization of transcriptional regulation of *rovA* by PhoP and RovA in *Yersinia pestis*. PLoS One *6*, e25484.

Zhang, Y., Wang, L., Han, Y., Yan, Y., Tan, Y., Zhou, L., Cui, Y., Du, Z., Wang, X., Bi, Y., et al. (2013). Autoregulation of PhoP/PhoQ and positive regulation of the cyclic AMP receptor protein-cyclic AMP complex by PhoP in *Yersinia pestis*. J. Bacteriol. *195*, 1022–1030.

Zheng, D., Constantinidou, C., Hobman, J.L., and Minchin, S.D. (2004). Identification of the CRP regulon using in vitro and in vivo transcriptional profiling. Nucleic Acids Res. *32*, 5874–5893.

Zhou, D., Han, Y., Qin, L., Chen, Z., Qiu, J., Song, Y., Li, B., Wang, J., Guo, Z., Du, Z., et al. (2005). Transcriptome analysis of the Mg^{2+}-responsive PhoP regulator in *Yersinia pestis*. FEMS Microbiol. Lett. *250*, 85–95.

Zieg, J., Silverman, M., Hilmen, M., and Simon, M. (1977). Recombinational switch for gene expression. Science *196*, 170–172.

Zurek, L., Schal, C., and Watson, D.W. (2000). Diversity and contribution of the intestinal bacterial community to the development of *Musca domestica* (Diptera: Muscidae) larvae. J. Med. Entomol. *37*, 924–928.

Zurek, L., Denning, S.S., Schal, C., and Watson, D.W. (2001). Vector competence of *Musca domestica* (Diptera: Muscidae) for *Yersinia pseudotuberculosis*. J. Med. Entomol. *38*, 333–335.

Supplements

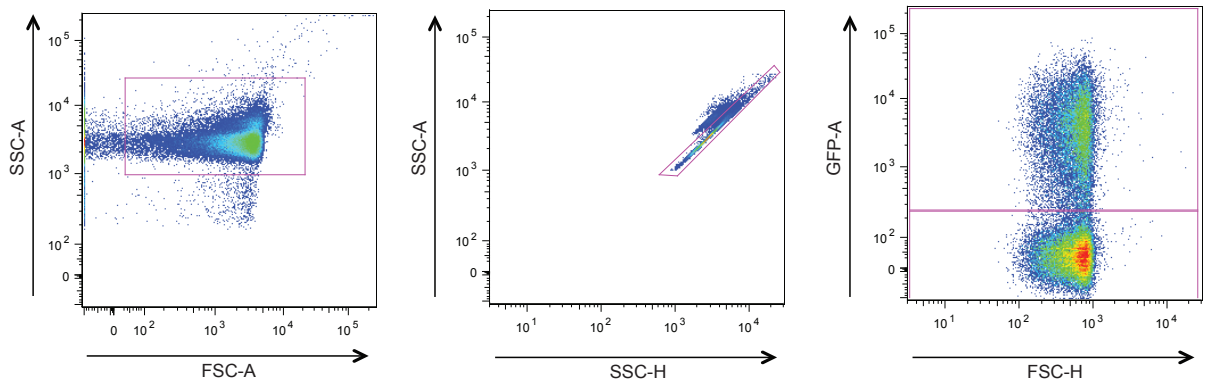

Fig. S1 Gating strategy for bacteria of *in vitro* cultures.
Exemplary gating strategy of bacteria, which were grown to exponential growth phase and fixed with 4% paraformaldehyde. At first, bacteria were gated according to their size. Then duplets were excluded and eGFP-positive and eGFP-negative cells were gated dependent on the fluorescence intensity.

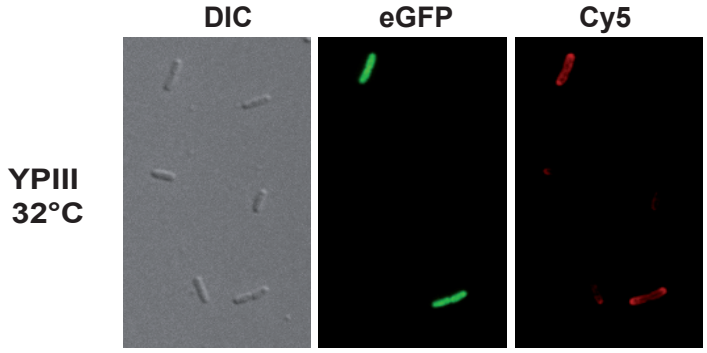

Fig. S2 Amount of Invasin on the cell surface equals RovA-dependent eGFP$_{LVA}$ expression.
Y. pseudotuberculosis YPIII cells harboring plasmid pKH70 (P$_{rovA}$-*egfp*$_{LVA}$) were grown to exponential growth phase at 32°C, fixed with 4% paraformaldehyde and stained with a specific monoclonal InvA antibody. As secondary antibody IgG-Cy5 was used. The cells were visualized using the Axiovert II fluorescence microscope (Zeiss) (performed by Nuss, A. M.).

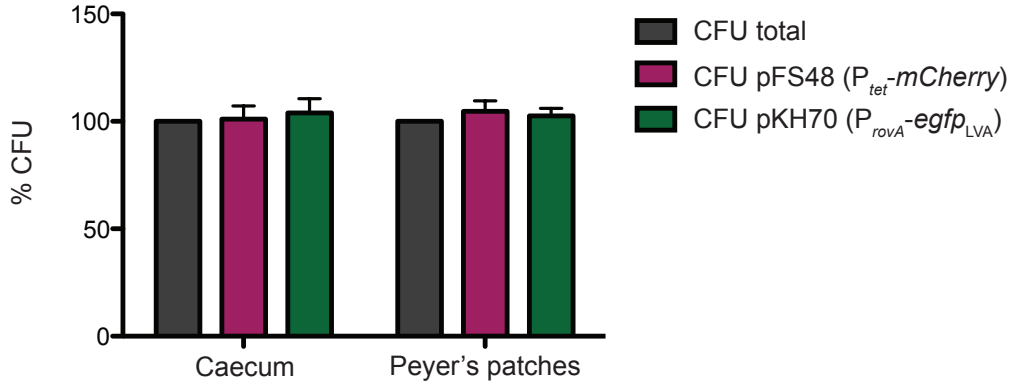

Fig. S3 Plasmid loss three days after infection of mice.
BALB/c mice (n=11) were orally infected with $2*10^8$ CFU of either *Y. pseudotuberculosis* YPIII wild type or YPIII $RovA_{P98S,\ G116A,\ SG127/128IK}$ (YP287) harboring plasmids pFS48 (P_{tet}-*mCherry*) and pKH70 (P_{rovA}-*egfp*$_{LVA}$). Three days post infection the number of bacteria in caecum and Peyer's patches was determined by plating on LB-agar with and without antibiotics. Data were normalized to CFUs without antibiotics.

$$\frac{\mathbf{d}r}{\mathbf{d}t} = \alpha_0 + \alpha \frac{r^{h_a}}{k_a(T)^{h_a} + r^{h_a}} \frac{k_r(T)^{h_r}}{k_r(T)^{h_r} + r^{h_r}} - \delta(T) \cdot r$$

α_0	basal production rate of RovA
α	maximum induced production rate of RovA
r	concentration of RovA
T	temperature
k_a	binding constant for activating binding site
h_a	Hill coefficient for activating binding site
k_r	binding constant for inhibitory binding site
h_r	Hill coefficient for inhibitory binding site
δ	degradation and dilution rate of RovA

Fig. S4 Differential equation for bistable *rovA* expression.
The differential equation describes the parameters involved in the establishment of bistable *rovA* expression (Müller J.; Münch R., unpublished data).

Danksagung

Zunächst möchte ich mich bei meiner Mentorin Prof. Dr. Petra Dersch für die gute Betreuung meiner Arbeit bedanken. Danke, für deine Unterstützung und Motivation während der gesamten Zeit sowie dein Vertrauen in meine Arbeit.

Prof. Dr. Susanne Engelmann möchte ich für die Übernahme des Koreferates danken. Ebenfalls danken möchte ich Prof. Dr. André Fleißner für die Teilnahme an der Promotionskommission.

Weiterhin bedanke ich mich bei den Teilnehmern meines *Thesis Committees* Prof. Dr. Eva Medina und Prof. Dr. Melanie Brinkmann.

Der „Helmholtz International Graduate School for Infection Research“ danke ich für die Finanzierung von Weiterbildungen und Konferenzen.

Aaron Nuss möchte ich für seine gute Betreuung danken. Vielen Dank für deine vielen guten Ratschläge, die gute Zusammenarbeit, deine Hilfsbereitschaft und das Korrekturlesen meiner Arbeit.

Des Weiteren möchte ich mich bei der gesamten Arbeitsgruppe MIBI für die schöne Zeit bedanken, insbesondere bei dem „großen“ Labor für die tolle Arbeitsatmosphäre. Danke Carina für deine ruhige und geduldige Art, für dein Verständnis sowie die vielen schönen Heimfahrten mit dem Fahrrad und Ausflüge in die Schwimmhalle.

Außerdem möchte ich meinem Büro danken, besonders Jörn für die vielen produktiven und unterhaltsamen Gespräche sowie seine Geduld immer wieder meine kleinen Panikattacken auszuhalten. Vielen Dank auch an Maik und Wiebke vor allem für die Versorgung mit Nervennahrung, die manchen grauen Tag etwas heller gemacht hat.

Ein ganz großes Dankeschön geht an Rebecca und Tanja für die Unterstützung und Kraft, die sie mir gegeben haben sowie ihr jederzeit offenes Ohr für meine Sorgen. Danke, dass ihr nicht nur beruflich, sondern auch privat immer für dich da gewesen seid.

Mein besonderer Dank gilt zudem Marion dafür, dass sie mir in einer schwierigen Zeit beiseite gestanden hat und diese Zeit für mich erträglicher gemacht hat. Danke,

dass du auch in der Ferne immer für mich da bist. Unsere abendlichen Spaziergänge werde ich nie vergessen.

Meinen Eltern und Großeltern danke ich von ganzem Herzen für ihre bedingungslose Unterstützung. Ebenfalls bedanken möchte ich mich bei Martin, der sich viele Stunden mit meiner Arbeit beschäftigt hat. Ein ganz besonderes Dankeschön geht an meine Schwester Katharina. Vielen Dank, dass du immer für mich da warst und bist, mir immer Rückhalt und Kraft gibst und ich jederzeit auf dich zählen kann! Zudem möchte ich Sten danken, der mir immer viel Verständnis entgegengebracht hat, mich fortwährend unterstützt hat und mein Fels in der Brandung war.